



AN ABSTRACT OF THE DISSERTATION OF

Luke A. Pangle for the degree of Doctor of Philosophy in Water Resources Science presented on August 7, 2013.

Title: Ecohydrological mediation of water budget partitioning and time scales of subsurface flow in a seasonally semi-arid grassland.

Abstract approved:

---

Jeffrey J. McDonnell

Understanding how the interactions and feedbacks between plant function, climate, and soils ultimately affects the terrestrial water balance and subsurface flow processes is major challenge in scientific hydrology. This dissertation summarizes the findings of a manipulative climate warming experiment, an observational field study that utilized stable-isotope tracers, and associated modeling analyses that I used to examine the physiological and physical mechanisms by which grassland ecosystems mediate water-balance partitioning and transit times of water flowing through the subsurface.

Utilizing the climate-controlled mesocosm experiment, I examined the responses of evapotranspiration, soil moisture, and potential groundwater recharge to a 3.5°C temperature increase in a grassland ecosystem experiencing a Mediterranean climate. I hypothesized that a warmer climate would cause a shift in the soil-water balance toward greater evapotranspiration, and less recharge. The results showed that warming treatments enhanced evapotranspiration during the spring. However, this reduced soil moisture more rapidly, resulting in less evapotranspiration during the summer than occurred under ambient temperatures, and no difference when considered over the entire year. Groundwater recharge was reduced during late-spring storms relative to the ambient temperature treatment, but these reductions were a small fraction of the annual total, and were offset by slightly greater recharge in the fall under warming treatments. The results highlighted the potential for interactions between climate, vegetation, and

soils to moderate the hydrological response to climate warming, particularly in environments where precipitation is seasonal and out of phase with the vegetation growing season.

I conducted additional field studies that utilized three lysimeters with surface conditions ranging from bare soil through two stages of aggrading grassland vegetation. Using hydrometric data, stable-isotopes as conservative tracer, and two hydrograph-separation techniques I evaluated whether aggrading grassland vegetation and root systems alter time scales of subsurface flow, and how this alteration may influence potential groundwater recharge. I tested the hypothesis that soil structural change under aggrading vegetation would enhance the rapid infiltration of precipitation-event water, resulting in greater potential recharge during individual storms. Contrary to this expectation, results from both hydrograph-separation techniques showed that precipitation-event water comprised 0 – 6% of potential recharge among all the storm events I analyzed, being greatest under bare soil, and always zero in grasslands ranging in age from 3.8 – 5.9 years. These results contradicted my original hypothesis, and were attributed to the low intensity of local precipitation, large soil-water storage potential, and the predominantly shallow rooting tendency of the grassland vegetation. In a final analysis I used stable-isotope measurements and a linear-time-invariant convolution approach to model mean-transit times and transit-time distributions of subsurface flow under each surface condition, and over the entire water year. The results showed that mean-transit times were not significantly different in the presence of aggrading vegetation.

From these analyses I concluded that physical alteration of the soil by aggrading plant root systems was not an ecohydrologically significant mechanism in this system. Ex post facto analyses showed that, at the time scale of individual storm events, the reduction of effective precipitation by interception and evaporative loss from the grassland canopies was of much greater importance—even with very low leaf area indices. At the annual time scale, root expansion enabled much greater exploitation of soil water during the summer drought, causing a shift from a recharge-dominated to an evapotranspiration-dominated soil-water balance within the first year of growth.

©Copyright by Luke A. Pangle

August 7, 2013

All Rights Reserved

Ecohydrological mediation of water budget partitioning and time scales of subsurface  
flow in a seasonally semi-arid grassland

by  
Luke A. Pangle

A DISSERTATION  
submitted to  
Oregon State University

in partial fulfillment of  
the requirements for the  
degree of

Doctor of Philosophy

Presented August 7, 2013  
Commencement June 2014

Doctor of Philosophy dissertation of Luke A. Pangle presented on  
August 7, 2013

APPROVED:

---

Jeffrey J. McDonnell, representing Water Resources Science

---

Director of the Water Resources Graduate Program

---

Dean of the Graduate School

I understand that my thesis will become part of the permanent collection of Oregon State University libraries. My signature below authorizes release of my dissertation to any reader upon request.

---

Luke A. Pangle, Author

## ACKNOWLEDGEMENTS

I thank my advisor, Jeff McDonnell, for welcoming me into his research group, for providing funding support and research opportunities, for serving as a very helpful editor of my writing, and most of all for his unshakably optimistic attitude and timely encouragement. One of the most important lessons learned during this process was how to remain persistent when my efforts seemed sure to fail. The times I recall being least encumbered by such doubts were often after a meeting with Jeff. Thanks for the support, Jeff.

I thank Jillian Gregg for the terrific opportunity to work at the Terracosm facility, for funding support during the first 15 months of my work, for sharing equipment and resources that enabled much of the research herein, and for her careful and thoughtful contributions as a co-author on the first manuscript presented here. I learned a lot from Jillian during our editing sessions about how to write concisely and effectively. Thanks, Jillian.

I thank my other committee members, Maria Dragila, Renee Brooks, and Jay Noller. Thanks to Maria for introducing me to hydrology—her soil physics course was the first hydrology-related course I had ever taken at the time, and it really peaked my interest. Also, thanks to Maria for generously writing letters of support for several scholarship opportunities I pursued, some successfully, and for helping me think through some of the modeling tasks associated with my third chapter. Thanks to Renee for sharing her passion for stable-isotope research, through our interactions in the Isotopics course and through our personal discussions about papers and parts of my data. Also, thank you for assisting with a tracer-injection test at the Terracosms and for allowing me access to research facilities that aided my work. Thanks to Jay Noller for his service to the University while acting as my graduate council representative, and for being an enthusiastic participant in my committee meetings and comprehensive exams.

I greatly appreciated and enjoyed the comradery shared with lab members Cody Hale, Luisa Hopp, Julian Klaus, Tina Garland, Caroline Patrick, Chris Gabrielli, Jay Frentress, Lysette Munoz-Villers, Friso Holwerda, and Falko Stocker. Also, thanks to many peers who performed service with me as part of the Hydrophiles—our University

chapter of the American Water Resources Association—which made my graduate experience vastly more rich than it would have been otherwise. Thanks to Elena Berman and Manish Gupta for the collaboration in the development of some new isotope sampling techniques. Finally, I thank the many great instructors I had the opportunity to interact with during my coursework at Oregon State, and Mary Santelmann for directing an excellent graduate program and for offering me guidance and teaching-assistantship opportunities.

I gratefully acknowledge funding support from US Department of Energy grant #DE-FG02-05ER64048, DOE SBIR Grant #DE-FG02-08ER84976, the Oregon State University College of Forestry Fellowships Program, the Water Resources Graduate Program, and the American Water Resources Association.

## CONTRIBUTION OF AUTHORS

Chapter 2: Jillian Gregg secured funding for the Terracosm experiment and crafted the experimental design. She directed data collection activities and quality assurance measures at the Terracosm facility, and provided editing and feedback throughout the analysis and writing process. Jeff McDonnell helped formulate the research question and hypotheses and provided editing and feedback throughout the analysis and writing process.

Chapter 3: Jeff McDonnell helped formulate the research question and provided editing and feedback throughout the analysis and writing process. Jillian Gregg helped collect data and provided editing support during manuscript development.

Chapter 4: Jeff McDonnell helped formulate the research question and provided editing and feedback throughout the analysis and writing process. Jillian Gregg helped collect data and provided editing support during manuscript development.

## TABLE OF CONTENTS

	<u>Page</u>
1 Introduction.....	1
1.1 Introduction.....	2
1.2 References.....	6
2 Rainfall seasonality and an ecohydrological feedback offset the potential impact of climate warming on evapotranspiration and groundwater recharge.....	9
2.1 Introduction.....	10
2.2 Materials and Methods.....	12
2.21 Climate.....	12
2.22 Site Description.....	13
2.23 Climate Control and Experimental Treatments.....	14
2.24 Measurement and Calculation of Water Budget Components.....	15
2.25 Calculation of Reference Evapotranspiration.....	17
2.26 Data Analysis.....	18
2.3 Results.....	19
2.31 Evapotranspiration.....	19
2.32 Soil Moisture.....	20
2.33 Groundwater Recharge.....	21
2.4 Discussion.....	22
2.41 What caused the contrasting seasonal patterns of ET observed under warming treatments versus ambient temperature?.....	22
2.42 Why were there only small seasonal reductions of R, and no reduction over the entire water year?.....	24

TABLE OF CONTENTS (Continued)

	<u>Page</u>
2.43 How does the specific combination of climate, vegetation, and soil affect the general inference that can be made from this manipulative experiment?.....	25
2.5 Conclusions.....	27
2.6 References.....	28
3 Soil-water flow under aggrading grassland vegetation: seeking evidence of hydrologically significant soil alteration by roots.....	43
3.1 Introduction.....	44
3.2 Materials and Methods.....	46
3.21 Site Description.....	46
3.22 Lysimeter design and soils.....	47
3.23 Lysimeter vegetation.....	48
3.24 Hydrometric data collection.....	49
3.25 Stable isotope sampling and analysis.....	49
3.26 Analytical approach 1: hydrograph separation with TRANSEP....	50
3.27 Analytical approach 2: hydrograph separation with a two-component mixing model.....	55
3.28 Precipitation-event definition and selection.....	56
3.3 Results.....	57
3.4 Discussion.....	59
3.41 Why was the event-water contribution to potential recharge negligible?.....	59
3.42 Ex post facto analysis of canopy-interception effects on recharge generation.....	63
3.5 Conclusions and ecohydrological significance of these results.....	65
3.6 References.....	66
4 Effects of vegetation establishment on soil-water balance, flow and transit time.....	80



## LIST OF FIGURES

<u>Figure</u>	<u>Page</u>
2.1 (A) Average precipitation that occurred each month over the study period (October, 2007 – August, 2010).....	35
2.2 A photograph of the terracosms in an open field in Corvallis, Oregon, and a drawing illustrating the enclosed aboveground chamber, underlying lysimeter, and irrigation system.....	36
2.3 (A) Time series of temperature on days of the year 1 through 3 and 183 through 185 under ambient temperature, symmetric warming, and asymmetric warming.....	37
2.4 (A-C) Cumulative ET during spring (March 1 <sup>st</sup> until cessation of recharge), summer (time following spring until September 30 <sup>th</sup> ), and spring and summer combined for 2008, 2009, and 2010.....	38
2.5 (A) Monthly ET (bars) and reference ET <sub>o</sub> (lines) during March through September of 2008 and 2009, and during March through July of 2010.....	39
2.6 (A) Daily P from October 1, 2007 through July 31, 2010.....	40
2.7 The cumulative P (beginning October 1 <sup>st</sup> ) required to initiate 1 mm d <sup>-1</sup> of R during the fall season of each year.....	41
2.8 Cumulative R for the fall (November - December), spring (March 1 <sup>st</sup> until the cessation of R), and the complete water year for 2007 through 2010.....	42
3.1 (A) Time series of precipitation and recharge for each lysimeter from February 28 <sup>th</sup> to March 19 <sup>th</sup> , 2012.....	73
3.2 (Row 1) Time series of observed precipitation and recharge, and simulated effective precipitation and recharge using the TRANSEP approach for L1bs, L1g, and L10 (columns 1, 2, and 3, respectively).....	74
3.3 Time series of cumulative precipitation and modified time series of cumulative precipitation based on varying levels of assumed interception loss (combined water storage and evaporation from the plant canopy).....	76
3.4 Observed and simulated recharge under bare soil (L1bs), and simulated recharge driven by precipitation time series that were modified to reflect varying magnitudes of interception loss from a plant canopy.....	77

LIST OF FIGURES (Continued)

<u>Figure</u>	<u>Page</u>
3.5 Time series of the hydraulic gradient occurring from the soil surface to the base of the soil profile during the rainfall-recharge event occurring from March 12 <sup>th</sup> through March 14 <sup>th</sup> , 2012.....	78
4.1 Exemplary shapes of the dispersion model (equation 4.3) used as a transit-time distribution function given a constant mean-transit time, T, of 50 days and a range of D/vx values that indicate varying relative contributions of diffusive versus advective transport.....	99
4.2 Measured rates of weekly precipitation and calculated rates of effective precipitation (i.e. precipitation that contributes to recharge) for each lysimeter, based on equations 4.4-4.6.....	100
4.3 Boxplots showing the median, inter-quartile range, 10 <sup>th</sup> and 90 <sup>th</sup> (whiskers) and 5 <sup>th</sup> and 95 <sup>th</sup> (dots) percentiles of the posterior distribution of the parameter space for the mean-transit time, T, and the parameter D/vx for each lysimeter.....	101
4.4 (Left) Time series of the $\delta^{18}\text{O}$ composition of effective precipitation for the bare soil and grassland-covered lysimeters during the 2011-2012 water year.....	102
4.5 Volumetric water content at 0.05, 0.15, and 0.75 m soil depth within each lysimeter .....	103
4.6 Time series of recharge from each lysimeter during the 2011-2012 water year.....	104

## LIST OF TABLES

<u>Table</u>	<u>Page</u>
3.1 (A) Summary of storm characteristics and recharge response observed in L1bs, L1g, and L10, including recharge to precipitation ratios and the fraction of recharge that was contributed by event water (simulated using TRANSEP and calculated using a two-component mixing model with error bounds in parentheses).....	75
3.2 Total precipitation and interception loss from the L1g (0.9 - >2 year-old grassland) and L10 (>7-year-old grassland at the time of measurement) during six storms.....	79

## LIST OF APPENDIX FIGURES

<u>Figure</u>	<u>Page</u>
A1.1 Diagram illustrating the components of the new sample-acquisition system and site of field-deployment: 1) sketch of the custom manifold, 2) photo of manifold mounted to sample tray of a CTC LCPAL auto-sampler, with four incoming sample lines and outgoing waste line, 3) LGR Liquid Water Isotope Analyzer, 4) photograph illustrating the flow path from the four-channel peristaltic pump to the sample inflow ports on the base of the manifold, 5) precipitation collector, 6) vinyl tubing connecting each water source to the peristaltic pump, 7) tipping bucket gages, 8) lysimeter with bare soil surface, 9) lysimeter with grassland vegetation.....	128
A2.1 Measured moisture retention curves for the soil layers installed at 0-20 and 80-100 cm depth within the lysimeters.....	132
A2.2 Measured and simulated recharge that occurred under the bare soil condition (L1bs) in response to precipitation on March 12 <sup>th</sup> through March 14 <sup>th</sup> , 2012.....	133

## DEDICATION

My hard work would not have been enough to complete this dissertation; it also required enormous and unconditional support from my wife, Lauren. I dedicate this effort to her.

## **1. INTRODUCTION**

## 1.1 Introduction

The terrestrial hydrologic cycle is linked to many ecological processes, but we currently lack a complete mechanistic understanding of the interactions and feedbacks between these two domains. This knowledge gap limits our ability to fully describe and quantify the timing, magnitude, and characteristic time scales of water flows in the environment. Measurements of precipitation and net-radiation at the land surface enable reasonably accurate prediction of long-term water-balance partitioning over large spatial scales [*Budyko*, 1974; *Milly*, 1994; *Milly and Dunne*, 2002], based on the thermodynamics of latent and sensible heat exchange at the land surface and the conservation of mass. Yet, water-balance partitioning within specific ecosystems, and over shorter times scales (e.g. seasons), becomes much less predictable because of the many confounding physical and physiological influences of vegetation [*Donohue et al.*, 2007].

Plant canopies intercept precipitation and dramatically alter the amount and pathway of water that actually reaches the ground [*Crockford and Richardson*, 2000]; their leaf area, leaf-level physiological traits, rooting depth and architecture collectively influence the amount and timing of transpiration [*Katul et al.*, 2012; *Thompson et al.*, 2011]; and as reagents of physical change within the soil, plant roots can alter soil-hydraulic properties that influence infiltration versus runoff at the soil surface [*Thompson et al.*, 2010] and perhaps flow processes occurring at greater depth within the soil [*Angers and Caron*, 1998; *Ghestem et al.*, 2011]. Describing and quantifying these vegetation effects on the terrestrial water balance—and feedback mechanisms between vegetation, soils, and local climate—has become a focal point for research in ecohydrology [*Eagleson*, 2002], and for better understanding the potential impacts of climate change on the hydrologic cycle [*Porporato et al.*, 2004].

One research frontier in ecohydrology and climate-change science is to better understand how the evapotranspiration response to intra-annual variability and long-term changes in climate will affect less observable water flows belowground, such as groundwater recharge and subsurface stormflow. Soil-water storage is the nexus between these above- and below-ground flows [*Rodriguez-Iturbe et al.*, 1999]. The amount and

vertical distribution of root water uptake controls spatial and temporal trends of soil-water storage, which has a direct effect on groundwater recharge and runoff by setting antecedent soil-moisture conditions prior to storms, and by modifying hydraulic gradients that control the redistribution of infiltrated soil-water back to the atmosphere or toward the water table. While this ecohydrological link is understood qualitatively, rarely can we observe and quantify interactions between above- and below-ground water flows and soil moisture dynamics in open environmental systems because state variables and boundary conditions are often unknown or very difficult to measure, and experimental manipulation of hydroclimatic drivers may be impossible.

Another frontier in ecohydrology is to develop new understanding of what observed vegetation patterns aboveground can tell us about magnitudes and time-scales of water flow belowground (e.g. [Hwang *et al.*, 2012]). Better mechanistic understanding of ecohydrological controls on subsurface flow processes would improve our ability to predict the hydrological impacts of land-use and environmental change. Studies have shown a variety of mechanisms by which plants modify the physical and hydraulic properties of soils they inhabit [Angers and Caron, 1998, Jarvis, 2007] such that infiltration rates at the soil surface are enhanced. This ecohydrological process has been shown to mediate the partitioning of rainfall between infiltration and rapid runoff in arid environments [Thompson *et al.*, 2010] and under different land-use practices [Price *et al.*, 2010]. However, little work has been done to track the fate of this water belowground. Whether plant alteration of soil hydraulic properties is an ecohydrological mechanism that influences the magnitude of other soil-water balance components, such as groundwater recharge, and the characteristic transit-times of soil-water is unknown.

Transit times of water flow through the subsurface are of interest because their mean and distribution describe the complexity of flow-path lengths and flux rates of water molecules that enter soil as precipitation and ultimately contribute to groundwater recharge and streamflow. These transit-times also have biogeochemical significance as they influence the timing and magnitude of solute export from soils and catchments [van der Velde *et al.*, 2010]. Transit-time analyses have been advanced through improved capabilities for measuring environmental tracers (e.g. stable isotopes) and through the application of parsimonious transit-time-distribution models that rely on measured data

and typically only one to three parameters [Maloszewski and Zuber, 1982]. This approach has enabled the estimation of mean-transit times and transit-time distributions of baseflow from a range of catchments (reviewed by [McGuire and McDonnell, 2006]), and a small representation of soil types [Maloszewski *et al.*, 2006; Stumpp *et al.*, 2009a; Stumpp *et al.*, 2007; Stumpp *et al.*, 2009b], although the specific impacts of vegetation establishment and growth on soil-water transit times has not been systematically examined.

At the field and whole-catchment scale, investigations of ecohydrological controls on water balance partitioning and transit-times are challenging because variable-boundary conditions (e.g. whole-catchment precipitation or evapotranspiration) are often unknown or immeasurable, and experimental manipulations cannot be introduced. Small-scale laboratory experiments alleviate many of these challenges, and allow for specific environmental variables to be isolated, though new challenges are confronted regarding the scale-dependence of observed processes [Kleinhans *et al.*, 2010]). Mesoscale experiments—representing some scale between soil-cores on a lab bench and entire catchments—have proven useful for improving our mechanistic understanding of how ecohydrological processes mediate fluxes of water, carbon, and energy in response to experimental hydroclimatic treatments [Wu *et al.*, 2011]. This dissertation leverages a mesoscale experimental facility—the Terracosm experiment—to test some fundamental hypothesis about ecohydrological mechanisms that may influence soil-water budget partitioning and transit times of subsurface flow. Specifically, it addresses questions about how climate change impacts evapotranspiration, and what are the subsequent effects on soil-moisture dynamics and groundwater recharge, and it examines how the establishment and aggradation of plant communities may alter the time-scales of subsurface flow over daily to seasonal times scales, and the associated effects on overall water-budget partitioning.

### *1.11 Description of chapters*

In Chapter 1 I examine the question of how projected increases in average-annual temperature influence evapotranspiration, and what are the subsequent impacts on soil-moisture dynamics and potential groundwater recharge. I hypothesize that warming will

cause a shift in the water budget to greater evapotranspiration and reduced groundwater recharge, and test this hypothesis using the Terracosm experiment—a manipulative experiment including 12 above-ground sunlit climate-controlled chambers with underlying soil-filled lysimeters. The terracosms enable continuous monitoring of the combined responses of evapotranspiration, soil moisture, and potential groundwater recharge to a 3.5°C temperature increase in grassland ecosystems in a Mediterranean climate. The temperature manipulations are applied symmetrically throughout the day, and asymmetrically such that daily minimum temperatures are 5°C greater than ambient and daily maximum temperatures were only 2°C greater than ambient.

In Chapter 2 I utilize a series of three lysimeters with surface conditions that include bare soil and grassland ecosystems ranging in age from one to six years to evaluate the potential influence of aggrading vegetation on subsurface flow. Specifically, I address whether growth and establishment of grassland vegetation alters the time-scales of water transport through soils during storm events, and if there is an associated impact on potential groundwater recharge rates. Each lysimeter contains the same soil material and experiences the same hydroclimatic conditions, allowing me to isolate the specific impact of vegetation. Based on well-documented mechanisms by which root systems alter soil structural and hydraulic properties, I hypothesize that rapid transport of infiltrating water through the soil profile will be enhanced with aggrading vegetation, leading to greater rates of groundwater recharge during individual storms.

In Chapter 3 I utilize the same series of lysimeters to further investigate how potential plant effects on soil properties and soil-moisture dynamics influence transit times of water flow across the entire water year. I use measured time series of precipitation and recharge fluxes and stable-isotope tracers spanning the entire water year (or longer), and a linear-time-invariant convolution approach to modeling the observed time series of stable-isotopes in recharge. The modeling approach allows me to estimate mean-transit times and transit-time distributions for each lysimeter. The effects of aggrading vegetation on transport time scales are evaluated through comparative analysis of model results and parameters.

## 1.2 References

Angers, D. A., and J. Caron (1998), Plant-induced changes in soil structure: Processes and feedbacks, *Biogeochemistry*, 42(1-2), 55-72.

Budyko, M. I. (1974), *Climate and Life*, 508 pp., Academic, New York.

Crockford, R. H., and D. P. Richardson (2000), Partitioning of rainfall into throughfall, stemflow and interception: effect of forest type, ground cover and climate, *Hydrol. Process.*, 14(16-17), 2903-2920.

Donohue, R. J., M. L. Roderick, and T. R. McVicar (2007), On the importance of including vegetation dynamics in Budyko's hydrological model, *Hydrol. Earth Syst. Sci.*, 11(2), 983-995.

Eagleson, P. S. (2002), *Ecohydrology: Darwinian expression of vegetation form and function*, Cambridge University Press, Cambridge, UK.

Ghestem, M., R. C. Sidle, and A. Stokes (2011), The Influence of Plant Root Systems on Subsurface Flow: Implications for Slope Stability, *Bioscience*, 61(11), 869-879.

Hwang, T., L.E.Band, J.M. Vose, C. Tague, (2012), Ecosystem processes at the watershed scale: hydrologic vegetation gradient as an indicator for lateral hydrologic connectivity of headwater catchments, *Water Resources Research*, 48.

Jarvis, N. J. (2007), A review of non-equilibrium water flow and solute transport in soil macropores: principles, controlling factors and consequences for water quality, *Eur. J. Soil Sci.*, 58(3), 523-546.

Katul, G. G., R. Oren, S. Manzoni, C. Higgins, and M. B. Parlange (2012), Evapotranspiration: A process driving mass transport and energy exchange in the soil-plant-atmosphere-climate system, *Rev. Geophys.*, 50(3), RG3002.

Kleinhans, M. G., M. F. P. Bierkens, and M. van der Perk (2010), HESS Opinions On the use of laboratory experimentation: 'Hydrologists, bring out shovels and garden hoses and hit the dirt', *Hydrol. Earth Syst. Sci.*, 14(2), 369-382.

Maloszewski, P., and A. Zuber (1982), Determining the turnover time of groundwater systems with the aid of environmental tracers. 1. Models and their applicability, *J. Hydrol.*, 57(3-4), 207-231.

- Maloszewski, P., S. Maciejewski, C. Stumpp, W. Stichler, P. Trimborn, and D. Klotz (2006), Modelling of water flow through typical Bavarian soils: 2. Environmental deuterium transport, *Hydrological Sciences Journal-Journal Des Sciences Hydrologiques*, 51(2), 298-313.
- McGuire, K. J., and J. J. McDonnell (2006), A review and evaluation of catchment transit time modeling, *J. Hydrol.*, 330(3-4), 543-563.
- Milly, P. C. D. (1994), Climate, Interseasonal Storage of Soil-Water, and the Annual Water-Balance, *Adv. Water Resour.*, 17(1-2), 19-24.
- Milly, P. C. D., and K. A. Dunne (2002), Macroscale water fluxes - 2. Water and energy supply control of their interannual variability, *Water Resources Research*, 38(10), 9.
- Porporato, A., E. Daly, and I. Rodriguez-Iturbe (2004), Soil water balance and ecosystem response to climate change, *American Naturalist*, 164(5), 625-632.
- Price, K., C. R. Jackson, and A. J. Parker (2010), Variation of surficial soil hydraulic properties across land uses in the southern Blue Ridge Mountains, North Carolina, USA, *J. Hydrol.*, 383(3-4), 256-268.
- Rodriguez-Iturbe, I., A. Porporato, L. Ridolfi, V. Isham, and D. R. Cox (1999), Probabilistic modelling of water balance at a point: the role of climate, soil and vegetation, *Proc. R. Soc. London Ser. A-Math. Phys. Eng. Sci.*, 455, 3789-3805.
- Stumpp, C., W. Stichler, and P. Maloszewski (2009a), Application of the environmental isotope delta O-18 to study water flow in unsaturated soils planted with different crops: Case study of a weighable lysimeter from the research field in Neuherberg, Germany, *J. Hydrol.*, 368(1-4), 68-78.
- Stumpp, C., P. Maloszewski, W. Stichler, and S. Maciejewski (2007), Quantification of the heterogeneity of the unsaturated zone based on environmental deuterium observed in lysimeter experiments, *Hydrological Sciences Journal-Journal Des Sciences Hydrologiques*, 52(4), 748-762.
- Stumpp, C., P. Maloszewski, W. Stichler, and J. Fank (2009b), Environmental isotope (delta O-18) and hydrological data to assess water flow in unsaturated soils planted with different crops: Case study lysimeter station "Wagna" (Austria), *J. Hydrol.*, 369(1-2), 198-208.
- Thompson, S. E., C. J. Harman, P. Heine, and G. G. Katul (2010), Vegetation-infiltration relationships across climatic and soil type gradients, *J. Geophys. Res.-Biogeosci.*, 115.

Thompson, S. E., C. J. Harman, A. G. Konings, M. Sivapalan, A. Neal, and P. A. Troch (2011), Comparative hydrology across AmeriFlux sites: The variable roles of climate, vegetation, and groundwater, *Water Resources Research*, 47.

van der Velde, Y., G. H. de Rooij, J. C. Rozemeijer, F. C. van Geer, and H. P. Broers (2010), Nitrate response of a lowland catchment: On the relation between stream concentration and travel time distribution dynamics, *Water Resources Research*, 46.

Wu, Z. T., P. Dijkstra, G. W. Koch, J. Penuelas, and B. A. Hungate (2011), Responses of terrestrial ecosystems to temperature and precipitation change: a meta-analysis of experimental manipulation, *Glob. Change Biol.*, 17(2), 927-942.

**2. RAINFALL SEASONALITY AND AN ECOHYDROLOGICAL FEEDBACK  
OFFSET THE POTENTIAL IMPACT OF CLIMATE WARMING ON  
EVAPOTRANSPIRATION AND GROUNDWATER RECHARGE.**

Luke A. Pangle

Jillian W. Gregg

Jeffrey J. McDonnell

In Review *Water Resources Research*

350 Main Street, Malden, MA 02148

## 2.1 Introduction

Empirical evidence suggests that detectable intensification of the hydrologic cycle has occurred over the last several decades, whereby long-term records of evapotranspiration, specific humidity, precipitation and runoff show increasing trends at global [Huntington, 2006] and continental scales [Groisman *et al.*, 2004]. These changes are correlated with increases in air temperature, and raise questions about the potential impact of future climate warming on the terrestrial hydrologic cycle. However, at regional and sub-regional scales these trends vary qualitatively and quantitatively, or may be unapparent [Groisman *et al.*, 2004]. Other components of the hydrologic cycle (e.g. groundwater recharge) are critical in some ecosystems, but their response to past climate variability has been poorly monitored, and their potential response to future climate warming remains uncertain [Green *et al.*, 2011]. The interactions and feedbacks between local climate, vegetation, and soils may strongly influence how future climate warming alters water fluxes in specific ecosystems, yet these interactions and feedbacks are poorly understood [Norby and Luo, 2004; Wu *et al.*, 2011].

So what projections can be made about the impact of future climate warming on the annual water budget in specific ecosystems? An intuitive hypothesis is that warmer air temperatures would enhance evapotranspiration by increasing incoming long-wave radiation and increasing the vapor-pressure gradient from the land surface to the atmosphere. If there is no change in total precipitation, then to conserve mass, an increase in evapotranspiration should cause a reduction in groundwater recharge and direct runoff. This has been the underlying hypothesis for many water budget models to date. For example, Budyko [1974] postulated that the ratio of average-annual evapotranspiration to precipitation for large basins is controlled by an aridity index (based on temperature and the surface energy balance), and that the remaining fraction of average-annual precipitation contributes to runoff (including surface and groundwater contributions to river discharge, and assuming water storage in the landscape was constant over long time periods). Budyko developed a quantitative model based on these principles that provided a good fit to calculated values of these ratios for many catchments, and thus provided a framework for evaluating the climate-sensitivity of the

annual water budget through inter-basin comparison. However, subsequent analyses of this hypothesis revealed a systematic error; catchments in which precipitation was seasonal, and temporally out of phase with temperature, commonly had greater runoff and less evapotranspiration than predicted [Milly, 1994]—highlighting the important influence that local precipitation regimes may have on the overall water budget response to changing temperature [Luo *et al.*, 2008; Porporato *et al.*, 2004; Wu *et al.*, 2011].

The singular use of climatic indices for projecting the water budget response to climate warming may also be compromised at intra-annual time scales because this approach does not account for seasonal regulation of transpiration by plant stomata that can result from phenological change and insufficient soil water [Donohue *et al.*, 2007]. For example, in Mediterranean climates maximum-daily temperatures during the summer co-occur with daily evapotranspiration rates that may be well below maximum due to a limited soil water supply. Peak photosynthesis in these systems occurs during the spring [Ma *et al.*, 2007; Phillips *et al.*, 2011], when high evapotranspiration may also reduce soil-water storage and inhibit groundwater recharge during precipitation events. Each of these fluxes can vary widely among years due to climate variability [Montaldo *et al.*, 2008; Pumo *et al.*, 2008; Viola *et al.*, 2008] and associated changes in the timing of peak physiological activity [Ma *et al.*, 2007; Phillips *et al.*, 2011].

Despite theoretical expectations of increased evapotranspiration and reduced groundwater recharge and runoff in response to warmer temperatures, experimental examination of this problem has been lacking. Accurate measurement of the terrestrial hydrologic cycle continues to be a major challenge for hydrologists [Beven, 2006] and catchment-sized units that are used in observational studies of hydrological processes are beyond the spatial scale accessible for experimental control and manipulation. Small-scale manipulative experiments have improved our understanding of how some water budget components respond to projected temperature increases associated with global climate warming [Bell *et al.*, 2010b; De Boeck *et al.*, 2006; Dermody *et al.*, 2007; Fay *et al.*, 2002; Morgan *et al.*, 2004; Zavaleta *et al.*, 2003a; Zavaleta *et al.*, 2003b]. However, these studies have not captured the entire water budget; most often they omit subsurface flow processes, such as groundwater recharge, which is potentially the most important water budget component for consumptive water use by humans. Subsurface water flow is

not directly controlled by air temperature, however, evapotranspiration and groundwater recharge are interdependent, since both fluxes depend on soil moisture [Porporato *et al.*, 2004; Rodriguez-Iturbe *et al.*, 1999]. To date, there is little experimental evidence to suggest how climate-induced changes in evapotranspiration could affect groundwater recharge [Green *et al.*, 2011; Kundzewicz *et al.*, 2007, Taylor *et al.*, 2012].

Here we present a mesocosm experiment that examines how projected climate warming impacts evapotranspiration, soil moisture, and groundwater recharge in a grassland ecosystem experiencing a Mediterranean rainfall regime in the Pacific Northwest region of the USA. Average annual temperature in this region is projected to increase by 3.0°C by the year 2080, with no significant change in annual precipitation, based on the mean simulation results from an ensemble of 19 Global Climate Models driven by three CO<sub>2</sub> emissions scenarios [Mote and Salathe, 2010]. We focus on three main objectives: (1) to quantify how increased temperature affects seasonal and annual evapotranspiration, (2) to contrast the relative influence of warming-induced changes in physical factors (i.e. temperature and vapor-pressure deficit) and changes in the timing of ecological effects (i.e. peak-plant-physiological activity) on the evapotranspiration response, and (3) to quantify how warming-induced changes in evapotranspiration influence seasonal and annual groundwater recharge. We hypothesized that (1) increased temperature would increase annual evapotranspiration, specifically due to greater evapotranspiration occurring earlier in the spring season, (2) warming-enhanced evapotranspiration would reduce groundwater recharge during the spring due to lower soil moisture prior to precipitation events, and (3) warming-enhanced evapotranspiration would cause lower soil moisture preceding the onset of the rain season, thus requiring greater total precipitation to initiate recharge. The combined result of 2 and 3 would be an overall reduction of recharge at the annual time scale.

## **2.2 Materials and Methods**

### *2.2.1 Climate*

This work was conducted at the Terracosm facility (<http://www.teraglobalchange.org>) that is located in Corvallis, OR, USA (44.57, -123.29;

77 m.a.s.l.). The climate is ‘wet Mediterranean’ with mild temperatures and seasonal precipitation. Average temperature is 4.1°C in January and 19°C in August. Average annual precipitation is 1085 mm and is almost entirely rainfall (Hyslop Farm Climate Station; <http://cropandsoil.oregonstate.edu/hyslop/handbook>). The majority of rainfall occurs during the winter months with a prolonged dry period during the summer (Figure 1A). Rainfall intensity is low—rates of 3 mm h<sup>-1</sup> or less occurred during more than 90% of the hours with any recorded rainfall during the study period (Figure 1B).

### 2.22 Site Description

The Terracosm facility consists of twelve sun-lit climate-controlled chambers (hereafter referred to as terracosms). Each terracosm covers a flat-ground-surface area of 2 m<sup>2</sup> (1 x 2 m); the height ranges from 1.5 – 1.7 m along a sloping roof with a southerly aspect. The terracosms have an aluminum frame with three walls and a roof made of clear Teflon film, and a north-facing wall made of Plexiglas (Figure 2). They are essentially closed systems, though the chamber front and control valves are opened periodically to aid with climate control. A 2.3 m<sup>3</sup> polypropylene tank underlies each terracosm and acts as a non-weighing lysimeter. The lysimeter depth ranges from 1 – 1.3 m along a sloping base that enables drainage. The lysimeters were insulated (0.15 m of foam insulation, R value 60) and placed within larger steel containment structures in the soil.

The lysimeters were filled with soil that was excavated from a nearby prairie that had previously been undeveloped park lands. The soil is in the Dixonville series—moderately deep, well drained soils formed in clayey colluvium and basalt-derived residuum [Survey, 2012]. The soil was excavated during the summer of 2005 in five 0.2 m depth increments and large materials were removed using a 0.0245 m sieve. Particle size analysis using the pipette method [Gee and Bauder, 1986] showed that the textural class was silty clay loam at 0 – 0.6 m depth (29 – 38% clay), silt loam at 0.6 – 0.8 m depth (26% clay), and loam at 0.8 – 1.0 m depth (23% clay). Pea gravel was used to fill the base of the lysimeter and to provide a flat surface, and a layer of landscaping cloth was placed on top of the pea gravel to minimize root growth into the gravel and lysimeter

plumbing. Soils were then back-filled into the terracosms and packed using a uniform tamping procedure for each increment, yielding a soil profile with one meter depth.

Three annual forbs, eight perennial forbs, and three perennial grass species were planted in each terracosm to simulate a plant assemblage that resembled natural grasslands found in Oregon's Willamette Valley. Plants were started in a greenhouse during the summer of 2005, left over winter in a lath house, and transplanted into the terracosms after the last frost during April, 2006. Sixteen individuals of each species were transplanted into each terracosm in a randomized design that was replicated between terracosms. The plants grew on the repacked soils for one year under ambient environmental conditions before the chamber tops were installed and temperature treatments initiated on April 17, 2007. Here we report on data collected from October 1, 2007 until a temporary cessation of temperature treatments on July 26, 2010.

### *2.23 Climate Control and Experimental Treatments*

The terracosms' interior climate was monitored and controlled at a one-minute frequency. Detailed descriptions of the climate control features have been published previously [*Phillips et al.*, 2011; *Tingey et al.*, 2000]; here we summarize the controls most relevant to the hydrological processes being studied. Three temperature treatments were imposed (n=4 per treatment). The ambient-temperature treatment maintained the same temperature as measured at an adjacent climate station; the symmetric-warming treatment maintained a temperature that was constantly 3.5°C greater than ambient; and the asymmetric warming treatment maintained a temperature that was, on average, 3.5°C greater than ambient, though the minimum dawn temperature was 5°C greater than ambient, while the maximum midday temperature was only 2°C greater (Figure 3A). Soil warming occurred through heat transfer from the temperature-controlled airstream within the terracosm. The air was warmed with a thermal radiator and cooled with a chilling radiator that were located inside an air-handler system.

Air was continuously circulated through the terracosms, resulting in an approximate wind speed of 0.3 m s<sup>-1</sup> [*Tingey et al.*, 2000]. Relative humidity (RH) inside the terracosms was measured with Vaisala HMT337 relative humidity sensors (Vaisala, Inc.) and [CO<sub>2</sub>] was monitored with infrared gas analyzers (LI-6262, LI-COR, Inc.).

Relative humidity and  $[\text{CO}_2]$  were controlled to match ambient conditions measured at the adjacent climate station, and were maintained at the same levels between temperature treatments. Hence, absolute humidity was greater inside terracosms receiving warming treatments. The vapor-pressure deficit was, on average, 25% greater under both warming treatments than under ambient temperature. Under asymmetric warming, this relative difference varied with temperature, often exceeding 30% during the pre-dawn hours and dropping below 20% during the afternoon (Figure 3B).

#### *2.24 Measurement and Calculation of Water Budget Components*

Natural precipitation was captured as it fell on the terracosm roofs and routed to a closed container. After approximately 2 L (1 mm depth equivalent) accumulated the water was pumped through a roof-mounted sprinkler system with six low-pressure sprinkler heads over the following 40-60 seconds. The precipitation amount (P) was calculated as the product of the pump run time (s) and a calibration value ( $\text{L s}^{-1}$ ), then converted to units of depth (mm) by dividing by the  $2 \text{ m}^2$  soil-surface area. The system was calibrated approximately monthly.

Five TDR probes (CS610, Campbell Scientific, Inc.) were installed horizontally in each lysimeter during soil packing, at depths of 0.05, 0.15, 0.35, 0.55, and 0.75 m below the soil surface. Volumetric water content ( $\theta$ ) was measured at each probe location at a 36-minute interval using a Tektronix 1502b TDR Cable Tester (Tektronix, Inc.) that was operated in conjunction with a Campbell CR10 Data Logger and SDMX50 Coax Multiplexer. Three types of error were apparent in the  $\theta$  time series: 1) sporadic measurements that deviated beyond realistic values of  $\theta$ , 2) values that deviated from preceding  $\theta$  values by margins that would not occur realistically during rainfall infiltration and drying, and 3) periods when  $\theta$  values became static due to equipment malfunction. Any  $\theta$  values greater than 0.5, or less than 0.1, were omitted from the dataset because the vast majority of  $\theta$  values at all soil depths, and for all individual sensors, demonstrated that  $\theta$  normally remained within these limits. Any  $\theta$  measurement that differed from the previous or following value by more than 0.05 was omitted from the dataset. The 0.05 threshold was chosen because we observed that differences between subsequent measurements rarely exceeded 0.05 even following intense rainfall,

and a frequency distribution and box plot both showed these differences were normally distributed with a mean ( $\mu$ ) of zero and standard deviation ( $\sigma$ ) of 0.032, and that differences between consecutive measurements were less than 0.05 94% of the time. Any  $\theta$  values that differed from the mean of those measured at the same depth and time in the other eleven terracosms by more than  $|2\sigma|$  ( $n=11$ ) were considered outliers, and omitted. To account for short periods when  $\theta$  measurements were static due to equipment malfunction, any sequence of identical measurements occurring over three hours or more were omitted from the dataset. Identical consecutive measurements were clearly apparent because the numerical  $\theta$  values generated by the TDR system included more than five decimal places.

Average-daily  $\theta$  was calculated for each probe based on these edited short-term data (36-minute interval, 60 total probes). Among the 60 total probes, 7.5 – 91% of the average-daily values were missing due to the data omissions described above. Fifty-two of the 60 probes had 33% or less of the daily values missing, while 4 probes had greater than 50% of daily values missing. Least-squares regression functions were used to fill in the gaps in the dataset and create complete time series of average-daily  $\theta$  for each probe. A function was formulated between daily  $\theta$  values for each probe (dependent variable), and the average of the daily  $\theta$  values for each probe occupying the same soil depth and receiving the same temperature treatment ( $n=3$ , independent variable). Linear functions provided the best fits, though a second-order polynomial or exponential function helped eliminate bias in the residuals in a few cases. The coefficient of determination for all fitted functions was 0.90 or greater.

Total volumetric water content of the entire soil volume ( $\theta_{\text{tot}}$ ) was estimated at a daily time-step using a weighted average of the daily  $\theta$  values for each probe:

$$\theta_{\text{tot}} = 0.1\theta_5 + 0.15\theta_{15} + 0.2\theta_{35} + 0.2\theta_{55} + 0.35\theta_{75} \quad (1)$$

where the subscripts on the right-hand side of the equation indicate the TDR probe depth. The weighting coefficients represent the fraction of the total soil volume that each probe was assumed to represent.

The lysimeter drainage was used as a proxy for potential groundwater recharge (R). We extracted soil cores from each terracosm once annually, and found less than 10% of total root biomass at 0.8 – 1 m soil depth, which was similar to vertical root

distributions reported by Schenk and Jackson [2002] for multiple prairie ecosystems. Hence, even if the soil profile were extended to greater depth, it is not likely that water draining beyond one meter depth would be taken up by plant roots in this ecosystem. Soil-water that percolated to the sloped base of the lysimeters drained through an exit pipe to a tipping-bucket gauge where it was measured in 0.004 mm increments. The tipping-bucket gauges were calibrated approximately monthly during the study period. No R data are reported from January 2010, due to equipment replacement during that time. Errors existed in the R dataset due to occasional clogs in the outflow pipe and equipment failure. These errors were manually removed using a written record of equipment failure that was maintained throughout the experiment. Linear interpolation was used to fill most of the data gaps. If the data gap was too long to be filled the data from that terracosm did not contribute to the treatment average for that season or year.

Evapotranspiration (ET) was calculated on a monthly and seasonal basis (seasons defined in Section 2.6 below) as the residual component of the water balance (i.e.  $ET = P - R - \Delta S$ ), where P and R represent cumulative-monthly or seasonal precipitation and groundwater recharge, respectively. The  $\Delta S$  was calculated as the difference between  $\theta_{tot}$  on the last day of the month and the last day of the previous month, or the last day of the season and the day prior to the beginning of that season. Most of the  $\theta_{tot}$  values used to calculate  $\Delta S$  relied on interpolated data for at least one of the five TDR probes. However, 90% of these  $\theta_{tot}$  values relied on interpolated data for only two, or less, of the five probes utilized in equation 1. Hence, the interpolation scheme used to replace missing daily  $\theta$  values did not unduly influence the  $\Delta S$  and ET calculations because the correlations used were strong, and the  $\theta_{tot}$  calculations relied mostly on actual measured data. The slow rate of infiltration and the delayed R response to P events prevented the calculation of ET using the water budget approach at the daily time scale, and lead to unrealistic ET values at the monthly timescale during winter months due to the frequency of P events. Hence, we limited our ET calculations to the months of March through September, which is also the time most relevant to address our hypotheses.

### *2.25 Calculation of Reference Evapotranspiration*

To approximate the potential influence of symmetric and asymmetric warming on grassland ET we calculated reference evapotranspiration ( $ET_o$ ) for each temperature treatment. These estimates reflect the physical influence of temperature and vapor-pressure deficit (VPD) (Figure 3) in the absence of water limitation. Reference ET was calculated at an hourly time-step using a standardized form of the Penman-Monteith model as outlined by Allen et al. [1998]. This approach utilized aerodynamic and surface resistance terms that represent a uniform grass canopy of 0.12 m height that is well watered [Allen et al., 1998]. The input data required for the model included solar radiation, temperature, relative humidity, and local latitude and longitude. Hourly solar radiation data from a pyranometer (LI-200, LI-COR, Inc.) were obtained from the Agrimet climate station (<http://www.usbr.gov/pn/agrimet/agrimetmap/crvoda.html>) located approximately 10.5 kilometers northeast of our study site. The temperature and relative humidity data were those measured within the terracosms.

### 2.26 Data Analysis

We used a single-factor analysis of variance (ANOVA) to test for the effect of temperature on ET and R. We also included a block effect in the ANOVA model, and used the Brown-Forsythe test [Kutner et al., 2005] to confirm the assumption of equal variances among treatment groups. Temperature and block were treated as fixed effects. We tested for differences in cumulative ET among treatments during the “hydrological spring” (hereafter referred to as spring), which we defined as the period from March 1<sup>st</sup> until the last day during which R was greater than zero for at least one temperature treatment; the “hydrological summer” (hereafter referred to as summer), defined as the period from the cessation of R until September 30<sup>th</sup>; and for the combined spring and summer period. The last day during which R was greater than zero (i.e. the last day of spring for our purpose) wasn’t exactly the same among treatments in some years. However, any additional R that occurred after the specified date was negligible for any treatment (0.1 mm or less). We tested for differences in cumulative R during the initial recharge period during the fall (November – December), during the spring, and for the entire water year (October 1<sup>st</sup> – September 30<sup>th</sup>). Gaps in the ET and R data due to equipment malfunction resulted in an unbalanced experimental design for some

comparisons. We accounted for this by utilizing a regression approach to ANOVA [Kutner *et al.*, 2005], whereby a “full” linear statistical model (i.e. one that contains a term describing temperature effects) is compared to a “reduced” model that omits the term describing the temperature effects. The reduced model represents the null hypothesis that temperature had no statistically significant impact on the response variable. The alternative hypothesis of a significant temperature effect is accepted if the full model accounts for a significantly greater fraction of the total variance. For any ANOVA that yielded a type-one error probability of 0.1 or less (i.e.  $p\text{-value} \leq 0.1$ ) we proceeded with Tukey’s procedure for multiple-pairwise comparisons of factor level means to specify which temperature levels were significantly different.

## 2.3 Results

### 2.3.1 Evapotranspiration

Evapotranspiration was greater under both warming treatments ( $ET_{\text{sym}}$  and  $ET_{\text{asy}}$ ) during the spring, but less during the summer, resulting in no significant difference in total ET between either warming treatment and the ambient temperature treatment ( $ET_{\text{amb}}$ ) over the combined spring and summer period (Figures 4A-C). The spring period (defined as March 1<sup>st</sup> until the cessation of R) lasted until May 14<sup>th</sup>, May 23<sup>rd</sup>, and June 15<sup>th</sup> in 2008, 2009, and 2010, respectively. Cumulative  $ET_{\text{sym}}$  and  $ET_{\text{asy}}$  during spring were, on average, 37 mm (21%) and 24 mm (12%) greater than  $ET_{\text{amb}}$ , respectively (Figures 4A-C,  $p$ -values were 0.10, 0.02, and 0.05 in 2008, 2009, and 2010, respectively).  $ET_{\text{sym}}$  was significantly greater than  $ET_{\text{asy}}$  during spring of 2008 (Tukey multiple-mean comparison,  $\alpha=0.1$ ), but not in the following years. Evapotranspiration under ambient temperature during the summer was, on average, 21 mm (9%) and 25 mm (12%) greater than  $ET_{\text{sym}}$  and  $ET_{\text{asy}}$ , respectively (Figure 4A-C,  $p$ -values were 0.0006 and 0.16 in 2008 and 2009, respectively). A similar trend was emerging during 2010, though cumulative ET for this summer period did not include the months of August and September since the temperature treatments were temporarily stopped during this period of plant dormancy. These contrasting spring and summer trends resulted in no significant difference in ET

between any temperature treatment during the combined spring and summer period (Figure 4A-C, p-value of 0.44 in 2008 and 0.61 in 2009).

Evapotranspiration increased from March through May and maximum-monthly ET occurred during May of each year (except during June, 2010, for the asymmetric warming treatment), and ET declined from May until reaching minimum-monthly totals during August (Figure 5A). Reference ET increased from March until reaching maximum-monthly totals during July—two months later than actual ET—then declined during August and September, though less rapidly than actual ET.

The warming-treatment effects on ET (i.e.  $ET_{\text{sym}} - ET_{\text{amb}}$  and  $ET_{\text{asy}} - ET_{\text{amb}}$ ) were greater than the projected effects on  $ET_o$  (i.e.  $ET_{o,\text{sym}} - ET_{o,\text{amb}}$  and  $ET_{o,\text{asy}} - ET_{o,\text{amb}}$ ) during the spring, and less during the summer (Figure 5B). In April, 2009,  $ET_{\text{sym}}$  and  $ET_{\text{asy}}$  were 21 mm and 19 mm greater than  $ET_{\text{amb}}$ , though the projected differences in  $ET_o$  were only 6 mm and 5 mm, respectively (Figure 5B). There were similar differences between the actual-and-projected-effect sizes of symmetric warming in April, 2008 and May, 2010, but less apparent differences under asymmetric warming. Averaged over three years, cumulative  $ET_{\text{sym}}$  and  $ET_{\text{asy}}$  during the spring were 37 mm (8.6) and 24 mm (6.9) greater than  $ET_{\text{amb}}$  (n=3 years,  $\sigma$  in parentheses), respectively, whereas  $ET_{o,\text{sym}}$  and  $ET_{o,\text{asy}}$  were only 16.8 mm (4.2) and 16.9 mm (7.5) greater than  $ET_{o,\text{amb}}$ . During the summer, projected  $ET_{o,\text{sym}}$  and  $ET_{o,\text{asy}}$  remained, on average, 32.1 mm (0.6) and 27.8 mm (0.6) greater than  $ET_{o,\text{amb}}$  (n=2 years), whereas actual  $ET_{\text{sym}}$  and  $ET_{\text{asy}}$  were 28 mm (7.6) and 29 mm (11.0) less than  $ET_{\text{amb}}$ , respectively (Figure 5B).

### 2.32 Soil Moisture

Volumetric soil moisture of the entire soil volume followed a seasonal cycle controlled by precipitation (Figure 6A-B). There was a transition from dry to wet conditions at the onset of precipitation in the fall, persistently wet conditions throughout the winter, and a transition from wet to dry conditions during the spring as precipitation decreased. During 2008, the minimum  $\theta_{\text{tot}}$  (calculated as average  $\theta_{\text{tot}}$  for the last seven days of September) was 0.18 (0.01), 0.17 (0.01), and 0.17 (0.01) for the ambient, symmetric, and asymmetric warming treatments, respectively; in 2009 these values were 0.17 (0.01), 0.16 (0.01), and 0.17 (0.01). During the spring,  $\theta_{\text{tot}}$  declined to lower values

earlier under symmetric and asymmetric warming than under ambient temperature. The maximum difference in  $\theta_{\text{tot}}$  between ambient and warming treatments was 0.05 and 0.04 for symmetric and asymmetric warming, respectively, and occurred in late May or early June of each year. In general, the trajectory of  $\theta_{\text{tot}}$  decline under ambient temperature lagged that observed under warming treatments by 1-2 weeks. For example, on June 1, 2009,  $\theta_{\text{tot}}$  was 0.26 and 0.27 under symmetric and asymmetric warming treatments, though  $\theta_{\text{tot}}$  under ambient temperature did not decline to 0.27 until June 16 (Figure 6B). A similar comparison beginning at July 1, 2009 showed a time lag for soil drying in the ambient chambers of eight days.

### 2.33 Groundwater Recharge

Groundwater recharge was initiated during November or December (Figure 6C). The cumulative precipitation required to initiate R was nearly identical among temperature treatments in 2007, 61 and 23 mm less under symmetric and asymmetric warming compared to ambient temperature in 2008 ( $p = 0.13$ ), and 30 and 17 mm less under symmetric and asymmetric warming compared to ambient temperature in 2009 ( $p = 0.08$ , Figure 7). These differences in cumulative precipitation typically occurred over the course of several hours during a single heavy rainstorm, and there was great variability among individual terracosms within any temperature treatment (Figure 7).

Groundwater recharge was marginally greater under both warming treatments than under ambient temperature during fall (November – December), though these differences were only significant in fall 2009 ( $p = 0.04$ , Figure 8A-C). Recharge was similar among all treatments throughout the remainder of the winter. During spring, the last large storm that caused R resulted in greater R under ambient temperature than under both warming treatments (Figure 6C). For example, average R from May 4<sup>th</sup> to May 23<sup>rd</sup>, 2009 was 16.6 (2.85), 6.35 (3.36), and 8.42 (2.30) mm under ambient temperature, symmetric warming, and asymmetric warming, respectively ( $n=4$ ;  $\sigma$  in parentheses). Similar differences were observed in June, 2010, and smaller differences in April, 2008 (Figure 6C). However, the reductions in R that occurred during these late-spring storm events had a small relative effect—they represented 4%, or less, of total annual R that occurred under ambient temperature in any year. Cumulative R over the entire spring

period was significantly reduced by warming treatments only during 2010 (Figure 8C, p-values were 0.84, 0.34, and 0.07 in 2008, 2009, and 2010, respectively). There were no significant differences in average-annual R between any temperature treatments across all three years (Figure 8A-C, p-values were 0.49, 0.22, and 0.48).

## 2.4 Discussion

Contrary to our hypothesis, we found that a 3.5°C increase in temperature did not significantly increase ET or reduce R over the entire water year. While the timing and magnitude of ET and R were affected at seasonal time scales, these effects were both positive and negative, depending on the season, resulting in no net difference in either flux at the annual time scale. In the following discussion we assess which factors are responsible for the contrasting seasonal patterns of ET and R, and how the vegetation, climate, and soils specific to this experiment affect the general inference that can be made from our results. Since cumulative seasonal fluxes were not significantly different between symmetric and asymmetric warming treatments, hereafter we discuss the general contrasts between both “warming treatments” and ambient temperature conditions.

### *2.4.1 What caused the contrasting seasonal patterns of ET observed under warming treatments versus ambient temperature?*

Evapotranspiration was greater under warming treatments than under ambient temperature during the spring (Figure 4A-C), which was consistent with our first hypothesis. The comparison of  $ET_0$  with actual ET helped to distinguish the relative importance of warming-induced changes in the physical environment (temperature and VPD) and the ecological effect of earlier peak-physiological activity by the vegetation. Specifically,  $ET_0$  provides an estimate for the potential change in ET expected in response to the warming influence on VPD in the absence of water limitation. Differences in the magnitude of the warming effect on actual ET versus  $ET_0$  then reflect the relative contribution of plant canopy growth, photosynthesis, and stomatal conductance to the overall ET response (the plant functions that dictate the resistance parameters in the Penman-Monteith model, but are held constant when estimating  $ET_0$ ).

In 2009, the warming treatments enhanced actual ET during April (relative to ambient temperature) by a margin that was two-fold greater than projected using the  $ET_0$  calculations. This discrepancy was likely due to acceleration of the timing of peak-seasonal photosynthesis that accompanied the increases in VPD. Phillips et al. [2011] showed that warming treatments accelerated the timing of peak-daily photosynthesis within the terracosc grasslands by an average of two weeks—from mid-May to late-April, 2009. In a similar Mediterranean grassland ecosystem in California, Zavaleta et al. [2003a] also showed a warming-induced acceleration in the timing of canopy greenness and the absorption of radiant energy in the photosynthetically active range. Our results, considered alongside those of Phillips et al. [2011], suggest that warming-induced changes in the timing of peak photosynthesis may have an equal, or greater, impact on ET during the spring season in Mediterranean climates than does enhanced VPD.

Evapotranspiration was drastically reduced during the summer in response to limited soil moisture, as illustrated by the stark contrast between ET and  $ET_0$  (Figure 5). The decline in ET occurred earlier under warming treatments compared to ambient temperature and paralleled similar observed declines in photosynthesis [Phillips et al., 2011]. As  $\theta$  diminishes, uptake of soil water by plants is limited, causing reductions in photosynthesis, leaf area, and the overall ET component of the water budget [Bell et al., 2010a; Bell et al., 2010b; Porporato et al., 2004; Porporato et al., 2001; Ryu et al., 2008]. In this Mediterranean climate ET increases steadily throughout the spring at the same time that the frequency and magnitude of precipitation steadily decreases. As a result of these opposing trends, soil moisture declines steadily toward a seasonal minimum value following the last spring rains. The warming treatments accelerated ET during the spring, but it came at the cost of earlier water stress and plant senescence at the onset of the summer dry period, whereas plants growing under ambient temperature were able to continue transpiring at a greater rate later into the season. This negative ecohydrological feedback caused a reduction in ET during the summer that offset the enhancement of ET that occurred during spring, resulting in no difference in total ET during the combined spring and summer period. The results of this manipulative experiment support the conclusions of Angert et al. [2005], who interpreted hemispherical-scale fluctuations in atmospheric  $[CO_2]$  and concluded that enhanced  $CO_2$

uptake by vegetation during warmer spring periods did not lead to greater CO<sub>2</sub> uptake over the entire growing season, presumably due to drought-induced reductions in photosynthetic activity during late summer.

This negative feedback may have had a secondary biophysical effect, where, despite greater temperature and VPD, the rate of bare-soil evaporation after plant senescence was too low to sustain the cumulative increase in ET that had developed under warming treatments during the spring. As the plants senesce, the transpiration component of ET would have decreased concomitant with declining rates of photosynthesis [Phillips *et al.*, 2011; Ryu *et al.*, 2008], while the fraction of ET attributable to bare soil evaporation was likely to have increased [Zhongmin *et al.*, 2009]. However, the rate of evaporation from the soil was near a water-limited-minimal rate, where evaporation from the soil surface is limited by exceedingly slow unsaturated-liquid-water flow from deeper soil layers. Additionally, senescing plant tissue has been shown to increase the albedo of the land surface in similar grasslands [Baldocchi *et al.*, 2004], and the dense mat of senesced plant tissue that remained after the growing season may have diminished advective vapor transport from the underlying soil surface by the wind, therefore inhibiting evaporation from the soil.

#### *2.42 Why were there only small seasonal reductions of R, and no reduction over the entire water year?*

We anticipated that warming-enhanced ET during the spring season would reduce pre-storm soil moisture, thereby causing a decline in R [Lehmann *et al.*, 2007; McMillan, 2012]. While there were reductions in R under warming treatments during the final large precipitation event of each spring (Figure 6C), these reductions were only a marginal fraction of R that occurred across the entire spring season. One exception was a significant seasonal effect during the spring of 2010 (Figure 8C). Differences in the timing and intensity of P—compared with the timing of soil drying—may help explain why significant warming effects on R emerged only during the spring of 2010. Total precipitation during June, 2010 was 63 mm, compared to only 15 mm in 2009 and 29 mm in 2008, and included 47 mm of cumulative P over a three-day period. This relatively intense P event was sufficient to generate R for all treatments, and occurred after the

maximum difference in  $\theta_{\text{tot}}$  had developed between the warming treatments and the ambient temperature treatment during late May. In contrast, the P events that generated the last R in 2008 and 2009 occurred during late April and early May, respectively, before the maximum treatment difference in  $\theta_{\text{tot}}$  had developed. Hence, in Mediterranean climates the impact of warmer air temperatures on R depends on the frequency and intensity of P events during the spring—high-intensity storms occurring late in the spring may generate less R in a warmer climate than similar storms occurring earlier in the spring, as the former are more likely to occur under greater pre-storm deficits in soil-water storage.

Contrary to our expectation that warming-enhanced ET would cause lower minimum  $\theta_{\text{tot}}$  at the end of the summer season [Cai *et al.*, 2009], differences in minimum  $\theta_{\text{tot}}$  were only marginally lower under warming treatments than under ambient temperature, and surprisingly, the cumulative P required to initiate R in the fall was significantly less under warming treatments in 2009 (Figure 7). Although highly variable among individual terracosms, this lower threshold P amount contributed to greater cumulative R under warming treatments during the fall, which offset the reduction of R that occurred during the following spring. While minimum  $\theta_{\text{tot}}$  at the end of the summer drought was only marginally lower under warming treatments, the duration of very low  $\theta_{\text{tot}}$  was extended more substantially. For example,  $\theta_{\text{tot}}$  was below 0.2 under warming treatments for 106-117 days in 2008 and 89-103 days in 2009, compared to only 81 and 61 days under ambient temperature. Longer periods of very low soil moisture could have increased the vertical extent of soil cracks in these clay soils, potentially enabling deeper infiltration through preferential flow processes [Jarvis, 2007] and earlier occurrence of R. This effect was recently demonstrated in agricultural soils by Sanders *et al.* [2012], though we have no direct evidence to evaluate this mechanism and can only offer it as speculation.

#### *2.43 How does the specific combination of climate, vegetation, and soil affect the general inference that can be made from this manipulative experiment?*

It is important to recognize what conditions may support, or detract from, the general inference that can be made from experiments or model simulations. We were

unable to assess potential spatial variability of the outcomes we observed, though this is undoubtedly important [Tague *et al.*, 2009; Thompson *et al.*, 2011]. The strengths of our approach included precision climate control, well-defined system boundary conditions, and the ability to simultaneously monitor the treatment response of ET,  $\theta$ , and R—capabilities that could not be matched by observational studies in the open environment—though the intensive nature of the experiment obviously limited the spatial extent and replication.

Most notably, the Mediterranean rainfall regime and associated temporal trends in soil moisture emerged as dominant influences in this study, and exerted important control over seasonal carbon fluxes as well [Phillips *et al.*, 2011]. In environments where rainfall is seasonally out of phase with temperature, the linkage between ET and temperature is less robust [Milly, 1994; Potter *et al.*, 2005; Pumo *et al.*, 2008; Viola *et al.*, 2008]. Different results might be expected in more humid environments where P occurs more uniformly throughout the year or in phase with vegetative growth, and where the frequency and intensity of rainfall determines how often plant stress may result in reduced ET [Porporato *et al.*, 2004; Porporato *et al.*, 2001].

The negative feedback mechanism of lower ET during summer resulting from greater ET during the spring under warming treatments may be unique to grassland ecosystems due to the nearly complete senescence of aboveground tissues and suppressed physiological activity during extended drought periods. Further, grassland ecosystems have been shown to have lower water use efficiency than forests, and more intensively exploit soil water when it is available [Ponton *et al.*, 2006; Teuling *et al.*, 2010]. Trees may shed part of their foliage during drought and regulate stomatal aperture to limit water loss, but water stress in trees may occur later in the season [Baldocchi *et al.*, 2004] due to their greater water use efficiency and more expansive root systems. Hence, warming-induced increases in ET during the spring may result in a greater annual total in forests, unlike the response we observed. Last, the negative feedback we observed may be unlikely in grasslands that contain C<sub>4</sub> species that demonstrate greater water-use efficiency and less susceptibility to water stress during drought [Baldocchi, 2011; Morgan *et al.*, 2011; Morgan *et al.*, 2004].

The high water-storage capacity of the silty-clay loam soils used in this experiment had important effects on the R response to warming. Green et al. [2007] completed a unique modeling analysis that examined the interactive effects of vegetation type (forest versus grassland), various soil textures, and prevailing rainfall regime (seasonal versus non-seasonal rainfall) on R. Their work identified important interactions between all three variables that ultimately determined if climate warming increased or decreased R, and to what extent. One salient finding of their work was the importance of soil texture and water storage capacity; specifically, they showed that finer textured soils consistently buffered the R response (whether positive or negative) to climate alteration and associated changes in ET, whereas more significant R responses occurred in sandy soils with lower storage capacity. Our soils contain a greater clay fraction than any of those simulated by Green et al. [2007]. Hence, the warming-enhancement of ET we observed may have had a greater impact on R during the spring given a more coarsely textured soil.

Last, our experiment did not include elevated atmospheric [CO<sub>2</sub>], which is expected under future climate conditions. Manipulative experiments in other Mediterranean grasslands have shown that elevated [CO<sub>2</sub>] can enhance the water-use efficiency of photosynthesis by reducing stomatal conductance, resulting in less overall transpiration and soil water depletion due to root uptake [*Field et al.*, 1997, *Fredeen et al.*, 1997]. In particular, Fredeen et al. [1997] showed that ET was reduced and soil moisture remained greater under elevated [CO<sub>2</sub>] relative to ambient levels, and the decline of soil moisture during the summer drought was delayed by about ten days. Had elevated [CO<sub>2</sub>] been included in our experiment, the warming-induced enhancement of ET during the spring may have been less, and warming-induced declines in soil moisture and ET during the summer may have been delayed.

## **2.5 Conclusions**

Results of our study demonstrate that the annual partitioning of P to ET and R in a Mediterranean-grassland ecosystem could be unaltered by climate warming. Warming caused greater ET during the spring (relative to ET under ambient temperature), but this

led to more rapid depletion of soil moisture and reduced ET during the summer. Despite warming-enhanced ET, reductions in total soil-water storage became great enough to reduce R only during the final storm event of the spring. These reductions in R were marginal relative to total R that occurred during the spring season, or were offset by greater R under warming treatments at the onset of fall rains, which we speculatively attribute to potential warming effects on the hydraulic properties of the silty-clay soils used in this experiment. Our results confirm the general view that interactions and feedbacks between climate, vegetation, and soil moisture ultimately dictate the ecosystem water balance response to climate warming [Angert *et al.*, 2005; De Boeck *et al.*, 2006; Green *et al.*, 2007; Green *et al.*, 2011; Jung *et al.*, 2010; Zavaleta *et al.*, 2003a].

## 2.6 References

- Allen, R. G., L. S. Pereira, D. Raes, and M. Smith (1998), Crop evapotranspiration - Guidelines for computing crop water requirements—FAO Irrigation and drainage paper 56, *FAO – Food and Agriculture Organization of the United Nations, Rome*, 300, 6541.
- Angert, A., S. Biraud, C. Bonfils, C.C. Henning, W. Buermann, J. Pinzon, C.J. Tucker, I. Fung, (2005), Drier summers cancel out the CO<sub>2</sub> uptake enhancement induced by warmer springs, *Proceedings of the National Academy of Sciences of the United States of America*, 102(31), 10823-10827, doi: 10.1073/pnas.0501647102.
- Baldocchi, D. (2011), Global change: The grass response, *Nature*, 476(7359), 160-161, doi: 10.1038/476160a.
- Baldocchi, D. D., L. K. Xu, and N. Kiang (2004), How plant functional-type, weather, seasonal drought, and soil physical properties alter water and energy fluxes of an oak-grass savanna and an annual grassland, *Agricultural and Forest Meteorology*, 123(1-2), 13-39, doi: 10.1016/j.agrformet.2003.11.006.
- Bell, J. E., E. S. Weng, and Y. Q. Luo (2010a), Ecohydrological responses to multifactor global change in a tallgrass prairie: A modeling analysis, *J. Geophys. Res.-Biogeosci.*, 115, G04042, doi: 10.1029/2009JG001120.

- Bell, J. E., R. Sherry, and Y. Q. Luo (2010b), Changes in soil water dynamics due to variation in precipitation and temperature: An ecohydrological analysis in a tallgrass prairie, *Water Resources Research*, 46, W03523, doi: 10.1029/2009WR007908.
- Beven, K. (2006), Searching for the Holy Grail of scientific hydrology:  $Q(t) = (S, R, \Delta t)A$  as closure, *Hydrology and Earth System Sciences*, 10(5), 609-618, doi: 10.5194/hess-10-609-2006.
- Budyko, M. I. (1974), *Climate and Life*, 508 pp., Academic, New York.
- Cai, W., T. Cowan, P. Briggs, and M. Raupach (2009), Rising temperature depletes soil moisture and exacerbates severe drought conditions across southeast Australia, *Geophysical Research Letters*, 36, L21709, doi: 10.1029/2009GL040334.
- De Boeck, H. J., C. Lemmens, H. Bossuyt, S. Malchair, M. Carnol, R. Merckx, I. Nijs, and R. Ceulemans (2006), How do climate warming and plant species richness affect water use in experimental grasslands?, *Plant and Soil*, 288(1-2), 249-261, doi: 10.1007/s11104-006-9112-5.
- Dermody, O., J. F. Weltzin, E. C. Engel, P. Allen, and R. J. Norby (2007), How do elevated CO<sub>2</sub>, warming, and reduced precipitation interact to affect soil moisture and LAI in an old field ecosystem?, *Plant and Soil*, 301(1-2), 255-266, doi: 10.1007/s11104-007-9443-x.
- Donohue, R. J., M. L. Roderick, and T. R. McVicar (2007), On the importance of including vegetation dynamics in Budyko's hydrological model, *Hydrology and Earth System Sciences*, 11(2), 983-995, doi: 10.5194/hess-11-983-2007.
- Fay, P. A., J. D. Carlisle, B. T. Danner, M. S. Lett, J. K. McCarron, C. Stewart, A. K. Knapp, J. M. Blair, and S. L. Collins (2002), Altered rainfall patterns, gas exchange, and growth in grasses and forbs, *Int. J. Plant Sci.*, 163(4), 549-557, doi: 10.1086/339718.
- Field, C.B., C.P. Lund, N.R. Chiariello, and B.E. Mortimer, (1997), CO<sub>2</sub> effects on the water budget of grassland microcosm communities, *Glob. Change Biol.*, 3(3), 197-206, doi: 10.1046/j.1365-2486.1997.t01-1-00096.x.
- Fredeen, A.L., J.T. Randerson, N.M. Holbrook, C.B. Field, (1997), Elevated atmospheric CO<sub>2</sub> increases water availability in a water-limited grassland ecosystem, *Journal of the American Water Resources Association*, 33(5), 1033-1039, doi: 10.1111/j.1752-1688.1997.tb04122.x.

Gee, G. W., and J. W. Bauder (1986), Particle-size Analysis, in *Methods of Soil Analysis. Part 1. Physical and Mineralogical Methods*, edited by E. A. Klute, American Society of Agronomy-Soil Science Society, Madison, WI.

Green, T. R., B.C. Bates, S.P. Charles, and P.M. Fleming (2007), Physically based simulation of potential effects of carbon dioxide-altered climates on groundwater recharge, *Vadose Zone J*, 6(3), 597-609, doi: 10.2136/vzj2006.0099.

Green, T. R., M. Taniguchi, H. Kooi, J. J. Gurdak, D. M. Allen, K. M. Hiscock, H. Treidel, and A. Aureli (2011), Beneath the surface of global change: Impacts of climate change on groundwater, *J. Hydrol.*, 405(3-4), 532-560, doi: 10.1016/j.jhydrol.2011.05.002.

Groisman, P. Y., R. W. Knight, T. R. Karl, D. R. Easterling, B. M. Sun, and J. H. Lawrimore (2004), Contemporary changes of the hydrological cycle over the contiguous United States: Trends derived from in situ observations, *J. Hydrometeorol.*, 5(1), 64-85, doi: 10.1175/1525-7541(2004)005<0064:CCOTHC>2.0.CO;2.

Huntington, T. G. (2006), Evidence for intensification of the global water cycle: Review and synthesis, *J. Hydrol.*, 319(1-4), 83-95, doi: 10.1016/j.jhydrol.2005.07.003.

Jarvis, N. J. (2007), A review of non-equilibrium water flow and solute transport in soil macropores: principles, controlling factors and consequences for water quality, *European Journal of Soil Science*, 58(3), 523-546, doi: 10.1111/j.1365-2389.2007.00915.x.

Jung, M., G. Bonan, A. Cescattii, J.Q. Chen, R. de Jeu, A.J. Dolman, W. Eugster, D. Gerten, D. Gianelle, N. Gobron, J. Heinke, J. Kimball, B.E. Law, L. Montagnani, Q.Z. Mu, B. Mueller, K. Oleson, D. Papale, A.D. Richardson, O. Roupsard, S. Running, E. Tomelleri, N. Viovy, U. Weber, C. Williams, E. Wood, S. Zaehle, K. Zhang (2010), Recent decline in the global land evapotranspiration trend due to limited moisture supply, *Nature*, 467(7318), 951-954, doi: 10.1038/nature09396.

Kundzewicz, Z. W., L. J. Mata, N. W. Arnell, P. Doll, B. Kabat, K. A. Jimenez, T. Miller, Z. Oki, S. Shiklomanov, and I. A. Shiklomanov (2007), Freshwater resources and their management, *Climate Change 2007: Impacts, Adaptation and Vulnerability, Contribution of Working Group II to the Fourth Assessment Report of the Intergovernmental Panel on Climate Change*, M.L. Parry, O.F. Canziani, J.P. Palutikof, P.J. van der Linden and C.E. Hanson, Eds., Cambridge University Press, Cambridge, UK, 173-210..

Kutner, M. H., C. J. Nachtsheim, J. Neter, and W. Li (2005), *Applied Linear Statistical Models*, McGraw-Hill/Irwin, New York, NY.

Lehmann, P., C. Hinz, G. McGrath, H. J. Tromp-van Meerveld, and J. J. McDonnell (2007), Rainfall threshold for hillslope outflow: an emergent property of flow pathway connectivity, *Hydrology and Earth System Sciences*, *11*(2), 1047-1063, doi: 10.5194/hessd-3-2923-2006.

Luo, Y. Q., D. Gerten, G. Le Maire, W.J. Parton, E.S. Weng, X.H. Zhou, C. Keough, C. Beier, P. Ciais, W. Cramer, J.S. Dukes, B. Emmett, P.J. Hanson, A. Knapp, S. Linder, D. Nepstad, L. Rustad, (2008), Modeled interactive effects of precipitation, temperature, and [CO<sub>2</sub>] on ecosystem carbon and water dynamics in different climatic zones, *Glob. Change Biol.*, *14*(9), 1986-1999, doi: 10.1111/j.1365-2486.2008.01629.x.

Ma, S., D.D. Baldocchi, X. Liukang, and T. Hehn, (2007), Inter-annual variability in carbon dioxide exchange of an oak/grass savanna and open grassland in California, *Agricultural and Forest Meteorology*, *147*, 157-171, doi: 10.1016/j.agrformet.2007.07.008.

McMillan, H. K. (2012), Effect of spatial variability and seasonality in soil moisture on drainage thresholds and fluxes in a conceptual hydrological model, *Hydrol. Process.*, *26*(18), 2838-2844, doi: 10.1002/hyp.9396.

Milly, P. C. D. (1994), Climate, interseasonal storage of soil-water, and the annual water-balance, *Adv. Water Resour.*, *17*(1-2), 19-24, doi: 10.1016/0309-1708(94)90020-5.

Montaldo, N., J. D. Albertson, and M. Mancini (2008), Vegetation dynamics and soil water balance in a water-limited Mediterranean ecosystem on Sardinia, Italy, *Hydrol. Earth Syst. Sci.*, *12*(6), 1257-1271, doi: 10.5194/hess-12-1257-2008.

Morgan, J. A., D. R. LeCain, E. Pendall, D. M. Blumenthal, B. A. Kimball, Y. Carrillo, D. G. Williams, J. Heisler-White, F. A. Dijkstra, and M. West (2011), C4 grasses prosper as carbon dioxide eliminates desiccation in warmed semi-arid grassland, *Nature*, *476*(7359), 202-205, doi: 10.1038/nature10274.

Morgan, J. A., D.E. Pataki, C. Korner, H. Clark, S.J. Del Grosso, J.M. Grunzweig, A.K. Knapp, A.R. Mosier, P.C.D. Newton, P.A. Niklaus, J.B. Nippert, R.S. Nowak, W.J. Parton, H.W. Polley, M.R. Shaw (2004), Water relations in grassland and desert ecosystems exposed to elevated atmospheric CO<sub>2</sub>, *Oecologia*, *140*(1), 11-25, doi: 10.1007/s00442-004-1550-2.

Mote, P. W., and E. P. Salathe (2010), Future climate in the Pacific Northwest, *Clim. Change*, 102(1-2), 29-50, doi: 10.1007/s10584-010-9848-z.

Norby, R. J., and Y. Q. Luo (2004), Evaluating ecosystem responses to rising atmospheric CO<sub>2</sub> and global warming in a multi-factor world, *New Phytologist*, 162(2), 281-293, doi: 10.1111/j.1469-8137.2004.01047.x.

Phillips, C. L., J. W. Gregg, and J. K. Wilson (2011), Reduced diurnal temperature range does not change warming impacts on ecosystem carbon balance of Mediterranean grassland mesocosms, *Glob. Change Biol.*, 17(11), 3263-3273, doi: 10.1111/j.1365-2486.2011.02483.x.

Ponton, S., L. B. Flanagan, K. P. Alstad, B. G. Johnson, K. Morgenstern, N. Kljun, T. A. Black, and A. G. Barr (2006), Comparison of ecosystem water-use efficiency among Douglas-fir forest, aspen forest and grassland using eddy covariance and carbon isotope techniques, *Glob. Change Biol.*, 12(2), 294-310, doi: 10.1111/j1365-2486.2005.01103.x.

Porporato, A., E. Daly, and I. Rodriguez-Iturbe (2004), Soil water balance and ecosystem response to climate change, *American Naturalist*, 164(5), 625-632, doi: 10.1086/424970.

Porporato, A., F. Laio, L. Ridolfi, and I. Rodriguez-Iturbe (2001), Plants in water-controlled ecosystems: active role in hydrologic processes and response to water stress - III. Vegetation water stress, *Adv. Water Resour.*, 24(7), 725-744, doi: 10.1016/S0309-1708(01)00006-9.

Potter, N. J., L. Zhang, P. C. D. Milly, T. A. McMahon, and A. J. Jakeman (2005), Effects of rainfall seasonality and soil moisture capacity on mean annual water balance for Australian catchments, *Water Resour. Res.*, 41(6), W06007, doi: 10.1029/2004WR003697.

Pumo, D., F. Viola, and L. V. Noto (2008), Ecohydrology in Mediterranean areas: a numerical model to describe growing seasons out of phase with precipitations, *Hydrology and Earth System Sciences*, 12(1), 303-316, doi: 10.5194/hess-12-303-2008.

Rodriguez-Iturbe, I., A. Porporato, L. Ridolfi, V. Isham, and D. R. Cox (1999), Probabilistic modelling of water balance at a point: the role of climate, soil and vegetation, *Proc. R. Soc. London Ser. A-Math. Phys. Eng. Sci.*, 455, 3789-3805, doi: 10.1098/rspa.1999.0477.

Ryu, Y., D. D. Baldocchi, S. Ma, and T. Hehn (2008), Interannual variability of evapotranspiration and energy exchange over an annual grassland in California, *Journal of Geophysical Research-Atmospheres*, 113, doi: 10.1029/2007JD009263.

Sanders, E. C., M. R. Abou Najm, R. H. Mohtar, E. Kladvko, and D. Schulze (2012), Field method for separating the contribution of surface-connected preferential flow pathways from flow through the soil matrix, *Water Resources Research*, 48, doi: 10.1029/2011WR011103.

Schenk, H. J., and R. B. Jackson (2002), The global biogeography of roots, *Ecological Monographs*, 72(3), 311-328, doi: 10.1046/j.1365-2745.2002.00682.x.

Survey, N. C. S. (2012), National Cooperative Soil Characterization Database, edited, Natural Resource Conservation Service; United States Department of Agriculture.

Tague, C., K. Heyn, and L. Christensen (2009), Topographic controls on spatial patterns of conifer transpiration and net primary productivity under climate warming in mountain ecosystems, *Ecohydrology*, 2(4), 541-554, doi: 10.1002/eco.88.

Taylor, R.G., B. Scanlon, P. Doll, M. Rodell, R. van Beek, Y. Wada, L. Longuevergne, M. Leblanc, J.S. Famiglietti, M. Edmunds, L. Konikow, T.R. Green, J. Chen, M. Taniguchi, M.F.P. Bierkens, A. MacDonald, Y. Fan, R.M. Maxwell, Y. Yechieli, J.J. Gurdak, D.M. Allen, M. Shamsudduha, K. Hiscock, P.J.F. Yeh, I. Holman, H. Treidel (2012), Ground water and climate change, *Nature Climate Change*, 3(4), 322-329, doi: 10.1038/nclimate1744.

Teuling, A. J., S.I. Seneviratne, R. Stöckli, M. Reichstein, E. Moors, P. Ciais, S. Luysaert, B. van den Hurk, C. Ammann, C. Bernhofer, E. Dellwik, D. Gianelle, B. Gielen, T. Grünwald, K. Klumpp, L. Montagnani, C. Moureaux, M. Sottocornola, and G. Wohlfahrt (2010), Contrasting response of European forest and grassland energy exchange to heatwaves, *Nat. Geosci.*, 3(10), 722-727, doi: 10.1038/ngeo950.

Thompson, S. E., C. J. Harman, P. A. Troch, P. D. Brooks, and M. Sivapalan (2011), Spatial scale dependence of ecohydrologically mediated water balance partitioning: A synthesis framework for catchment ecohydrology, *Water Resources Research*, 47, doi: 10.1029/2010WR009998.

Tingey, D. T., R. S. Waschmann, D. L. Phillips, and D. M. Olszyk (2000), The carbon dioxide leakage from chambers measured using sulfur hexafluoride., *Environmental and Experimental Botany*, 43, 101-110, doi: 10.1016/S0098-8472(99)00051-9.

Viola, F., E. Daly, G. Vico, M. Cannarozzo, and A. Porporato (2008), Transient soil-moisture dynamics and climate change in Mediterranean ecosystems, *Water Resources Research*, 44, doi: 10.1029/2007WR006371.

Wu, Z. T., P. Dijkstra, G. W. Koch, J. Penuelas, and B. A. Hungate (2011), Responses of terrestrial ecosystems to temperature and precipitation change: a meta-analysis of experimental manipulation, *Glob. Change Biol.*, 17(2), 927-942, doi: 10.1111/j.1365-2486.2010.02302.x.

Zavaleta, E. S., B. D. Thomas, N. R. Chiariello, G. P. Asner, M. R. Shaw, and C. B. Field (2003a), Plants reverse warming effect on ecosystem water balance, *Proceedings of the National Academy of Sciences of the United States of America*, 100(17), 9892-9893, doi: 10.1073/pnas.1732012100.

Zavaleta, E. S., M. R. Shaw, N. R. Chiariello, B. D. Thomas, E. E. Cleland, C. B. Field, and H. A. Mooney (2003b), Grassland responses to three years of elevated temperature, CO<sub>2</sub>, precipitation, and N deposition, *Ecological Monographs*, 73(4), 585-604, doi: 10.1890/02-4053.

Zhongmin, H., Y. Guirui, Z. Yanlian, S. Xiaomin, L. Yingnian, S. Peili, W. Yanfen, S. Xia, Z. Zemei, Z. Li, and L. Shenggong (2009), Partitioning of evapotranspiration and its controls in four grassland ecosystems: Application of a two-source model, *Agricultural and Forest Meteorology*, 149, 1410-1420, doi: 10.1016/j.agrformet.2009.03.014.

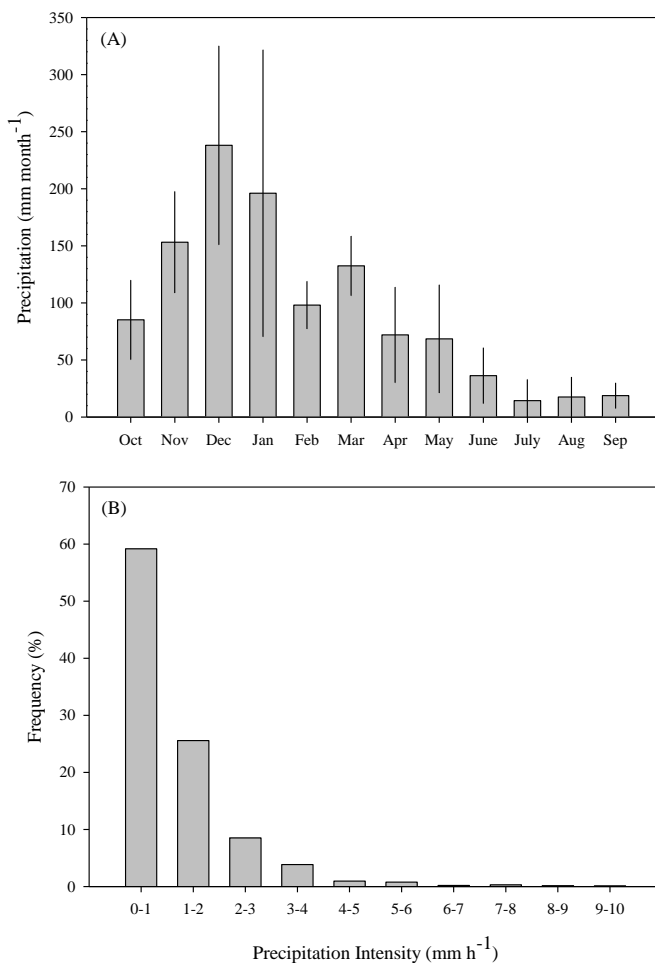


**Figure 2.1.** (A) Average precipitation that occurred each month over the study period (October, 2007 – August, 2010). Error bars represent plus and minus one standard deviation ( $n = 3$ , except  $n=2$  for August and September). (B) The frequency distribution of precipitation intensity during the same period (calculated based on hourly totals grouped into 1-mm increments).

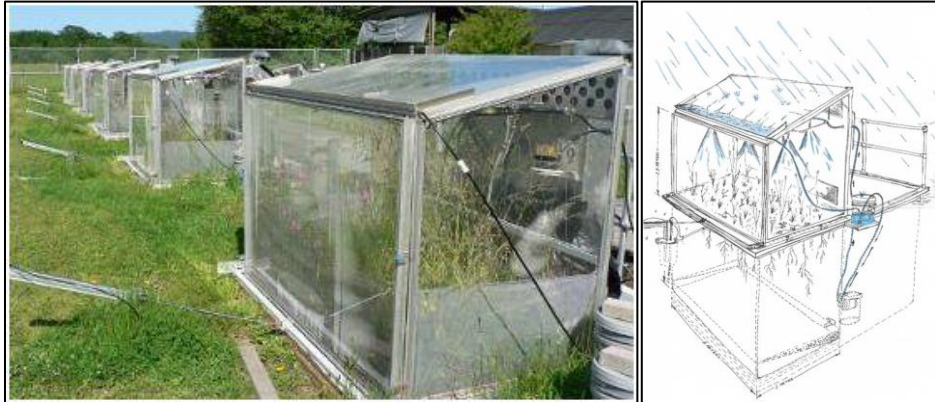
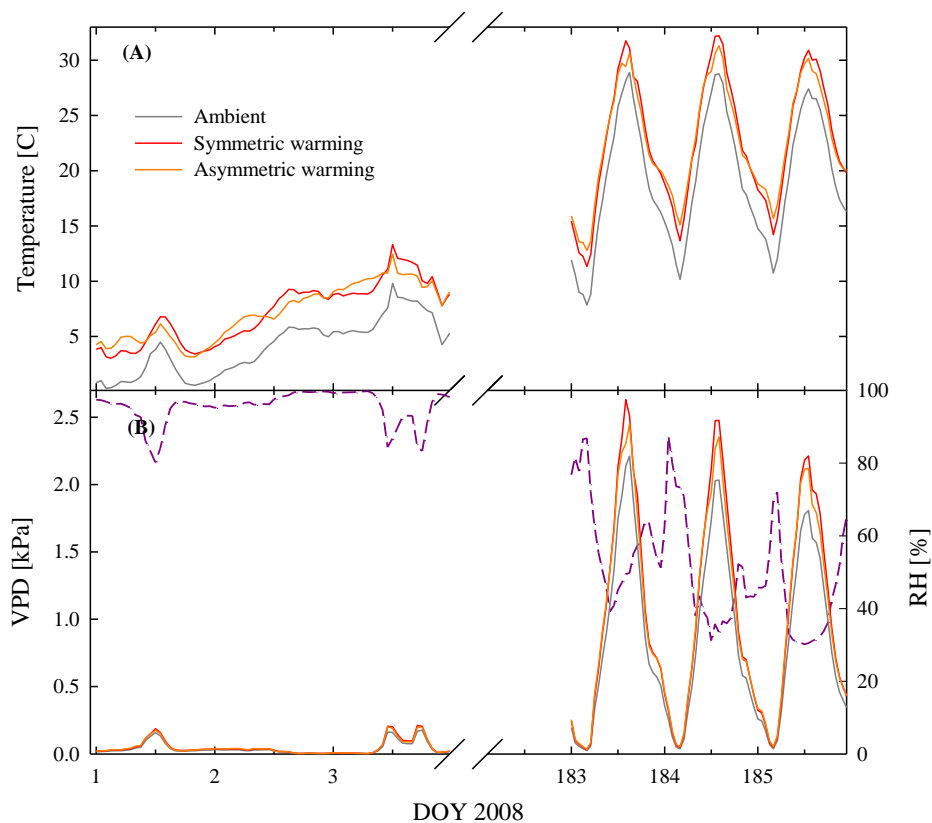
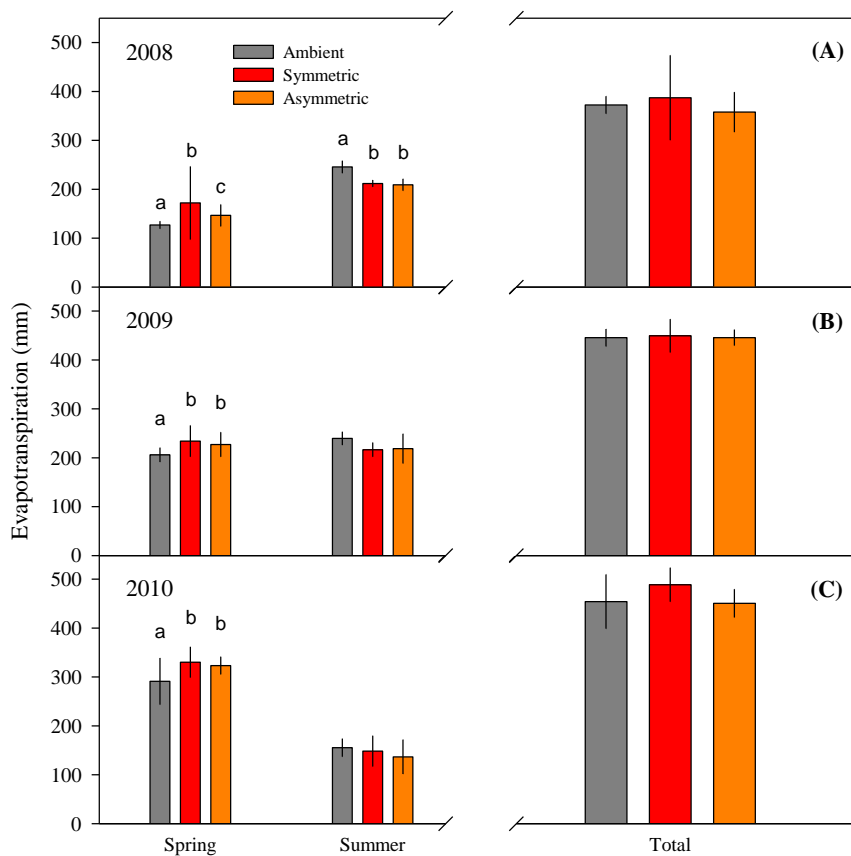


Figure 2.2. A photograph of the terracosms in an open field in Corvallis, Oregon, and a drawing illustrating the enclosed aboveground chamber, underlying lysimeter, and irrigation system. Additional photographs and diagrams can be viewed at [www.teraglobalchange.org](http://www.teraglobalchange.org).



**Figure 2.3.** (A) Time series of temperature on days of the year 1 through 3 and 183 through 185 under ambient temperature, symmetric warming, and asymmetric warming. (B) Time series of vapor pressure deficit over the same time span. The purple dashed line represents relative humidity, which was maintained at ambient levels under all three temperature treatments.



**Figure 2.4.** (A-C) Cumulative ET during spring (March 1<sup>st</sup> until cessation of recharge), summer (time following spring until September 30<sup>th</sup>), and spring and summer combined for 2008, 2009, and 2010. Evapotranspiration totals during 2010 do not include August or September, as treatments temporarily ceased on July 26, 2010 during plant dormancy. Error bars indicate 90% confidence intervals. Where present, letters indicate differences among temperature treatments associated with a p-value of 0.1 or less.

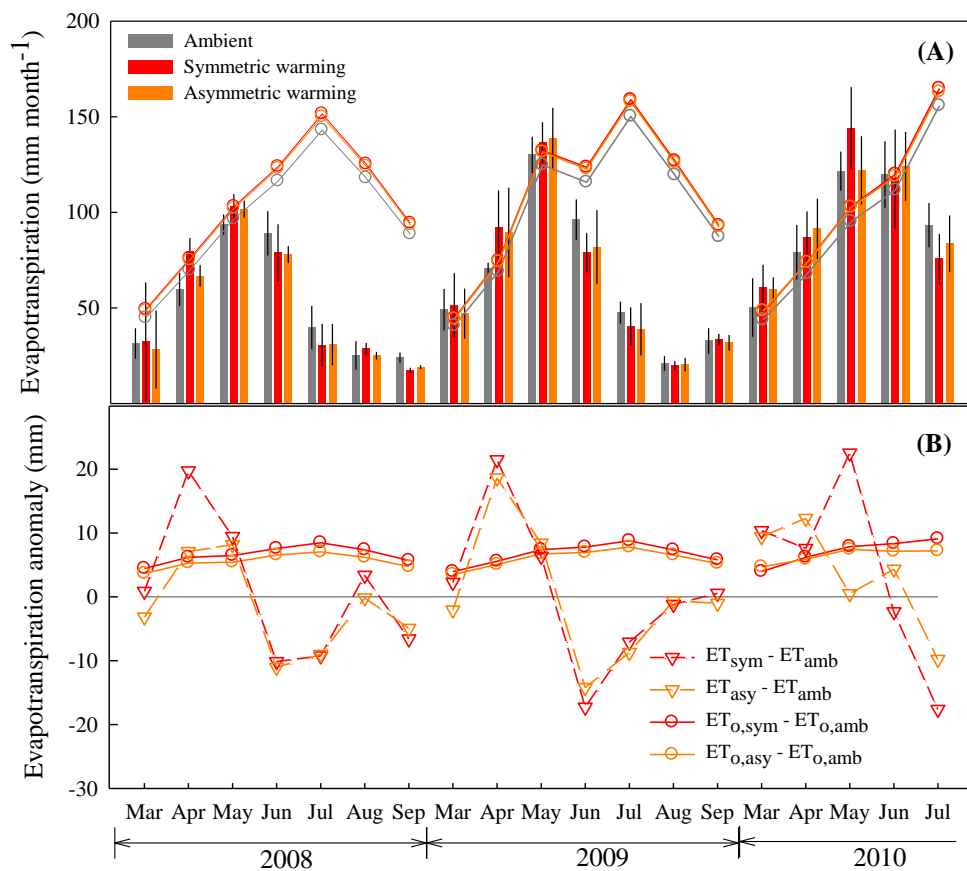


**Figure 2.5.** (A) Monthly ET (bars) and reference  $ET_o$  (lines) during March through September of 2008 and 2009, and during March through July of 2010. Error bars indicate 90% confidence intervals. (B) The magnitude of the warming effect on actual ET (i.e.  $ET_{\text{sym}} - ET_{\text{amb}}$  and  $ET_{\text{asy}} - ET_{\text{amb}}$ ) and reference  $ET_o$  (i.e.  $ET_{\text{o,sym}} - ET_{\text{o,amb}}$  and  $ET_{\text{o,asy}} - ET_{\text{o,amb}}$ ). Each point represents the difference in average-monthly ET between the respective temperature treatment and the ambient temperature treatment (horizontal line).

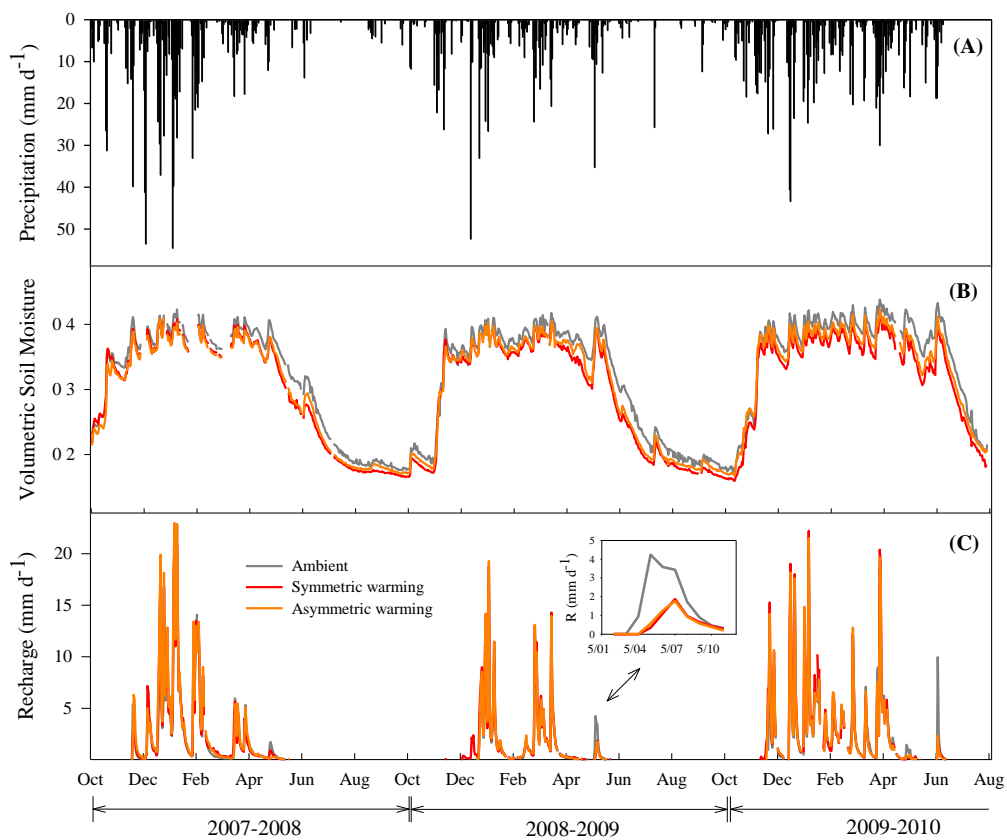


**Figure 2.6.** (A) Daily P from October 1, 2007 through July 31, 2010. (B) Average-daily volumetric water content for each treatment during the same period. Each value is the treatment average of the volumetric water content of the entire soil volume, calculated using equation 1. (C) Average-daily R for each treatment. The inset graph highlights an example of the differences in R observed among treatments during the final R event of the spring (here expanded only for 2009).

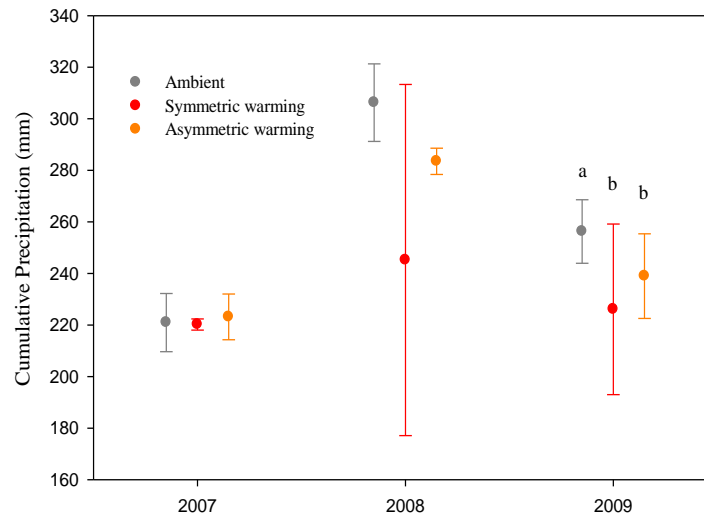
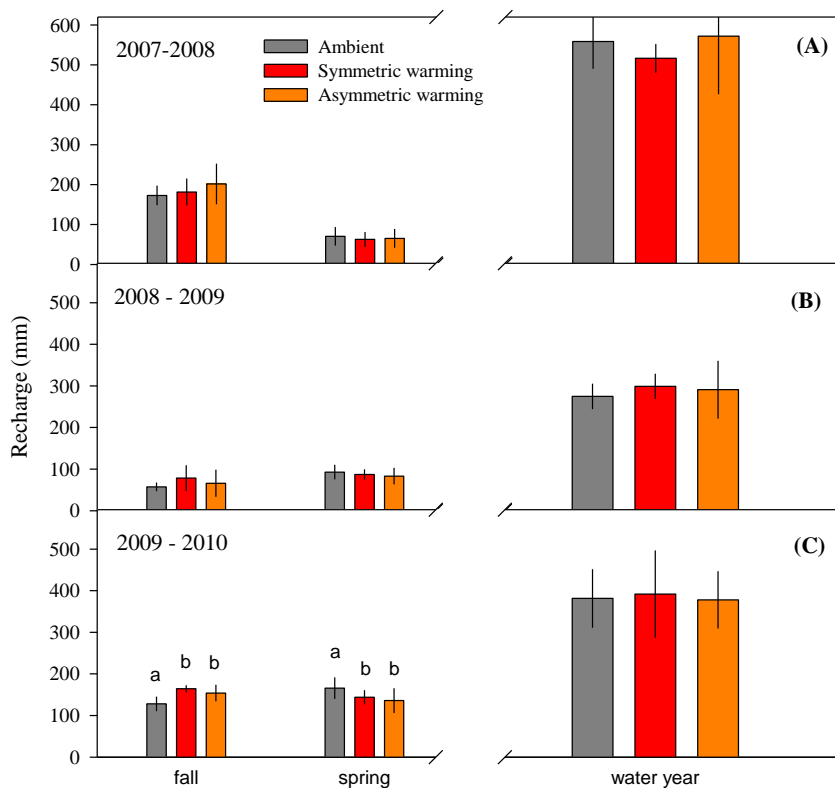


Figure 2.7. The cumulative P (beginning October 1<sup>st</sup>) required to initiate 1 mm d<sup>-1</sup> of R during the fall season of each year. Error bars represent 90% confidence intervals. Different lower-case letters indicate differences among treatments with  $p = 0.1$  or less.



**Figure 2.8.** Cumulative R for the fall (November - December), spring (March 1<sup>st</sup> until the cessation of R), and the complete water year for 2007 through 2010. Error bars indicate 90% confidence intervals. Where present, letters indicate differences among temperature treatments associated with a p-value of 0.1 or less. No data were available for January 2010 due to equipment replacement during that time. Hence, the reported R for that water year is less than the actual amount.

**3. SOIL-WATER FLOW UNDER AGGRADING GRASSLAND VEGETATION:  
SEEKING EVIDENCE OF HYDROLOGICALLY SIGNIFICANT SOIL  
ALTERATION BY ROOTS**

Luke A. Pangle

Jillian W. Gregg

Jeffrey J. McDonnell

### 3.1. Introduction

A growing body of research speculates on the many influences of plants and plant roots on subsurface flow in soils [Ghestem *et al.*, 2011]. While we know that plants induce hydraulically significant changes to the structure and porosity of soils they inhabit, the hydrologic impact of these physical changes on the vadose-zone water balance is poorly understood.

Studies have shown that the continued growth, decay, and regrowth of root mass has the effect of excavating new macropores in soils [Angers and Caron, 1998; Edwards *et al.*, 1988; Luxmoore, 1981; Noguchi *et al.*, 1997; Rasse *et al.*, 2000; Tippkotter, 1983] that may conduct water and solutes at much greater flux rates than possible in the bulk-soil matrix [Beven, 1981; Beven and Germann, 1982; Beven and Germann, 2013; Dragila and Wheatcraft, 2001; Lange *et al.*, 2009; Mitchell *et al.*, 1995; Nimmo, 2007; Noguchi *et al.*, 1997; Rasse *et al.*, 2000]. For example, Rasse *et al.* [2000] conducted hydraulic measurements on soil cores collected from field plots with and without an alfalfa crop, and showed that saturated-hydraulic conductivity was 57% greater in the presence of alfalfa after only two years of growth—a result that was attributed to root-induced increases in total porosity and macroporosity.

Plant roots also create local zones of greater bulk density as they permeate a fixed soil volume [Bruand *et al.*, 1996; Dexter, 1987], inducing heterogeneity in soil porosity and pore diameters. Plant stems and canopies can exacerbate the potential hydrological influence of these belowground effects by intercepting incident precipitation over large areas and funneling the water to concentrated areas of infiltration at the base of plant stems, where preferential flow through excavated root channels may accelerate infiltration to greater soil depth [Johnson and Lehmann, 2006].

In addition to excavating new pore space, uptake of soil water by roots and exudation of organic residues has been shown to alter hydraulically-significant soil structural properties [Angers and Caron, 1998; Bengough, 2012; Bronick and Lal, 2005]. Soil regions immediately adjacent to plant roots undergo amplified wetting and drying cycles that enhance the aggregation of soil particles by facilitating cleaving at zones of weakness in the soil, particularly in clay-bearing soils that demonstrate shrinking and

swelling tendencies [*Caron et al.*, 1992; *Jastrow*, 1987; *Materechera et al.*, 1992]. Organic exudates from plant roots and mycorrhizal fungi can serve as bonding agents that facilitate the cohesion of microaggregates into larger macroaggregates [*Angers and Caron*, 1998; *Materechera et al.*, 1992; *Rillig et al.*, 2002] yielding inter-aggregate pore spaces with greater diameter and conductivity than found within the aggregate. Further, organic exudates are known to coat macropore surfaces found near roots [*Ellerbrock and Gerke*, 2004], conveying some degree of hydrophobicity that may inhibit infiltration of water films from macropores into the smaller pores of the soil matrix, thus enhancing longitudinal flow within the pore.

While the suite of possible mechanisms by which plants influence the soil-pore space have been proposed and described, the collective impact of these mechanisms on the vadose-zone water balance has rarely been explored. This is due in part to our inability to see below the soil surface and track water flow and transport within the root zone—as absorbed by plant roots and transpired back to the atmosphere, or percolating beyond the root zone and contributing to groundwater recharge. Studies have demonstrated that solute tracers are dispersed through soil macropores—often generated by root growth—at rates that far exceed the effective Darcian velocity (reviewed by [*Jarvis*, 2007]). Nevertheless, the magnitude of water actually traveling through these pores and the water balance component to which it ultimately contributes has rarely been quantified. Additionally, plant-induced macroporosity in soils has been shown to accelerate infiltration of precipitation (or irrigation) at the soil surface, which can have an important impact on hydrologic partitioning by affecting the amount of precipitation that contributes to surface runoff versus infiltration into the subsurface [*Price et al.*, 2010; *Thompson et al.*, 2010; *Weiler and Naef*, 2003]. The results from these studies, in particular, suggest that plant-induced changes to soil hydraulic properties have the potential to significantly impact the overall vadose-zone water balance, inspiring the postulation that vegetation can be actively managed to achieve desirable soil hydraulic properties and hydrologic response [*Lange et al.*, 2009; *Macleod et al.*, 2007].

Here we address the overarching question: Does the coevolution of plant and soil systems enhance rapid-subsurface water flow sufficiently to alter the overall vadose-zone water balance? We utilized a chronosequence of vegetated lysimeters with surface

conditions ranging from bare soil to a six-year-old grassland ecosystem in a Mediterranean climate, hydrometric and stable-isotope tracer data, and two hydrograph separation techniques to target plant root development effects on flow and transport. In this Mediterranean climate there is a high frequency of rain storms with short inter-storm drying periods occurring during the late-fall and winter seasons when plant physiological activity is low. These conditions offer a unique opportunity to isolate and examine how aggrading grassland vegetation, as a physical perturbation to the soil environment, affects infiltration and potential groundwater recharge. We test the hypothesis that rapid-time-source contributions to potential groundwater recharge will be enhanced as the grassland ecosystem aggrades, due to the documented effects that developing root and shoot systems exert on soil physical properties, and that the fraction of precipitation that contributes to potential groundwater recharge during individual storm events will increase.

## **3.2. Materials and Methods**

### *3.2.1 Site description*

This work was conducted at the Terracosm facility in Corvallis, OR, USA. For this analysis we utilized a single Terracosm (hereafter abbreviated L10) and two additional lysimeters (L1bs and L1g) that were constructed to replicate the lysimeter design used for L10, but were not covered by a Teflon-walled aboveground chamber as was L10 (as part of a climate-warming experiment [*Pangle et al.*, 2013a; *Phillips et al.*, 2011]). Though enclosed by a chamber, the air temperature, [CO<sub>2</sub>], and relative humidity conditions within L10 were controlled to track those measured at an adjacent climate station. The main difference in meteorological conditions experienced by L10 versus L1bs and L1g was wind speed and duration. The wind speed inside L10 was generated by a fan and approximately constant at 0.3 m s<sup>-1</sup>, whereas L1bs and L1g experienced ambient wind conditions. Below we describe the design features of these three units that are important for the comparisons made in this work.

### 3.22 Lysimeter design and soils

The L10 lysimeter was constructed of polypropylene with a total volume of 2.3 m<sup>3</sup>. The two-dimensional area from a plan view was 2 m<sup>2</sup> (2 x 1 m), and the depth ranged from 1-1.3 m along a base with constant slope angle (30%) that facilitated water flow to a drainage port at the downslope side of the lysimeter base. The lysimeter was encased in a larger aluminum containment structure. The bottom was filled with pea gravel to a volume of 0.3 m<sup>3</sup>—such that it filled the wedge-shaped base and provided a flat surface upon which the soils were placed. A sheet of landscaping cloth was placed on top of the gravel layer to inhibit root growth into the gravel and lysimeter plumbing. The remaining 2 m<sup>3</sup> of the lysimeter volume was filled with soil, resulting in a soil depth of 1 m. The soil was excavated from a prairie site near Corvallis, Oregon, USA in depth increments of 0.2 m. Each depth-specific layer of soil was air dried and passed through a 0.0245 m sieve to remove stones and large organic material, then each 0.2-m-depth increment was filled into the lysimeter in the same orientation as extracted from the field. A weighted tamping tool and systematic tamping procedure were used to achieve the greatest possible consistency in bulk density of soils filled into the various lysimeters. The same tamping procedure was used on a smaller control volume of soil that could be placed on a scale, indicating the bulk density of the repacked soil was 1.1 g cm<sup>-3</sup>. Particle size analysis using the pipette method [Gee and Bauder, 1986] showed that the textural class was silty clay loam at 0 – 0.6 m depth (29 – 38% clay), silt loam at 0.6 – 0.8 m depth (26% clay), and loam at 0.8 – 1.0 m depth (23% clay).

L1bs and L1g each consisted of a lysimeter with 1 m<sup>3</sup> volume—1 m<sup>2</sup> area from a plan view (1 x 1 m) with 1 m total depth. Each had a flat base, rather than sloping, with four drainage ports (0.0254 m diameter). Their base was filled with the same pea gravel to a depth of only 0.05 m; the same landscaping cloth was placed overtop the pea gravel, and the remaining 0.95 m depth was filled with the same soil material, in the same orientation, and using the same tamping procedure as was used for L10. These two lysimeters were filled with soil during December, 2010. They were covered with a tarp and first exposed to precipitation on March 3, 2011.

### 3.23 *Lysimeter vegetation*

Three annual forbs, eight perennial forbs, and three perennial grass species were planted in L10 to simulate a plant assemblage that resembled natural grasslands found in Oregon's Willamette Valley. For L10, plants were started in a greenhouse during the summer of 2005, left over winter in a lath house, and transplanted into L10 after the last frost during April, 2006. Sixteen individuals of each species were transplanted in a randomized design with a planting density of 112 individuals per m<sup>2</sup>. The plants grew on the repacked soils for one year before the chamber top was installed on L10 during April, 2007.

The same assemblage of species was planted with the same density in L1g on May 15, 2011, while L1bs was left with a bare soil surface. This analysis includes data collected from L1bs and L1g from February through March, 2012, representing a bare soil condition and grassland aggradation over 290-310 days (0.8 y, including one growing season and one dormant period), respectively. We present data from L10 from December, 2009; March, 2010; and for the same period during February through March, 2012, representing grassland aggradation over 3.75, 3.9, and approximately 5.9 years, respectively. Based on the replication of the soil material, initial species composition and planting density, and nearly homogenous climatic conditions experienced at each lysimeter, we attribute differences observed in response variables to the influence of these varied stages of aggrading vegetation.

### 3.24 *Hydrometric data collection*

Incident precipitation (P), volumetric-soil moisture ( $\theta$ ), and potential groundwater recharge [i.e. lysimeter drainage (R)] were measured for each lysimeter. Incident precipitation on L1bs and L1g was measured with a tipping bucket gage and HOBO Event Logger (Onset Computer Corporation, Inc.; Bourne, MA) in increments of 0.14 mm, while incident precipitation on L10 was captured on the chamber roof, routed to a storage container until approximately 1 mm accumulated, then pumped onto the vegetated surface of L10 over approximately 60 seconds using six low-pressure sprinkler heads. Though the mechanisms of precipitation delivery differed between the three lysimeters, cumulative precipitation during individual storm events was nearly identical,

as were maximum one-hour precipitation intensities (shown later in Table 3.1). Recharge was measured with tipping bucket gages at L1bs and L1g at 0.005 mm increments, while a custom-made gage was used on L10 that measured in 0.03 mm increments.

Volumetric-soil moisture was measured with a TDR system that included four TDR probes (CS610, Campbell Scientific, Inc.) installed horizontally at depths of 0.05, 0.15, 0.35, and 0.75 m below the soil surface, and a Tektronix 1502b TDR Cable Tester (Tektronix, Inc.) that was operated in conjunction with a Campbell CR10 Data Logger and SDMX50 Coax Multiplexer. Volumetric-water content was measured at each probe location every 36 minutes. Data from all probes were manually edited to remove erroneous data points using procedures described by Pangle et al. [2013a]. The probes at 0.35 m depth in L1bs and L1g failed, so data from that soil depth were omitted from the analysis for L10 as well.

### *3.25 Stable isotope sampling and analysis*

Intensive sampling of P and R was conducted during select storm events for analysis of their stable-isotope composition ( $\delta^{18}\text{O}$  and  $\delta^2\text{H}$ ), though here we report only the  $\delta^{18}\text{O}$  data. For storms occurring during March, 2012, sampling was done using a new automated and high-frequency sampling and analysis system described by Pangle et al. [2013b] (Appendix 1), which enabled sub-hourly sample collection and analysis of P from a precipitation collector and R from L1bs and L1g. We conducted manual sampling of R from L10 at the same time. Sampling of R during other storm events was done manually at sub-hourly intervals, on average, with lower sampling frequency occurring overnight during some storms. Manual sampling of P relied on a sequential sampling device similar to that reported by Kennedy et al. [1979], with 12 bottles and a catch area of 0.03 m<sup>2</sup>. Each sample represented a fraction of the total precipitation that occurred between sample collection dates. That fraction was determined by dividing each individual sample volume by the total volume of water collected in all 12 bottles, then multiplying that fractional value by the actual precipitation amount that occurred between collection dates. The stable isotope composition measured in each sample was then assumed to represent the average isotopic composition of that portion of total

precipitation. The samples were stored in glass vials with sealed caps at room temperature prior to analysis.

The ratio  $^{18}\text{O}:^{16}\text{O}$  (and  $^2\text{H}:^1\text{H}$ ) in water samples was measured with a Los Gatos Research Liquid Water Isotope Analyzer (Los Gatos Research, Mountain View, CA). Isotopic ratios were converted to  $\delta$  notation and reported in per mil values [ $(\text{‰})$ , parts per thousand relative to an external standard] using the Vienna Standard Mean Ocean Water (VSMOW):

$$\delta^{18}\text{O} = \left( \frac{^{18}\text{O}:^{16}\text{O}_{\text{sample}}}{^{18}\text{O}:^{16}\text{O}_{\text{vsmow}}} - 1 \right) \times 1000 \quad (3.1)$$

The analytical accuracy was limited by the accuracy of the external standards, which was  $\pm 1$  and  $0.2 \text{ ‰}$  for  $\delta^2\text{H}$  and  $\delta^{18}\text{O}$ , respectively. Among all analyses included here, the mean analytical precision was  $0.50$  (range =  $0.18 - 0.73$ ) and  $0.12$  (range =  $0.04 - 0.15$ ) per mil for  $\delta^2\text{H}$  and  $\delta^{18}\text{O}$ , respectively—quantified as the sample-standard-deviation of all measured external standard values multiplied by two.

### 3.26 Analytical approach 1: hydrograph separation with TRANSEP

We used two isotope-based hydrograph-separation techniques to quantify the time-source contributions to total R during individual storms, and to compare how these time-source contributions to R differ under a bare soil condition and varying stages of aggrading grassland vegetation. The approaches we use both assume that R is comprised of two distinct time-source components; these are called “pre-event” and “event” water:

$$R = R_{\text{pe}} + R_{\text{e}} \quad (3.2)$$

where R is total potential recharge,  $R_{\text{pe}}$  is recharge generated from pre-event water, and  $R_{\text{e}}$  is recharge generated by event water. Pre-event water refers to water molecules that were stored within the soil-pore space prior to the precipitation event of interest, whereas event water refers to water molecules that infiltrated the soil-pore space during the precipitation event. The isotopic composition of R at any point in time is calculated as a sum:

$$\delta_R(t) = \delta_{pe}(t)R_{pe}(t) + \delta_e(t)R_e(t) \quad (3.3)$$

where  $\delta_R$ ,  $\delta_{pe}$ , and  $\delta_e$  are the  $\delta$  values (here  $\delta^{18}\text{O}$ ) of total R, pre-event water, and event water, respectively. The first method we used was a transfer-function hydrograph-separation technique (TRANSEP, [Weiler *et al.*, 2003]). The TRANSEP method requires measured P, R, and the  $\delta$  values from both fluxes to derive two metrics of interest for our comparison: 1) a time series of the fraction of total P that generates R during the storm event, and 2) a time series of the fraction of total R that is generated by event water versus pre-event water.

The first step of the TRANSEP method is a non-linear function proposed by Jakeman and Hornberger [1993] that approximates the fraction of incoming precipitation that contributes to recharge as opposed to evaporation—either during the current or subsequent storm events. Infiltration and recharge during storm events are highly non-linear processes, resulting from variable initial soil-water content and the non-linear relationships between soil-water content and the associated water pressure and hydraulic conductivity, and because of system-specific thresholds that must be met before flow may proceed across some control surface of interest (in our case the base of a soil profile). A conceptual underpinning of the effective precipitation is that it represents the fraction of total precipitation that occurs during approximately steady state conditions (steady soil-water content and associated soil-hydraulic properties) and therefore yields linearly-scaled outflow amounts. The empirical function proposed by Jakeman and Hornberger [2003] to estimate effective precipitation is shown below:

$$s(t) = b_1 p(t) + (1 - b_2^{-1})s(t - \Delta t) \quad (3.4)$$

$$s(t = 0) = b_3 \quad (3.5)$$

$$p_{\text{eff}}(t) = p(t)s(t) \quad (3.6)$$

where  $s(t)$  is the antecedent precipitation index that is calculated as a function of the historical precipitation record dating back to a specified start time, and weighted based on the parameter  $b_2$ ; the parameter  $b_3$  is the initial antecedent precipitation index at the

specified start time; the parameter  $b_1$  is iteratively adjusted throughout the simulation period to ensure that the effective precipitation equals the actual recharge amount, and  $p_{\text{eff}}(t)$  is the effective precipitation at time  $t$  [Jakeman and Hornberger, 1993]. This set of equations introduces the first two unknown parameters in this analytical approach ( $b_2$  and  $b_3$ ). The  $p_{\text{eff}}$  time series is then used to simulate  $R$  and  $\delta_R$ .

The outflow (in our case  $R$ ) is simulated by linear convolution of the  $p_{\text{eff}}$  time series with a time-invariant transfer function, as below:

$$R(t) = \int_0^t g(\tau) p_{\text{eff}}(t - \tau) d\tau \quad (3.7)$$

where the hydrologic-transfer function,  $g(\tau)$ , is a probability-density function that represents the system response to  $p_{\text{eff}}$ . The responsiveness of the system to  $p_{\text{eff}}$  depends on soil-specific properties such as pore structure and connectivity that influence the propagation of pressure waves and actual flow velocities of water molecules through the soil—the factors that control the magnitude and timing of the outflow response. Our use of a time-invariant hydrologic-transfer function assumes that under near-steady state conditions, which are delineated based on the  $p_{\text{eff}}$  model, all these sources of complexity in the soil can be represented by a single function that assigns probability to the range of time scales at which  $R$  can occur in response to  $P$ .

After simulating  $R(t)$ , the second step in the TRANSEP method is to simulate the time series of observed  $\delta^{18}\text{O}$  values in  $R$ . Equations 3.2 and 3.3 above can be combined and rewritten to solve for  $\delta_R(t)$  as shown below:

$$\delta(t) = \frac{R_e(t)}{R(t)} [\delta_e(t) - \delta_{pe}] + \delta_{pe} \quad (3.8)$$

The unknown variables in this equation are  $R_e(t)$  and  $\delta_e(t)$ , with  $R_e(t)$  being the variable of primary interest.  $R_e(t)$  is expected to vary depending on the intensity and duration of  $P$  that occurs during the storm, and therefore the fraction of  $p_{\text{eff}}$  that contributes to  $R$  during the current storm event. This fraction,  $f(t)$ , is modeled using the same function as for  $p_{\text{eff}}$  (equations 3.4-3.6), but with  $s$  replaced by the fraction  $f$  and the parameter  $b_3$  is set to

zero since in principle there can be no  $p_{\text{eff}}$  contribution to  $R$  prior to the beginning of the storm. Given this functional form for  $f$ ,  $R_e(t)$  is then estimated through two steps. First, the isotopic composition of event water is approximated as:

$$\delta_e(t) = \frac{\int_0^t \delta_p(t - \tau) p_{\text{eff}}(t - \tau) f(t - \tau) h_e(\tau) d\tau}{\int_0^t p_{\text{eff}}(t - \tau) f(t - \tau) h_e(\tau) d\tau} \quad (3.9)$$

where  $\delta_p$  is the time-varying isotopic composition of precipitation and  $h_e(\tau)$  is the function that describes the distribution of transit times experienced by water molecules included in  $p_{\text{eff}}$  that contribute to  $R$  during the current storm event. The denominator in the above equation defines  $R_e$ —the total amount of recharge comprised of event water—and can be combined with equation 3.7 above to calculate the fraction of total  $R$  that is comprised of event water:

$$\frac{R_e(t)}{R(t)} = \frac{\int_0^t p_{\text{eff}}(t - \tau) f(t - \tau) h_e(\tau) d\tau}{\int_0^t p_{\text{eff}}(t - \tau) g(\tau) d\tau} \quad (3.10)$$

Last, the isotopic composition of  $R$  can be simulated by substituting equations 3.7 and 3.9 into equation 3.8, yielding:

$$\begin{aligned} \delta_R(t) = & \frac{1}{R(t)} \int_0^t \delta_p(t - \tau) p_{\text{eff}}(t - \tau) f(t - \tau) h_e(\tau) d\tau \\ & - \frac{\delta_{pe}}{R(t)} \int_0^t p_{\text{eff}}(t - \tau) f(t - \tau) h_e(\tau) d\tau + \delta_{pe} \end{aligned} \quad (3.11)$$

The functions  $g(\tau)$  and  $h_e(\tau)$  defined in equations 3.7 and 3.9, respectively, may take on a variety of functional forms with varying theoretical underpinnings [Kirchner *et al.*, 2000; Maloszewski and Zuber, 1982; Weiler *et al.*, 2003]. Executing the TRANSEP method requires selection of a functional form for each, and determination of the optimal parameter values that minimize the differences between simulated and observed values of  $R$  and  $\delta_R$ . Similar to Weiler *et al.* [2003], we utilized the optimization scheme proposed

by Abbaspour et al. [2001] to search for a parameter set that minimized an objective function computed as the average of the Nash-Sutcliffe efficiency [Nash and Sutcliffe, 1970] and the root-mean-square error subtracted from one. We found that R was best simulated using the two-parallel-linear reservoir model [Weiler et al., 2003]:

$$g(\tau) = \frac{\phi}{\tau_f} \exp\left(-\frac{\tau}{\tau_f}\right) + \frac{1-\phi}{\tau_s} \exp\left(-\frac{\tau}{\tau_s}\right) \quad (3.12)$$

Conceptually, this model implies that the water flow through the soil profile occurs in two domains—fast and slow—where the distribution of response times in each domain is described by an exponential function, with parameters  $\tau_f$  and  $\tau_s$  describing the mean response time in the fast and slow flow reservoirs, respectively. The parameter  $\phi$  describes the fraction of water or tracer that is partitioned to the fast versus slow reservoirs. One additional parameter,  $\eta$ , describes the time lag between precipitation and activation of the hydrologic response.  $\delta_R$  was best simulated using an analytical form of the advection-dispersion equation [Maloszewski and Zuber, 1982]:

$$h_e(\tau) = \left[ \left( \frac{4\pi\tau D}{v_x T} \right)^{-\frac{1}{2}} \exp \left[ -\frac{T \left( 1 - \frac{\tau}{T} \right)^2 v_x}{4D\tau} \right] \right] \tau^{-\frac{1}{2}} \quad (3.13)$$

The final important component in our application of this method is the designation of  $\delta^{18}\text{O}$  values that represents pre-event water (equation 3.8 and 3.11). Typically, this value is assigned based on the measured value of  $\delta^{18}\text{O}$  observed in flow prior to a storm event, and remains constant throughout the simulation period. However, we observed that  $\delta^{18}\text{O}$  in R samples collected throughout the entire year showed long-term trends that likely result from inter-storm variability in mean  $\delta^{18}\text{O}$  in precipitation. Our high-frequency data also revealed gradual linear trends in  $\delta_R$  within and between days. It was necessary to account for these trends when designating  $\delta_{pe}$ , and we did so by specifying  $\delta_{pe}$  as a function of time, where each value of  $\delta_{pe}(t)$  was calculated based on linear interpolation between 1) the mean  $\delta^{18}\text{O}$  value of R samples collected during the recession flow prior to a storm, and 2) the mean  $\delta^{18}\text{O}$  value of R samples collected during the recession flow

following the storm. The sample sizes available to calculate means 1 and 2 above ranged from three to eight among the storm events we analyzed. We simulated  $R$  and  $\delta_R$  at a 15-minute time step using TRANSEP for a series of storm events (Table 3.1) that were delineated based on criteria described in section 3.28 below.

### 3.27 Analytical approach 2: hydrograph separation with a two-component mixing model

The second hydrograph-separation technique was a two-component mixing model. While TRANSEP is regarded as the “state-of-the-art” method for tracer-based hydrograph separation, few studies have actually compared the results of TRANSEP with those from two-component mixing models [Lyon *et al.*, 2009; Weiler *et al.*, 2003]. We applied both methods to identify the full range of  $R_e$  estimates that could result based on the contrasting approaches. The two-component mixing model is similarly based on equations 3.2, 3.3, and 3.8 from above. In lieu of the linear-time-invariant convolutions and parameter-optimization scheme, the mixing model solves equation 3.8 for  $R_e$  using measured values of  $R$ ,  $P$ ,  $\delta_R$  and  $\delta_{pe}$  (with  $\delta_{pe}$  varying linearly throughout the storm as described above). The remaining term,  $\delta_e$ , relies on prior calculation of  $p_{eff}$  and the variable  $f$  in the TRANSEP method, but for the two-component mixing model it is calculated as a flux-weighted and time-varying average of the  $\delta^{18}O$  measured sequentially in precipitation (i.e. the event water source):

$$\delta_e(t) = \frac{\sum_{t=0}^t P(t)\delta_P(t)}{\sum_{t=0}^t P(t)} \quad (3.14)$$

The assumptions invoked in the application of the two-component mixing model have been outlined previously [Buttle, 1994; Sklash and Farvolden, 1979], and three are relevant for our application:

- 1) The isotopic composition of the event and pre-event water sources are distinctly different.
- 2) The isotopic composition of event water is constant in time, or temporal variations can be measured and included in equation 3.14 above.

- 3) The isotopic composition of pre-event water is constant in time (at the time-scale of individual precipitation events) and throughout the soil pore space.

The first assumption is generally valid during storm events because of the rainout effect, where the  $\delta$  values in precipitation tend to decline during storms to more negative values than are observed in the streamflow or soil-water drainage. The rainout effect invalidates the second assumption, although temporal variations in  $\delta_e$  can be accounted for by using equation 3.14. The third assumption can rarely be validated unless extensive spatial and temporal sampling of the soil water can be accomplished before and during storms. We observed temporal trends  $\delta_{pe}$  and accounted for them as noted previously.

The two-component mixing model described above is subject to uncertainty due to limits of analytical precision and designation of  $\delta_{pe}$ —the latter being of greatest importance. Genereux [1998] demonstrated how a general equation for error propagation in parameters that are calculated based on multiple independent measurements, when applied to equation 3.8 above, yields the following:

$$W_{f_{pe}} = \left\{ \left[ \frac{f_{pe}}{(\delta_e - \delta_{pe})} W_{\delta_{pe}} \right]^2 + \left[ \frac{f_e}{(\delta_e - \delta_{pe})} W_{\delta_P} \right]^2 + \left[ \frac{-1}{(\delta_e - \delta_{pe})} W_{\delta_R} \right]^2 \right\}^{\frac{1}{2}} \quad (3.15)$$

where  $W_{f_{pe}}$  is the uncertainty associated with the calculated fraction of pre-event water in R; and the other W terms are the uncertainty associated with pre-event water, P, and R. For  $\delta_{pe}$  the measure of uncertainty we used was the mean of the standard deviations of R samples collected in the recession flows that preceded, and followed, a particular storm, multiplied by two. The measure of uncertainty associated with  $\delta_P$  and  $\delta_R$  were the mean analytical precision values reported in section 3.25. Similar to the TRANSEP application, a 15-minute time step was used to calculate  $R_e$  and the associated uncertainty using the two-component mixing model.

### 3.28 Precipitation-event definition and selection

We delineated individual storm events as periods of precipitation separated by a rainless period of at least six hours. If an extended rainless period followed a storm event, the event was considered to continue until R ceased to enable the best estimates of

R to P ratios. In some cases, a new event began while recession flow from the previous event was continuing; in that case we calculated R:P for the full time range encompassing all constituent events.

### 3.3 Results

Four storm events were delineated during February 28<sup>th</sup> to March 20<sup>th</sup>, 2012. These included 126 mm of precipitation for L1bs and L1g, and 134 mm for L10 (11% of total precipitation during the 2011-2012 water year). These storms generated 120, 100, and 99 mm of R from L1bs, L1g, and L10—15, 20, and 21% of their respective annual totals (Figure 3.1A). Sampling was conducted for two additional events for L10 that occurred during December, 2009, and March, 2010. The combined manual and automated sampling [Pangle *et al.*, 2013b] and analysis of stable isotopes in each water flux yielded average sampling rates of 0.83 mm/sample for precipitation and 0.54, 0.47, and 1.34 mm per sample for R from L1bs, L1g, and L10, respectively.  $\delta^{18}\text{O}$  values in precipitation ranged from -3.05 to -21.48 ‰, with a standard deviation of 3.21 ‰. This variability was markedly dampened in the R flux, with ranges of 5.43, 4.36, and 2.28 ‰ and standard deviations of only 0.67, 0.91, and 0.64 ‰ for L1bs, L1g, and L10, respectively. Notably, the standard deviations and ranges in R were largely influenced by the consistently decreasing trend of  $\delta^{18}\text{O}$  values over the entire study period, rather than short-term fluctuations occurring within individual storm events (Figure 3.1B).

The monitored events occurred under continuously high antecedent moisture conditions that were similar among all three lysimeters, as indicated by measurements of volumetric water content at 0.05, 0.15, and 0.75 m soil depth (Figure 3.1C-E). Small differences in volumetric water content existed between the different lysimeters at particular depths, but these were offset typically by opposing differences observed at other depths, for example,  $\theta$  at 0.05 m depth was lower in L1g than in L1bs and L10, but greater at 0.75 m depth. Importantly, all  $\theta$  values at all depths ranged from 0.36 to 0.49 for the entire period of analysis—a range corresponding to maximum pore-water pressures between -10 and 0 kPa gage pressure (i.e. near field saturation; Figure A2.1).

Recharge amount and the  $\delta^{18}\text{O}$  composition of R were simulated reasonably well with the TRANSEP method, and the ratio  $R_e:R$  was consistently low, or zero, among all lysimeters and storm events when estimated with TRANSEP and the two-component mixing model. Figure 3.2 shows the results for the March 12<sup>th</sup> through March 14<sup>th</sup>, 2012 event. Actual and simulated R was greatest under the bare soil condition (32 mm), and decreased to 24 and 21 mm under 0.8- and 5.9-year-old grassland vegetation, respectively. Similarly, the ratio of simulated-effective precipitation to actual precipitation decreased from 0.96 under bare soil to 0.73 and 0.63 under the same two stages of aggrading vegetation (Figure 3.2, row 1). The TRANSEP method simulated totals of R for this event that matched the observed values from each lysimeter to within 2 mm. An average of the Nash-Sutcliffe efficiency index and one minus the root-mean-square error was used as a measure of goodness of fit, and equaled 0.89, 0.86, and 0.86 for L1bs, L1g, and L10, respectively.

TRANSEP also captured transient fluctuations in  $\delta^{18}\text{O}$  that occurred during the rising limb of the hydrograph under the bare soil condition and 0.9-year-old grassland cover, but with less accuracy than the simulated R amounts (averaged Nash-Sutcliffe and 1-RMSE values = 0.27, 0.42, and 0.6), and without accurately simulating the minimum  $\delta^{18}\text{O}$  value observed under the bare soil condition (Figure 3.2, row 2). Both TRANSEP simulations and the two-component mixing-model calculations indicated that event-water contributions to total R were minimal under the bare soil and 0.9-year-old grassland—occurring almost exclusively at the onset of the rising limb of the hydrograph—and negligible under the 5.9-year-old grassland (Figure 3.2, row 3). The TRANSEP results suggested a small but continuous contribution of event-water to total R over several hours, whereas results from the two-component mixing model indicated greater instantaneous contributions of event water to total R, but occurring over much shorter time intervals (Figure 3.2, row 3).

Table 3.1 summarizes the storm characteristics, recharge response to precipitation, flux-weighted mean  $\delta^{18}\text{O}$  values for P and R, and event-water contributions to total R during all storm events that were intensively sampled in during February through March, 2012, and two additional events where intensive manual sampling was conducted from L10 during December, 2009 and March, 2010. These results emphasize

that among all storms and surface conditions the event-water contribution to total R was very small or zero. In fact, detectable event water contributions to total R were only apparent during two storms under bare soil, one storm under 0.8-year-old grassland cover, and not at all under grassland cover ranging in age from 3.8 to 5.9 years. Event-water contributions to total R were always greatest under bare soil—when they occurred at all—and despite the different temporal trends of  $R_e$  estimated with the TRANSEP and mixing-model approaches (Figure 3.2), each method yielded similar magnitudes of  $R_e$ . Similarly, the ratio R:P was consistently greatest under bare soil, and declined by 15-36% under varying stages of grassland aggradation (Table 3.1A-B). The storms that generated these R responses were generally of great intensity for this region, with maximum-hourly precipitation rates that fall within the top 10<sup>th</sup> percentile of those recorded in a 10-year-long precipitation dataset (2002-2012) collected at a climate station located approximately 10 km northeast of our study site [*Bureau of Reclamation*, 2013]. The difference between  $\delta^{18}\text{O}$  in P versus R ranged from 0.86 per mil (L1bs, March 14<sup>th</sup> through 16<sup>th</sup>) to 3.79 per mil (L1bs, March 12<sup>th</sup> through March 14<sup>th</sup>)—resulting in signal to noise ratios ranging from 7.17 to 31.58, where noise is the stated analytical precision.

### 3.4 Discussion

#### 3.41 Why was the event-water contribution to potential recharge negligible?

By excavating new pore space, promoting fractures and aggregation in a fine-textured soil with intrinsic shrinking and swelling tendencies, and through deposition of organic substances within these macropore spaces, the aggradation of a grassland community in a fine-textured silty-clay soil should enhance the likelihood of preferential and rapid water flow through the soil profile [*Jarvis et al.*, 2009]. Nevertheless, our results clearly indicate little to no rapid transfer of event water beyond the root zone (0.95 – 1-m depth) during individual storm events.

While most studies of macropore-flow processes utilize solute tracers, the use of stable isotopes is beneficial here because they are part of the water molecules and reflect directly their transport distances and time scales. This is in contrast to solute tracers that can move at varying rates within the soil-water continuum due to advection and diffusion

[Jones *et al.*, 2006]. Other studies that utilized stable-isotopes and/or hydrograph-separation methods also indicated that flow from lysimeters or drain tiles was dominated by water existing in the soil-pore space prior to the storm event [Stumpp and Malowszewski, 2010; Cullum, 2009]. An alternative approach to infer the relative hydrologic importance of non-equilibrium flow through macropores has been to apply flow models that do, or do not, explicitly account for these processes, and see how well, or poorly, the models simulate measured soil moisture or soil-water pressure measurements, water-table levels, or lysimeter fluxes. Herbst *et al.* [2005] concluded that non-equilibrium macropore flow was a relatively small fraction of total flux from five cropped lysimeters, whereas Cuthbert and Tindimugaya [2010] concluded that preferential flow through macropores was an important mechanism for generating groundwater recharge based on the poor performance of a uniform-flow version of the Richards equation, and on the observation of rapid changes in well-water levels during storms even under very dry antecedent conditions. Our measurements and analyses cannot preclude the occurrence of rapid event water flow through plant-induced macropores, but they do confirm that if this type of flow occurred, it did not occur over sufficiently long duration or depth within the soil profile to comprise a significant fraction of the water that flowed beyond the root zone during individual storm events—the flux that would potentially alter water balance partitioning by contributing to groundwater recharge. Retrospectively, we can identify other attributes of the system and the local hydro-climatology that may explain this result, including 1) relatively low precipitation intensity upon soils with substantial water-storage capacity, 2) the root architecture of the dominant grassland species and the fraction of the soil profile that contained significant root mass, and 3) the potential inhibiting influence of rainfall interception by the plant canopy.

Though relatively large and intense for this region, the storms we analyzed were mostly insufficient to cause rapid translocation (*i.e.* within the time span of a storm event) of event water through the soil profile. For that to occur, event water that infiltrates the soil surface must reach pressures sufficient to enter previously air-filled macropore space—perhaps created by one of the aforementioned plant-related mechanisms—then flow through that pore space, traversing the soil profile before being subject to lateral

infiltration into the smaller-diameter pores of the soil matrix. Several studies have shown the occurrence of these flow processes to be more likely when precipitation is of high intensity and long duration [Gish *et al.*, 2004; Horton and Hawkins, 1965; Williams *et al.*, 2000], because the rapid supply of water at the soil surface maintains high water pressure in the surficial pore space, and the continued supply over long time periods may sustain film flows through the macropore space over longer distances. If event water rapidly traversed the entire soil profile we would expect to see rapid fluctuations in the  $\delta^{18}\text{O}$  composition of recharge that mirror those observed in precipitation, but lagged in time and dampened somewhat depending on the degree of mixing with pre-event water in the soil. Instead, the  $\delta^{18}\text{O}$  of recharge was mostly stable during individual storms and deviated little from the  $\delta^{18}\text{O}$  composition of the pre-event water. These observations, combined with the results of the hydrograph separation analyses, suggest that recharge was generated almost entirely by the displacement of pre-event water that existed in the soil-pore space prior to the storm event [Williams *et al.*, 2002].

The vertical connectivity of root-induced macropore space in this grassland ecosystem may have been insufficient to allow for greater event water transport through the soil profile. The root systems of our mixed-species communities extended to the full depth of the lysimeters, though more than 70% of the total root mass was observed in the upper 0.4 m of the soil, and less than 10% was observed at 0.8-1 m depth (based on annual extraction and sorting of 1" diameter soil cores; data not shown)—a distribution that is similar to those reported for multiple other prairie ecosystems by Schenk and Jackson [2002]. If these root systems did enhance macroporosity in this silty-clay soil, the connectivity of this pore space would likely diminish along with the density of root mass at greater soil depth [Udawatta *et al.*, 2008]. Further, the perennial grass species in these communities comprised much of the ecosystem biomass, and are known to grow dense nets of fibrous roots in relatively shallow soil layers [Grevers and Dejong, 1990], in contrast to tap root systems of species such as alfalfa that excavate macropore space that is both continuous and vertically oriented [Li and Ghodrati, 1994; Mitchell *et al.*, 1995]. One species in this study, *Lupinus albicaulis*, had a tap root system, though it was competitively excluded by the other species over time.

The lack of vertical continuity of plant-induced macropore space, combined with the large water-storage capacity of these soils and the continuously high antecedent moisture conditions may explain why recharge was composed almost entirely of pre-event water. Each intensively-sampled storm event (except the December, 2009 event in L10) produced total rainfall that was less than 10% of the estimated pre-event water storage within the soil profile, and the soils remained near field saturation throughout the duration of this study period (saturation-moisture content based on moisture retention measurements described in Appendix 2). Wet antecedent conditions promote rapid event water movement through the soil profile, as shown in irrigation studies where tracers are sequentially added to the irrigation water, and those added later (i.e. with wetter antecedent moisture conditions) arrive more rapidly at the point of measurement [Jaynes *et al.*, 2001; Kung *et al.*, 2000]. This relationship is equivocal, though, as other reports highlight more rapid flow and transport processes during dry conditions [Hardie *et al.*, 2011; Nimmo, 2012]), particularly in soils where hydrophobic surfaces exist on macropore walls. The wet antecedent conditions observed in our study may have promoted rapid event-water transfer through plant-induced macropores in shallow soil where root density was greatest, but if the connectivity of these macropores was limited at depth, and water supply limited by rainfall intensity and duration, then the event water was likely to adsorbed into the soil matrix before traversing the entire profile [Horton and Hawkins, 1965]. In doing so, the newly infiltrating event water would contribute to the propagation of water-pressure through the soil profile that could readily displace the abundant pre-event water [Williams *et al.*, 2002], much of which was already held a low capillary tension.

Initially we expected interception, storage, and evaporative loss from the aggrading grassland canopies to have a small effect on the recharge response to precipitation, because the grassland species maintain only a small amount of living aboveground biomass during the winter and early spring (leaf area indices near one as late as March; data not shown). However, recharge to precipitation ratios were consistently highest under bare soil and lower under grassland vegetation, and during the March 12<sup>th</sup> – 14<sup>th</sup> storm, when there was an event-water contribution to total recharge, that fraction was greater under bare soil than under the young grassland cover, and zero

under the 5.9-year-old grassland. These results suggest that the reduction of effective precipitation by aboveground biomass had a more hydrologically significant effect than the putative plant-induced changes to the soil hydraulic properties—by reducing recharge to precipitation ratios and the apparent contribution of event water to total recharge during storm events.

### *3.42 Ex post facto analysis of canopy-interception effects on recharge generation*

In light of these results, we performed an ex post facto modeling analysis to evaluate quantitatively whether storage and evaporative loss of water from the grassland canopies could explain the declining recharge to precipitation ratios observed with aggrading vegetation. We used HYDRUS-1D ([Simunek *et al.*, 2012]; finite-element numerical solver of the Richards equation for variably-saturated flow) to simulate the recharge response that was observed during the March 12<sup>th</sup> – 14<sup>th</sup> storm event (Table 3.1, modeling approach detailed in Appendix 2). Keim *et al.* [2006] performed a similar analysis, where they used time-series of measured precipitation and throughfall to find transfer functions that represented the time-evolution of precipitation transfer through mature forest canopies [Keim and Skaugset, 2004], then used these transfer functions to modify the precipitation data that drove a hydrologic model of catchment runoff response. Lacking such data, we modified manually the input precipitation dataset to mimic 1, 4, 7, and 10 mm of interception loss from the grassland canopy—reflecting both water storage in the canopy and evaporative loss of this water during the storm event (Figure 3.3)—then simulated recharge using each modified precipitation time series.

The model accurately simulated the recharge response observed under the bare soil condition (<1 mm error in total R; RMSE = 0.06 mm 15 min<sup>-1</sup>), though with some systematic error during recession flow (Figure A2.2). The results show that by assuming four millimeters of interception loss the timing of the rising limb of the recharge hydrograph was delayed by approximately one hour, and total recharge was reduced by five millimeters relative to the bare-soil simulation where no canopy interception occurred (Figure 3.4). These changes are in good agreement with the approximately one-hour delay in the timing of the observed rising limb, and the observed eight millimeter reduction of total recharge under the 0.9-year-old grassland. Likewise, by simulating 10-

mm of interception loss the rising limb was delayed by about two hours with a 10-mm reduction in simulated recharge, which agreed well with the 1.5-hour delay and 12-mm reduction of total recharge observed for the 5.9-year-old grassland relative to the bare soil (Figure 3.4). The simulations also reveal the internal water-pressure dynamics that contributed to the different recharge responses (Figure 3.5). The storage and evaporative loss of water from the grassland canopies decreased the amount of precipitation that initially infiltrated into the soil, and delayed the formation of large hydraulic gradients that drove the infiltration of existing soil water deeper into the profile. Although the same maximum hydraulic gradient was ultimately reached under bare soil and grassland cover, the peak recharge rate was considerably lower under the 5.9-year-old grassland, partly due to the seepage-face boundary condition at the base of the lysimeters. For drainage to occur the soil water at the seepage face must reach pressures greater than atmospheric pressure, and due to the simulated interception losses and the associated delay in the formation of a large hydraulic gradient in the soil profile, this threshold pressure was also achieved later in time—most importantly, after the time when the peak hydraulic gradient formed (vertical lines on Figure 3.5).

So are the magnitudes of interception loss that we simulated conceivable? Reports from other grassland ecosystems suggest that canopy storage (i.e. the total amount of water that can be absorbed to plant biomass) may range from <1 to >2 mm [Clark, 1940; Couturier and Ripley, 1973; Yu *et al.*, 2012], and a significant amount of that storage can be attributed to accumulated detritus on the soil surface [Couturier and Ripley, 1973]. Some of these estimates of canopy storage in grasslands may be biased toward lower values, because the simple catchment devices used to measure throughfall cannot be located directly under the base of plants, especially the basal area of grasses such as *Festuca romeri* (a prominent species in our grasslands), although this is exactly where most plant tissue is concentrated. Total interception loss, however, includes both storage on live and dead plant matter and evaporative loss from these surfaces that occurs during the storm, and was shown to range from 14-22% of total-annual precipitation in the same systems [Couturier and Ripley, 1973]. Our own data, collected by placing an array of small cups underneath the grassland canopies during storms, indicate interception losses of 4 mm or more are plausible, though there was large variability even

within the small areas under consideration, including some measurements that appear to have been taken in concentrated drip zones where throughfall was actually greater than precipitation (Table 3.2).

We do acknowledge that the simple modifications we made to the precipitation time series for our simulations may skew the temporal dynamics of this interception loss, as they imply that the canopy storage is satiated and all evaporative loss from the canopy occurs at the onset of the storm, and afterward precipitation passes through the saturated canopy. The first 10 mm of precipitation on March 12<sup>th</sup> occurred between 12:00 and 18:00, when average temperature was 8°C and relative humidity was 82%. Hence, the interception and evaporative loss of 10 mm over that time period would seem exceptional unless the true canopy storage was greater than values reported for other grasslands in the literature. Also, while the TDR data indicate that antecedent moisture conditions were generally similar between the bare soil and vegetated lysimeters, these measurements represent a small fraction of the total soil volume, and resolving total antecedent soil-water storage to the order of millimeters is not possible. This leaves open the possibility that small differences in antecedent soil-water storage (i.e. a few millimeters) could have also contributed to the delayed hydrograph response and lower peak flows.

### **3.5 Conclusions and ecohydrological significance of these results**

While plant-induced changes to soil structure have been identified as important mechanisms for generating macropore flow and solute transport in soils [Angers and Caron, 1998; Jarvis, 2007], the effect of these changes on vadose-zone water balance partitioning is poorly understood. We hypothesized that well-documented changes to soil hydraulic properties associated with aggrading grassland vegetation would enhance rapid transport of event water through the soil profile, thus increasing the ratio of potential groundwater recharge to precipitation during individual storm events. Using a lysimeter study with known boundary conditions, high-frequency stable-isotope data, and two hydrograph separation techniques we showed that event-water contributions to potential recharge during storm events were always small or negligible, and actually decreased with aggrading vegetation. A retrospective modeling analysis showed that in this system

the putative belowground influences of aggrading vegetation were trumped by the impact of aboveground biomass on effective precipitation.

Plant-induced changes to soil hydraulic properties have been identified as potentially important determinants of the vadose-zone water balance as they may enhance infiltration of precipitation into the soil—providing soil moisture to support transpiration and ecosystem processes rather than contributing to rapid surface runoff [Bachmair *et al.*, 2012; Price *et al.*, 2010; Thompson *et al.*, 2010; Weiler and Naef, 2003]. Our analyses probed one stratum deeper to evaluate if the same plant-induced changes could enhance potential groundwater recharge, but the evidence contradicted this expectation, showing instead that the accumulation of biomass and detritus aboveground reduced the magnitude and timing of precipitation infiltration into the subsurface and significantly reduced potential recharge to precipitation ratios during storms—even with live LAI values as small as one, and during the wet winter season when vegetation growth was minimal. These contrasting biophysical effects of vegetation have been juxtaposed rarely, and we conclude that their net effect will be conditional on the intensity and duration of typical storms, soil-water storage capacity, root and canopy architecture of the dominant vegetation.

### 3.6 References

Abbaspour, K. C., R. Schulin, and M. T. van Genuchten (2001), Estimating unsaturated soil hydraulic parameters using ant colony optimization, *Adv. Water Resour.*, 24(8), 827-841.

Angers, D. A., and J. Caron (1998), Plant-induced changes in soil structure: processes and feedbacks, *Biogeochemistry*, 42(1-2), 55-72.

Bachmair, S., M. Weiler, and P. A. Troch (2012), Intercomparing hillslope hydrological dynamics: spatio-temporal variability and vegetation cover effects, *Water Resources Research*, 48.

Bengough, A. G. (2012), Water dynamics of the root zone: rhizosphere biophysics and its control on soil hydrology, *Vadose Zone Journal*, 11(2).

- Beven, K. (1981), Microporosity, mesoporosity, macroporosity and channeling flow phenomena in soils, *Soil Sci. Soc. Am. J.*, 45(6), 1245-1245.
- Beven, K., and P. Germann (1982), Macropores and water flow in soils, *Water Resources Research*, 18(5), 1311-1325.
- Beven, K., and P. Germann (2013), Macropores and water flow in soils revisited, *Water Resources Research*, Available online, DOI: 10.1002/wrcr.20156.
- Bronick, C. J., and R. Lal (2005), Soil structure and management: a review, *Geoderma*, 124(1-2), 3-22.
- Bruand, A., I. Cousin, B. Nicoullaud, O. Duval, and J. C. Begon (1996), Backscattered electron scanning images of soil porosity for analyzing soil compaction around roots, *Soil Sci. Soc. Am. J.*, 60(3), 895-901.
- Bureau of Reclamation, Dept. of the Interior, The Pacific Northwest Cooperative Agricultural Weather Network, <http://www.usbr.gov/pn/agrimet/>, accessed June, 2013.
- Buttle, J. M. (1994), Isotope hydrograph separations and rapid delivery of pre-event water from drainage basins, *Prog. Phys. Geogr.*, 18(1), 16-41.
- Caron, J., B. D. Kay, and J. A. Stone (1992), Improvement of structural stability of a clay loam with drying, *Soil Sci. Soc. Am. J.*, 56(5), 1583-1590.
- Clark, O. R. (1940), Interception of rainfall by prairie grasses, weeds, and certain crop plants, *Ecol. Monogr.*, 10(2), 243-277.
- Couturier, D. E., and E. A. Ripley (1973), Rainfall interception in mixed grass prairie, *Canadian Journal of Plant Science*, 53(3), 659-663.
- Cullum, R.F. (2009), Macropore flow estimations under no-till and till systems, *Catena*, 78(1), 87-91.
- Cuthbert, M.O., C. Tindimugaya (2010), The importance of preferential flow in controlling groundwater recharge in tropical Africa and implications for modelling the impact of climate change on groundwater resources, *Journal of Water and Climate Change*, 1(4), 234-245.
- Dexter, A. R. (1987), Compression of soil around roots, *Plant Soil*, 97(3), 401-406.

- Dragila, M.-I., and S. W. Wheatcraft (2001), Free Surface Films, in *Conceptual Models of Flow and Transport in the Fractured Vadose Zone*, edited, pp. 217-241, National Research Council, National Academy Press, Washington, D.C.
- Edwards, W. M., L. D. Norton, and C. E. Redmond (1988), Characterizing macropores that affect infiltration into nontilled soil, *Soil Sci. Soc. Am. J.*, 52(2), 483-487.
- Ellerbrock, R. H., and H. H. Gerke (2004), Characterizing organic matter of soil aggregate coatings and biopores by Fourier transform infrared spectroscopy, *Eur. J. Soil Sci.*, 55(2), 219-228.
- Gee, G. W., and J. W. Bauder (1986), Particle-size Analysis, in *Methods of Soil Analysis. Part 1. Physical and Mineralogical Methods*, edited by E. A. Klute, American Society of Agronomy-Soil Science Society, Madison, WI.
- Genereux, D. (1998), Quantifying uncertainty in tracer-based hydrograph separations, *Water Resources Research*, 34(4), 915-919.
- Ghestem, M., R. C. Sidle, and A. Stokes (2011), The influence of plant root systems on subsurface flow: implications for slope stability, *Bioscience*, 61(11), 869-879.
- Gish, T. J., K. J. S. Kung, D. C. Perry, J. Posner, G. Bubenzer, C. S. Helling, E. J. Kladviko, and T. S. Steenhuis (2004), Impact of preferential flow at varying irrigation rates by quantifying mass fluxes, *J. Environ. Qual.*, 33(3), 1033-1040.
- Grevers, M. C. J., and E. Dejong (1990), The characterization of soil macroporosity of a clay soil under 10 grasses using image-analysis, *Can. J. Soil Sci.*, 70(1), 93-103.
- Hardie, M. A., W. E. Cotching, R. B. Doyle, G. Holz, S. Lisson, and K. Mattern (2011), Effect of antecedent soil moisture on preferential flow in a texture-contrast soil, *J. Hydrol.*, 398(3-4), 191-201.
- Herbst, M., W. Fialkiewicz, T. Chen, T. Putz, D. Thiery, C. Mouvet, G. Vachaud, and H. Vereecken (2005), Intercomparison of flow and transport models applied to vertical drainage in cropped lysimeters, *Vadose Zone Journal*, 4(2), 240-254.
- Horton, J. H., and R. H. Hawkins (1965), Flow path of rain from the soil surface to the water table, *Soil Sci.*, 100(6), 377-383.
- Jakeman, A. J., and G. M. Hornberger (1993), How much complexity is warranted in a rainfall-runoff model, *Water Resources Research*, 29(8), 2637-2649.

- Jarvis, N. J. (2007), A review of non-equilibrium water flow and solute transport in soil macropores: principles, controlling factors and consequences for water quality, *Eur. J. Soil Sci.*, 58(3), 523-546.
- Jarvis, N. J., J. Moeys, J. M. Hollis, S. Reichenberger, A. M. L. Lindahl, and I. G. Dubus (2009), A conceptual model of soil susceptibility to macropore flow, *Vadose Zone Journal*, 8(4), 902-910.
- Jastrow, J. D. (1987), Changes in soil aggregation associated with tallgrass prairie restoration, *American Journal of Botany*, 74(11), 1656-1664.
- Jaynes, D. B., S. I. Ahmed, K. J. S. Kung, and R. S. Kanwar (2001), Temporal dynamics of preferential flow to a subsurface drain, *Soil Sci. Soc. Am. J.*, 65(5), 1368-1376.
- Johnson, M. S., and J. Lehmann (2006), Double-funneling of trees: Stemflow and root-induced preferential flow, *Ecoscience*, 13(3), 324-333.
- Jones, J. P., E. A. Sudicky, A. E. Brookfield, and Y. J. Park (2006), An assessment of the tracer-based approach to quantifying groundwater contributions to streamflow, *Water Resources Research*, 42(2), W02407.
- Keim, R. F., and A. E. Skaugset (2004), A linear system model of dynamic throughfall rates beneath forest canopies, *Water Resources Research*, 40(5).
- Keim, R. F., H. Meerveld, and J. J. McDonnell (2006), A virtual experiment on the effects of evaporation and intensity smoothing by canopy interception on subsurface stormflow generation, *J. Hydrol.*, 327(3-4), 352-364.
- Kennedy, V. C., G. W. Zellweger, and R. J. Avanzino (1979), Variations of rain chemistry during storms at two sites in Northern California, *Water Resources Research*, 15, 687-702.
- Kirchner, J. W., X. H. Feng, and C. Neal (2000), Fractal stream chemistry and its implications for contaminant transport in catchments, *Nature*, 403(6769), 524-527.
- Kung, K. J. S., E. J. Kladvik, T. J. Gish, T. S. Steenhuis, G. Bubenzer, and C. S. Helling (2000), Quantifying preferential flow by breakthrough of sequentially applied tracers: Silt loam soil, *Soil Sci. Soc. Am. J.*, 64(4), 1296-1304.
- Lange, B., P. Luescher, and P. F. Germann (2009), Significance of tree roots for preferential infiltration in stagnant soils, *Hydrol. Earth Syst. Sci.*, 13(10), 1809-1821.

Li, Y. M., and M. Ghodrati (1994), Preferential transport of nitrate through soil columns containing root channels, *Soil Sci. Soc. Am. J.*, 58(3), 653-659.

Luxmoore, R. J. (1981), Microporosity, mesoporosity, and macroporosity of soil, *Soil Sci. Soc. Am. J.*, 45(3), 671-672.

Lyon, S. W., S. L. E. Desilets, and P. A. Troch (2009), A tale of two isotopes: differences in hydrograph separation for a runoff event when using delta D versus delta O-18, *Hydrol. Process.*, 23(14), 2095-2101.

Macleod, C. J. A., A. Binley, S. L. Hawkins, M. W. Humphreys, L. B. Turner, W. R. Whalley, and P. M. Haygarth (2007), Genetically modified hydrographs: what can grass genetics do for temperate catchment hydrology?, *Hydrol. Process.*, 21(16), 2217-2221.

Maloszewski, P., and A. Zuber (1982), Determining the turnover time of groundwater systems with the aid of environmental tracers 1: models and their applicability, *J. Hydrol.*, 57(3-4), 207-231.

Materechera, S. A., A. R. Dexter, and A. M. Alston (1992), Formation of aggregates by plant-roots in homogenized soils, *Plant Soil*, 142(1), 69-79.

Mitchell, A. R., T. R. Ellsworth, and B. D. Meek (1995), Effect of root systems on preferential flow in swelling soil, *Commun. Soil Sci. Plant Anal.*, 26(15-16), 2655-2666.

Nash, J. E., and J. V. Sutcliffe (1970), River flow forecasting through conceptual models part 1 - A discussion of principles, *J. Hydrol.*, 10(3), 282-290.

Nimmo, J. R. (2007), Simple predictions of maximum transport rate in unsaturated soil and rock, *Water Resources Research*, 43(5).

Nimmo, J. R. (2012), Preferential flow occurs in unsaturated conditions, *Hydrol. Process.*, 26(5), 786-789.

Noguchi, S., Y. Tsuboyama, R. C. Sidle, and I. Hosoda (1997), Spatially distributed morphological characteristics of macropores in forest soils of Hitachi Ohta Experimental Watershed, Japan, *Journal of Forest Research*, 2(4), 207-215.

Pangle, L. A., J. W. Gregg, and J. J. McDonnell (2013a), Seasonal rainfall and an ecohydrological feedback offset the potential impact of climate warming on evapotranspiration and groundwater recharge, *Water Resources Research*, *In Review*.

- Pangle, L. A., J. Klaus, E. S. F. Berman, M. Gupta, and J. J. McDonnell (2013b), A new multi-source and high-frequency approach to measuring  $\delta^2\text{H}$  and  $\delta^{18}\text{O}$  in hydrological field studies, *Water Resources Research, In Review*.
- Phillips, C. L., J. W. Gregg, and J. K. Wilson (2011), Reduced diurnal temperature range does not change warming impacts on ecosystem carbon balance of Mediterranean grassland mesocosms, *Glob. Change Biol.*, 17(11) 3263-3273.
- Price, K., C. R. Jackson, and A. J. Parker (2010), Variation of surficial soil hydraulic properties across land uses in the southern Blue Ridge Mountains, North Carolina, USA, *J. Hydrol.*, 383(3-4), 256-268.
- Rasse, D. P., A. J. M. Smucker, and D. Santos (2000), Alfalfa root and shoot mulching effects on soil hydraulic properties and aggregation, *Soil Sci. Soc. Am. J.*, 64(2), 725-731.
- Rillig, M. C., S. F. Wright, and V. T. Eviner (2002), The role of arbuscular mycorrhizal fungi and glomalin in soil aggregation: comparing effects of five plant species, *Plant Soil*, 238(2), 325-333.
- Schenk, H. J., and R. B. Jackson (2002), The global biogeography of roots, *Ecol. Monogr.*, 72(3), 311-328.
- Simunek, J., M. Sejna, H. Saito, M. Sakai, and M. T. Van Genuchten (2012), The HYDRUS-1D software package for simulating the movement of water, heat, and multiple solutes in variably saturated media, Version 4.15, *HYDRUS Software Series*, 3, Department of Environmental Sciences, University of California Riverside, Riverside, California, USA, .
- Stumpp, C. and P. Maloszewski (2010), Quantification of preferential flow and flow heterogeneities in an unsaturated soil planted with different crops using the environmental isotope delta O-18, *Journal of Hydrology*, 394(3-4), 407-415.
- Thompson, S. E., C. J. Harman, P. Heine, and G. G. Katul (2010), Vegetation-infiltration relationships across climatic and soil type gradients, *J. Geophys. Res.-Biogeosci.*, 115.
- Tippkötter, R. (1983), Morphology, spatial arrangement and origin of macropores in some hapludalfs, West-Germany, *Geoderma*, 29(4), 355-371.
- Udawatta, R. P., S. H. Anderson, C. J. Gantzer, and H. E. Garrett (2008), Influence of prairie restoration on CT-measured soil pore characteristics, *J. Environ. Qual.*, 37(1), 219-228.

Weiler, M., and F. Naef (2003), An experimental tracer study of the role of macropores in infiltration in grassland soils, *Hydrol. Process.*, 17(2), 477-493.

Weiler, M., B. L. McGlynn, K. J. McGuire, and J. J. McDonnell (2003), How does rainfall become runoff? A combined tracer and runoff transfer function approach, *Water Resources Research*, 39(11).

Williams, A., D. Scholefield, J. Dowd, N. Holden, and L. Deeks (2000), Investigating preferential flow in a large intact soil block under pasture, *Soil Use and Management*, 16(4), 264-269.

Williams, A. G., J. F. Dowd, and E. W. Meyles (2002), A new interpretation of kinematic stormflow generation, *Hydrol. Process.*, 16, 2791-2803.

Yu, K. L., T. G. Pypker, R. F. Keim, N. Chen, Y. B. Yang, S. Q. Guo, W. J. Li, and G. Wang (2012), Canopy rainfall storage capacity as affected by sub-alpine grassland degradation in the Qinghai-Tibetan Plateau, China, *Hydrol. Process.*, 26(20), 3114-3123.

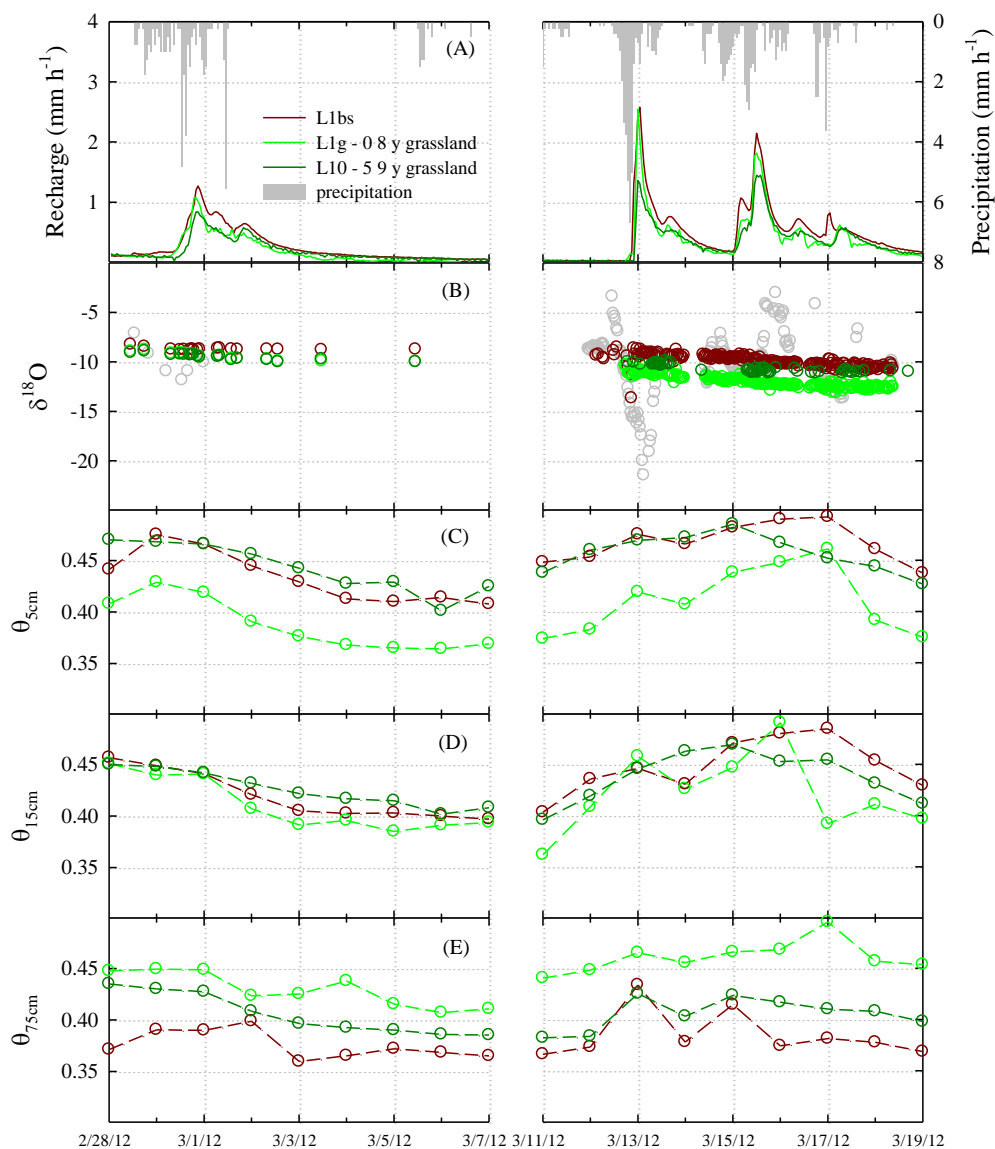


**Figure 3.1** (A) Time series of precipitation and recharge for each lysimeter from February 28<sup>th</sup> to March 19<sup>th</sup>, 2012. (B)  $\delta^{18}\text{O}$  composition of each water flux over the same time period (C-E) Volumetric soil moisture at 5, 15, and 75 cm soil depth. The x-axis break spans from March 7<sup>th</sup> to March 11<sup>th</sup>—a period with no precipitation.

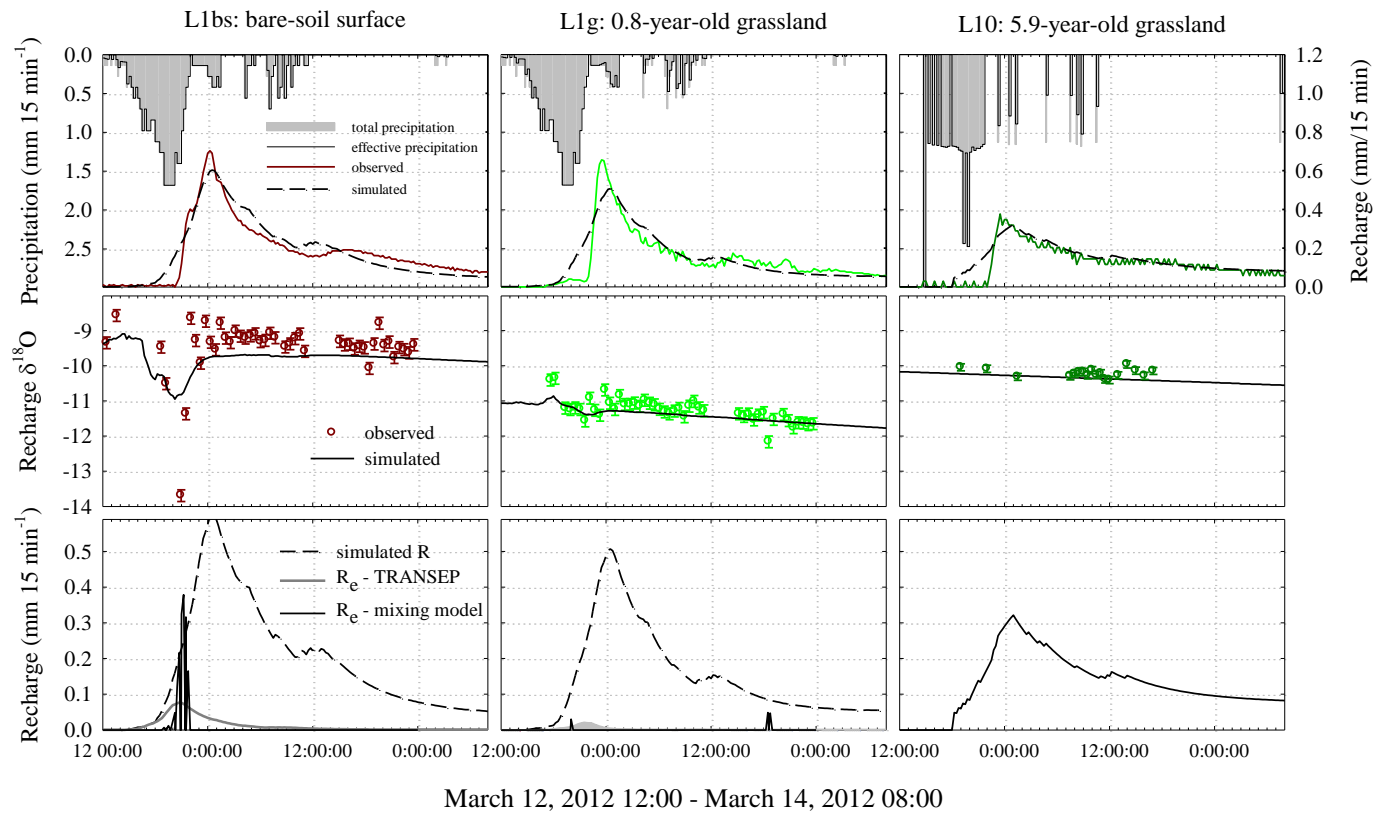


**Figure 3.2** (Row 1) Time series of observed precipitation and recharge, and simulated effective precipitation and recharge using the TRANSEP approach for L1bs, L1g, and L10 (columns 1, 2, and 3, respectively). (Row 2) Time series of observed and simulated  $\delta^{18}\text{O}$  in recharge. Error bars indicate the analytical precision as defined in section 3.25. (Row 3) Time series of recharge and the event-water contribution to recharge as simulated with TRANSEP, and calculated using a two-component mixing model.

	Grassland Age (y)	Time Range	P (mm)	$P_{\max}$ (mm h <sup>-1</sup> )	R:P	$\overline{\delta^{18}O_P}$	$\overline{\delta^{18}O_R}$	R <sub>e</sub> :R - TRANSEP	R <sub>e</sub> :R - Mixing Model
(A)	bs	2/28/12 11:30	36	3.8	0.97	-10.49	-8.72	0.00	0.00
	0.8	–	36	3.8	0.82	-10.49	-9.44	0.00	0.00
	5.9	3/5/12 00:00	37	3.6	0.82	-10.49	-9.50	0.00	0.00
	bs	3/12/12 12:00	38	6.7	0.95	-13.27	-9.48	0.04	0.06 (0.05-0.06)
	0.8	--	38	6.7		-13.27	-11.19	0.01	0.01 (0.00-0.01)
	5.9	3/14/2012 8:00	41	7.4		-13.27	-10.08	0.00	0.00
	bs	3/14/12 8:00	37	3.4	0.79	-9.03	-9.89	0.00	0.03 (0.01-0.03)
	0.8	--	37	3.4		-9.03	-11.16	0.00	0.00
	5.9	3/16/2012 16:00	40	3.6		-9.03	-10.02	0.00	0.00
	bs	3/16/12 16:00	15	3.9	0.71	-9.89	-10.46	0.00	0.00
	0.8	--	15	3.9		-9.89	-12.58	0.00	0.00
	5.9	3/19/2012 22:00	16	3.7		-9.89	-11.05	0.00	0.00
	3.8	12/14/09 – 12/19/09	67	4.4	0.66	-12.04	-8.33	0.00	0.00
	3.9	3/11/10 – 3/20/10	37	4.7	0.57	-8.18	-8.88	0.00	0.00
	(B)	bs	3/20/12 – 3/25/12	58	4.2	0.99			na
0.8		3/20/12 – 3/25/12	58	4.2	0.66			na	na
5.9		3/20/12 – 3/25/12	64	8.1	0.63			na	na

**Table 3.1** (A) Summary of storm characteristics and recharge response observed in L1bs, L1g, and L10, including recharge to precipitation ratios and the fraction of recharge that was contributed by event water (simulated using TRANSEP and calculated using a two-component mixing model with error bounds in parentheses). A single R:P ratio is reported for the three storm events occurring from March 12<sup>th</sup> through March 19<sup>th</sup> since recession flow never completely ceased between events. (B) Storm characteristics and R:P ratios for an additional storm occurring from March 20<sup>th</sup> to March 25<sup>th</sup>, 2012 (no isotope data collected for this event).

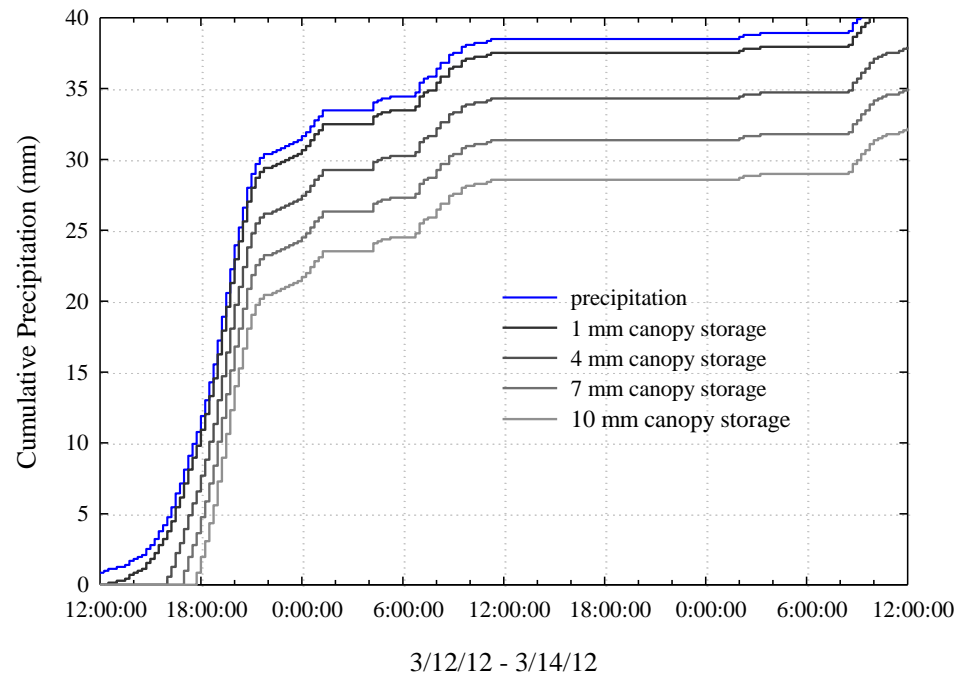


**Figure 3.3** Time series of cumulative precipitation and modified time series of cumulative precipitation based on varying levels of assumed interception loss (combined water storage and evaporation from the plant canopy).

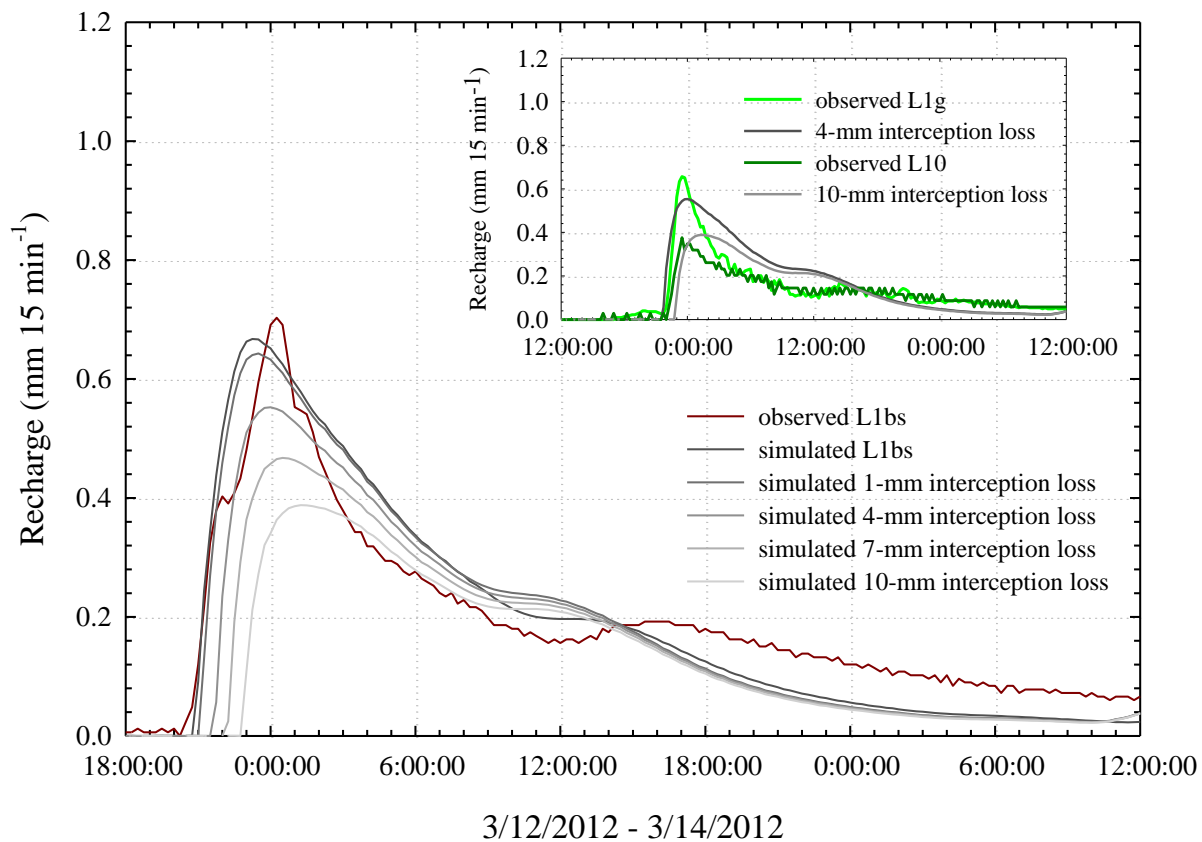


**Figure 3.4** Observed and simulated recharge under bare soil (L1bs), and simulated recharge driven by precipitation time series that were modified to reflect varying magnitudes of interception loss from a plant canopy. The inset shows the observed recharge under 0.8-year-old grassland (L1g) and 5.9-year-old grassland (L10) compared to simulated recharge assuming four and ten millimeters of interception loss.

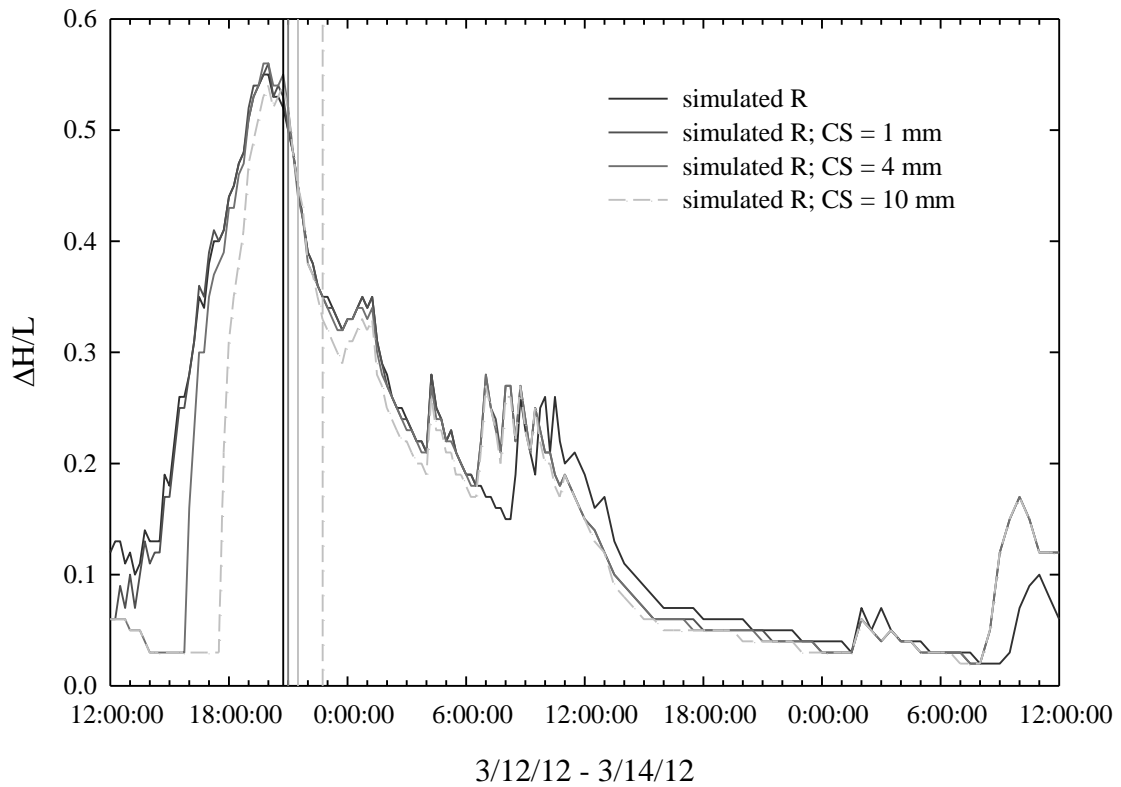


**Figure 3.5** Time series of the hydraulic gradient occurring from the soil surface to the base of the soil profile during the rainfall-recharge event occurring from March 12<sup>th</sup> through March 14<sup>th</sup>, 2012. Different time series represent the simulated hydraulic gradients assuming various interception losses from the aggrading grassland canopies. Vertical lines indicate the time at which the threshold pressure ( $h=0$ ) needed to initiate drainage was exceeded at the bottom boundary of the simulated soil profile.

	P (mm)	<u>L1g interception loss (mm)</u> median (1 <sup>st</sup> , 3 <sup>rd</sup> quartile)	<u>L10 interception loss (mm)</u> median (1 <sup>st</sup> , 3 <sup>rd</sup> quartile)
4/3/12 – 4/5/12	18.2	3.8 (-1.9, 6.3)	na
4/15/12 – 4/17/12	11.2	4.1 (0.8, 5.4)	na
4/25/12 – 4/27/12	9.2	3.1 (0.1, 5.4)	na
11/16/12 – 11/19/12	43.9	8.1 (3.6, 14)	na
6/17/13 – 6/20/13	4.2	3.8 (0.3, 4.1)	4.2 (-1.3, 4.2)
6/22/13 – 6/27/13	21.3	5.2 (-0.5, 5.8)	8.2 (1.2, 17.7)

Table 3.2 Total precipitation and interception loss from the L1g (0.9 - >2 year-old grassland) and L10 (>7-year-old grassland at the time of measurement) during six storms. Interception loss was calculated as the difference between total precipitation and the amount of precipitation collected in small cups (18 cm<sup>2</sup> surface area) placed beneath the plant canopy. The median and inter-quartile range are reported based on a sample size of 18 cups.

**4. EFFECTS OF VEGETATION ESTABLISHMENT ON SOIL-WATER  
BALANCE, FLOW AND TRANSIT TIME**

Luke A. Pangle

Jillian W. Gregg

Jeffrey J. McDonnell

## 4.1 Introduction

The effects of vegetation on transit times of water flow through soils are poorly understood. Nevertheless, soil-water transit times have key hydrological, biogeochemical, and ecological significance. The mean and distribution of soil-water transit times are indicative of the complexity of flow-path lengths that exist in the subsurface and are useful for comparative analysis of soils [Maloszewski *et al.*, 2006] and catchments [McGuire and McDonnell, 2006]. Soil-water transit times also influence soil-solution chemistry [Bastviken *et al.*, 2006], mass export into streams [Johnson *et al.*, 2007; van der Velde *et al.*, 2010], and the balance of infiltrating precipitation that may be available to support ecosystem productivity versus contributions to groundwater recharge or runoff.

The transit time of water flow through soils is defined as the difference between the exit-time of a water molecule from the soil and its entry time during a precipitation event. Whereas the stream channel defines the exit point from an entire catchment, quantifying the transit times that are specific to the soil requires a clearly defined boundary where exit times can be measured. This boundary is well defined for soils contained within lysimeters. To date, studies of transit times through soils contained within lysimeters have focused on the variability in mean-transit times as influenced by physical and hydraulic properties of the soil. For example, mean-transit times ranged from 7.5 to 59 weeks among a series of 1.5-2 m deep lysimeters containing gravel, sand, and loamy sand soil types at sites in Germany and Austria [Maloszewski *et al.*, 2006; Stumpp *et al.*, 2009a; Stumpp *et al.*, 2009b]. Vitvar and Balderer [1997] reported a mean-transit time of 26 weeks in a 2 m deep lysimeter in Switzerland that contained soil purportedly with an extensive macropore network.

In natural catchments, suction lysimeters have been used to sample a time series of water isotopes to compute soil-water mean-residence time (defined as the current time minus entry time). Such soil-water mean-residence times have ranged from 1-10 weeks at sampling depths ranging from 0.2 – 0.9 m [Asano *et al.*, 2002; McGuire and McDonnell, 2010; Stewart and McDonnell, 1991], though Muñoz-Villers [2012] reported a longer mean-residence time of six months for soil waters sampled at 1.2 m depth in a

mountain cloud forest with extremely permeable soils. In general, finer-textured soils with smaller diameter and more tortuous pore space may contribute to longer transit times, and higher rainfall amounts and intensities may cause shorter transit times

However, we still do not know the influence of vegetation on soil-water transit times. For instance, the growth and expansion of plant root systems may alter soil physical and hydraulic properties in ways that enhance rapid transport processes through soil macropores [*Angers and Caron, 1998; Jarvis, 2007*]. This phenomenon has been reported on widely in agricultural systems, often under ponded infiltration or irrigation applied over relatively short time periods, but the impact of plant root systems on mean-transit times in uncultivated soils and under natural precipitation regimes has not been investigated. Thompson et al. [2010] confirmed the strong relationship between aboveground plant biomass and infiltration rates in arid environments, where this alteration of soil hydraulics may enhance survivorship among plants, but found no strong evidence for a similar relationship in more humid environments. However, they examined only aboveground biomass, not roots, and whether plant-induced changes to soil hydraulics affect mean-transit times when considering the full depth of the soil profile is unknown.

Intuitively, and based on recent modeling analyses [*Botter et al., 2010; 2011; Heidbuchel et al., 2012; Rinaldo et al., 2011; van der Velde et al., 2012*], soil-water transit times are expected to be conditional on overall water budget partitioning, which is controlled by plant physiological function and root expansion. Plant transpiration and root uptake control the amount and distribution stored-soil water prior to storms—a key factor that influences whether newly infiltrating precipitation is adsorbed and stored within the soil pore space over long periods, or is rapidly transmitted through the soil profile. Works by [*Stumpp et al., 2009a; Stumpp et al., 2009b*] showed that mean-transit times of subsurface flow were very sensitive to the timing of crop rotations and variation in water-balance partitioning induced by different crop types, though the explanatory mechanism for these differences was not explicitly resolved.

To address the role of vegetation, field-based studies are needed that show how soil-water transit times are affected by the establishment and growth of vegetation communities. Pangle ([2013]; Chapter 3 of this document) utilized a controlled field

experiment that included three lysimeters with identical soil materials, but with surface conditions including bare soil and two stages of aggrading grassland vegetation. This enabled a comparison of subsurface flow processes occurring during individual storm events, where differences could be attributed to vegetation establishment and growth. Here we use the same field experiment to examine how vegetation influences transit times of soil water occurring over the entire water year. Our objectives are to 1) quantify soil-water transit times and the soil-water balance under each surface condition, 2) determine if soil alteration by root growth and expansion is a plausible mechanism that affects soil-water transit times, and 3) to evaluate how vegetation effects on the soil-water balance influence soil-water transit times.

## **4.2 Materials and Methods**

### *4.21 Site description and hydrometric data collection*

This work was conducted at the Terracosm facility in Corvallis, OR, USA [Phillips *et al.*, 2011]. We utilized a series of three lysimeters with surface conditions including bare soil (L1bs), and grassland ecosystems ranging in age from less than one to six years (L1g and L10). The lysimeter design, soils, and vegetation were described in sections 3.21-3.23 of this document. This work also relied on the same hydrometric measurements described in section 3.24, although the record of precipitation used in this analysis was measured with a tipping bucket gage (Hydrological Services Ltd., New South Wales, UK) at a weather station located approximately 10 km northeast of the study site [Bureau of Reclamation, 2013].

### *4.22 Stable isotope sampling and analysis*

Samples of precipitation were collected at the research site from late September, 2009 until June, 2012 using a sequential-sampling device similar to that presented by Kennedy *et al.* [1979], and described in section 3.25 of this document. The soil water draining from the lysimeter base was a reasonable proxy for potential groundwater recharge—given that local water-table levels are shallow during the wet winter in this environment, and since this water had percolated beyond the rooting zone—and is

hereafter referred to more simply as recharge, R. Recharge was sampled from L10 over the same period as precipitation, and from March, 2011 until June, 2012 from L1bs and L1g. Samples from L10 were collected in a plastic bottle that was attached to the outflow-tube from the lysimeter base; those from L1bs and L1g were collected in a closed plastic container with an attached funnel that channeled water flowing directly out of the tipping bucket gage. The ratio  $^{18}\text{O}:^{16}\text{O}$  (and  $^2\text{H}:^1\text{H}$ ) in water samples was measured with a Los Gatos Research Liquid Water Isotope Analyzer (Los Gatos Research, Mountain View, CA). Isotopic ratios were converted to  $\delta$  notation and reported in per mil values [‰, parts per thousand relative to an external standard] using the Vienna Standard Mean Ocean Water (VSMOW):

$$\delta^{18}\text{O} = \left( \frac{^{18}\text{O}:^{16}\text{O}_{\text{sample}}}{^{18}\text{O}:^{16}\text{O}_{\text{vsmow}}} - 1 \right) \times 1000 \quad (4.1)$$

The analytical accuracy was limited by the accuracy of the external standards, which was +/- 1 and 0.2 ‰ for  $\delta^2\text{H}$  and  $\delta^{18}\text{O}$ , respectively. Among all analyses included here, the mean analytical precision was 0.36 (range = 0.06 – 0.67) and 0.08 (range = 0.02 – 0.10) ‰ for  $\delta^2\text{H}$  and  $\delta^{18}\text{O}$ , respectively—quantified as the sample-standard-deviation of all measured external standard values multiplied by two.

#### 4.23 Estimation of soil-water transit times

We quantified the mean and distribution of transit-times of water molecules that traversed the soil profile using the linear-time-invariant convolution approach (LTIC). The conceptual underpinning of this approach (using notation specific to this analysis and  $\delta^{18}\text{O}$  as a conservative tracer) can be described as follows: the temporal variation of  $\delta^{18}\text{O}$  in recharge,  $\delta^{18}\text{O}_R$ , will mimic the temporal variation of  $\delta^{18}\text{O}$  in precipitation,  $\delta^{18}\text{O}_P$ , but lagged in time, and weighted by a transit-time-distribution function,  $g(\tau)$ , as shown below:

$$\delta^{18}\text{O}_R(t) = \int_0^t \delta^{18}\text{O}_P(t) \cdot g(t-\tau) d\tau \quad (4.2)$$

The transit-time-distribution function is a probability-density function with the independent variable,  $\tau$ , representing the range of times that water molecules may take to traverse the soil profile—indicative of the complexity of flow paths that exist in the soil-pore space—and the function describes the probability of each incremental transit time. We used a solution of the advection-dispersion equation [Kreft and Zuber, 1978; Maloszewski and Zuber, 1982] to represent  $g(\tau)$ :

$$g(\tau) = \left[ \left( \frac{4\pi\tau D}{vxT} \right)^{-\frac{1}{2}} \exp \left[ -\frac{T \left( 1 - \frac{\tau}{T} \right)^2 vx}{4D\tau} \right] \right] \tau^{-\frac{1}{2}} \quad (4.3)$$

where the parameter,  $T$ , represents the mean-transit time of water flowing through soil, and the parameter,  $D/vx$ , is a dimensionless number that describes the ratio of diffusive to advective transport within the soil (i.e. the inverse of the commonly known Peclet number). Figure 4.1 illustrates how the shape of this distribution changes given a constant  $T$  of 50 days, and  $D/vx$  ranging from 0.001 to 0.3.

The convolution of  $\delta^{18}\text{O}_p$  with equation 4.3 is a linear calculation, and based on the fundamental assumption that the transit-time distribution is time invariant; that is, its shape (defined by  $T$  and  $D/vx$ ) does not change despite varying precipitation rates and soil-water storage conditions. This assumption is not valid generally for water flow in variably-saturated soils because of the highly non-linear relationships between water content, water pressure, and effective conductivity. Nevertheless, in our Mediterranean climate soil-water content and water pressure are maintained at quasi-steady-state conditions during the wet winter season (i.e. soil-water contents at or near field saturation and soil water matric potential greater than -10 kPa for most of the time) when temperature and evaporative demand are consistently low, and rainfall is frequent. Since recharge from the soil volume occurs exclusively during this wet season, the LTIC approach can be reasonably applied in this system.

The time-invariance assumption can be further addressed by using a weighting function to delineate precipitation that occurs during quasi-steady-state conditions and effectively contributes to groundwater recharge, as opposed to being evaporated back into

the atmosphere or filling micropore space in the soil where it would be rendered relatively immobile [Brooks *et al.*, 2010]. We use the weighting function shown to be effective by [Stumpp *et al.*, 2009a], whereby the total precipitation during a time-step is reduced by the magnitude of evapotranspiration occurring during the same time. The  $\delta^{18}\text{O}_p$  time series used as input to equation 4.2 is then modified to  $\delta^{18}\text{O}_{\text{Peff}}$  as follows:

$$\delta^{18}\text{O}_{\text{Peff}}(t_i) = \frac{N \cdot P_{\text{eff},i}}{\sum_{i=1}^N P_{\text{eff},i}} \cdot (\delta^{18}\text{O}_{P,i} - \overline{\delta^{18}\text{O}_R}) + \overline{\delta^{18}\text{O}_R} \quad (4.4)$$

where N is the total number of time steps, and  $P_{\text{eff}}$  at each time step is calculated as:

$$P_{\text{eff},i} = P_i - ET_{o,i} \quad (4.5)$$

where  $ET_o$  is the calculated evapotranspiration for a reference grass canopy following the method described by Allen *et al.* [1998] and applied previously at this site by Pangle [2013]. The use of this simplified estimate was necessary since the lysimeters were non-weighing and actual ET could not be calculated at the weekly time step used in the application of equation 4.2. If equation 4.5 yielded a negative value, the absolute value of this difference was assumed to reduce  $P_{\text{eff}}$  during the previous week (or weeks), following the procedure below until  $P_{\text{eff},i}$  was equal to zero:

$$P_{\text{eff},i} = (P_i + P_{i-1} + \dots + P_{i-j}) - ET_{o,i} \quad (4.6)$$

During the dry summer period this recursive reduction of  $P_{\text{eff}}$  often spanned several weeks prior. We enforced a threshold value for j that was unique to each lysimeter so that  $P_{\text{eff}}$  for the entire year was similar to the observed annual recharge amount. This method represents a simple, data-based, and physically plausible way to delineate the fraction of total precipitation that contributes to recharge based on the hydroclimatic conditions that follow the precipitation event. A final manual adjustment to the  $P_{\text{eff}}$  time series was made based on observed soil moisture data (shown later in Figure 4.5), whereby  $P_{\text{eff}}$  was set to zero prior to November 21, 2011 for L1g and L10, and prior to

October 17, 2011 for L1bs. The difference in timing was based on the observation of when volumetric-water content at the measured depths of 0.05, 0.15, and 0.75 m all exceeded 0.25. This was the average value of volumetric-water content that corresponded with soil-matric potential of -10 kPa (Appendix 2, Figure A2.1). This manual adjustment was based on the assumption that precipitation that occurred at the onset of the rain season, when soil moisture levels had not yet reached quasi-steady state, would have filled much of the smallest-diameter and least conductive pore space that was vacated by evaporation and transpiration during the summer drought period, thus reducing the likelihood that its specific  $\delta^{18}\text{O}$  signature would influence the  $\delta^{18}\text{O}$  observed in recharge.

The methodology outlined above was applied to simulate  $\delta^{18}\text{O}_R$  in recharge from each lysimeter during the 2011-2012 water year. Previous applications of this method have shown that records of  $\delta^{18}\text{O}_P$  that occurred prior to the study period are needed [Hrachowitz *et al.*, 2011], because the  $\delta^{18}\text{O}_R$  measured in the initial outflow (here R, in other cases streamflow) may be influenced by the  $\delta^{18}\text{O}$  signature of precipitation that occurred prior to the measurement period, but has persisted in the subsurface and may still influence  $\delta^{18}\text{O}_R$  during the measurement period. To account for this possibility, we used measured precipitation and  $\delta^{18}\text{O}_P$  from September, 2009 through June, 2011, appended to the same data sets from September, 2011 through June, 2012, to simulate  $\delta^{18}\text{O}_R$  from December, 2011 through April, 2012 for L10. L1bs and L1g were fully saturated with local tap water prior to their first exposure to actual precipitation in March, 2011. For these two lysimeters we used measured precipitation amount from October, 2010 through May, 2012, the known  $\delta^{18}\text{O}$  composition of the tap water for the time preceding March, 2011, and measured values of  $\delta^{18}\text{O}_P$  thereafter to simulate  $\delta^{18}\text{O}_R$  from November, 2011 through May, 2012. Though L1bs and L1g were not actually receiving incident precipitation from October, 2010 through February, 2011, using measured precipitation amount and the constant  $\delta^{18}\text{O}$  of the tap water in equation 4.2 for that time period effectively simulated the  $\delta^{18}\text{O}$  of water stored in these soils (from the saturation with tap water) when they were first exposed to actual precipitation in March, 2011.

Finally, the parameters T and D/vx in equation 4.3, and their uncertainty, were estimated using a Bayesian approach recently adapted to two-parameter transit-time

models by [Hrachowitz *et al.*, 2010]. The initial possible distributions of T and D/vx were specified by uniform distributions with ranges 1-600 and 0.001-1, respectively, then reduced to 50-150 and 0.001-0.15 in a second iteration. The DREAM-ZS algorithm [Schoups and Vrugt, 2010; Ter Braak and Vrugt, 2008; Vrugt *et al.*, 2009] was used to search the possible parameter space during 50,000 model iterations, using three parallel chains in the Markov chain Monte Carlo simulation algorithm. The optimal parameter set was selected based on maximization of a log likelihood function and the parameter uncertainty is presented based on the derived posterior parameter distribution [Hrachowitz *et al.*, 2010]. The  $\delta^{18}\text{O}_R$  for each lysimeter was simulated using the optimal parameter values in equation 4.3 convolved with the input time series of  $\delta^{18}\text{O}_{\text{Peff}}$  (equation 4.2), and the accuracy of the simulation was evaluated based on the root-mean-squared error statistic.

### 4.3 Results

Total precipitation from October, 2011 through September, 2012 was 1185 mm. Using equations 4.4 – 4.6 we calculated effective precipitation amounts of 770, 501, and 479 mm for L1bs, L1g, and L10, respectively (Figure 4.2). The variable, j, in equation 4.6 was manually adjusted until these effective precipitation totals were similar in magnitude to the observed annual totals of recharge from each lysimeter (shown later in Figure 4.6). From October 17<sup>th</sup> – November 20<sup>th</sup>, 2011, there were 60 mm of effective precipitation for L1bs that were excluded from the  $P_{\text{eff}}$  total for L1g and L10. Effective precipitation was similar for all lysimeters, and nearly equal to total P, during most of the winter, and from March 19<sup>th</sup> throughout the spring season  $P_{\text{eff}}$  was greater for L1bs than L1g and L10 by 209 and 229 mm, respectively (Figure 4.2). Notably, 40, 59, and 62% of total annual  $P_{\text{eff}}$  for L1bs, L1g, and L10, respectively, occurred during two weeks of intense rain (12/26/11 – 1/2/12 and 1/16/2012 – 1/22/2012).

The estimated mean-transit times of water flow through the soil profile were 106, 101, and 94 days for L1bs, L1g, and L10, respectively (Figure 4.3). These differences were relatively small, however, considering the broadly overlapping inter-quartile ranges of the posterior distributions of T estimated for each lysimeter (Figure 4.3). The

parameter  $D/vx$ —indicating the relative contribution of diffusive versus advective transport—was very low under all surface conditions, generally similar for the young grassland (L1g) and bare soil lysimeter (L1bs), and lowest for the oldest grassland (L10) (Figure 4.3).

The weekly values of  $\delta^{18}\text{O}$  in  $P_{\text{eff}}$  ranged from -5.36 to -15.11‰ (Figure 4.4). The time series included  $\delta^{18}\text{O}$  values associated with  $P_{\text{eff}}$  from earlier in the fall and later in the spring for L1bs than either grassland lysimeter—corresponding to similar differences in  $P_{\text{eff}}$  (Figure 4.2). The transit-time distributions, based on equation 4.3 and the maximum likelihood parameter values shown in Figure 4.3, were similar between L1bs and L1g, though the distribution for L10 showed less range and greater probability density around the mean. The simulated time series of  $\delta^{18}\text{O}_R$  agreed generally with temporal trends in the observed values (Figure 4.4), although the simulated values did not reflect accurately the full range of  $\delta^{18}\text{O}_R$  for any lysimeter: simulated ranges were 1.24, 1.64, and 3.10 versus observed ranges of 2.65, 3.91, and 3.95 ‰ for L1bs, L1g, and L10, respectively. The root-mean-squared errors for each simulation (Figure 4.4) were 20% or less of this total range. The greatest simulation errors occurred during March, 2012, when the most negative values of  $\delta^{18}\text{O}_R$  were observed for all lysimeters.

There were distinct differences in soil moisture between the bare soil and grassland lysimeters during the fall and spring season. At 0.15 and 0.75 m soil depth, the seasonal minimum soil moisture values that occurred following the summer drought were substantially lower in both grassland lysimeters than under bare soil (Figure 4.5). The volume of water at 0.75 m soil depth under bare soil varied little throughout the summer drought period, showing only small increases in response to precipitation events during the fall, winter and spring. During the seasonal transition from wet to dry conditions in April and May, soil moisture also declined more rapidly in both grassland lysimeters than under bare soil (Figure 4.5).

These seasonal differences in soil moisture extended the period when quasi-steady-state conditions existed, and therefore the length of the  $P_{\text{eff}}$  and  $\delta^{18}\text{O}_{P_{\text{eff}}}$  time series for the bare soil versus grassland lysimeters (Figure 4.2 and 4.3). Similarly, 136 mm of R occurred under the bare soil from November 1<sup>st</sup> – December 26<sup>th</sup>, whereas only 1.8 and zero mm occurred in L1g and L10 (Figure 4.6). Smaller differences existed during the

spring of 2012, when R persisted at greater rates and later into the spring season under bare soil than in either grassland lysimeter.

#### 4.4 Discussion

The motivation for this study was to quantify soil-water transit times and the soil-water balance under bare soil and two stages of aggrading grassland vegetation, and to evaluate two potential mechanisms by which aggrading vegetation may influence soil-water transit times: 1) alteration of soil physical and hydraulic properties by root systems, and 2) vegetation effects on the soil-water balance and soil-moisture. The results indicate generally similar mean-transit times occurring under bare soil and grassland communities in their first and sixth years of growth, despite changes to soil hydraulic properties that may have occurred, and despite a substantial shifts in the soil-water balance observed even in the first year of plant growth.

##### *4.4.1 Soil-water mean-transit times: how fast and why?*

Our mean-transit time estimates (94 – 106 days; 13 – 15 weeks) are at the low end (more rapid end) of the range reported for other soil lysimeter studies (7.5 – 59 weeks) [Maloszewski *et al.*, 2006; Stumpp *et al.*, 2009a; Stumpp *et al.*, 2009b]. The soils studied by Maloszewski *et al.* [2006] included very coarse gravels and sands with estimated saturated hydraulic conductivity values ranging from 4 to more than 100 m d<sup>-1</sup> (except for one sand with saturated conductivity of 0.2 m d<sup>-1</sup>) [Maciejewski *et al.*, 2006]. Stumpp *et al.* [2009a] studied a sandy soil with a reported saturated conductivity of 1.19 m d<sup>-1</sup>, while the silty-clay loam soil we studied had an approximate saturated conductivity value of 0.93 m d<sup>-1</sup> (based on the van Genuchten-Mualem soil-hydraulic model [van Genuchten, 1980] that was fit to a measured moisture retention curve). Hence, it is somewhat surprising that we observed more rapid mean-transit times given the much finer-textured soil. However, the comparison is influenced in part by the fact that the effective flow-path length (i.e. lysimeter depth) examined in those studies was twice that reported on here (2 m versus our 0.95-1 m total depth at each lysimeter). Another possible cause for our shorter mean residence time may be differences in precipitation regime: total annual

precipitation at our site was greater than reported in those studies, and in our Mediterranean climate the precipitation is concentrated within a five-month period with low evaporative demand, whereas precipitation was more distributed throughout the year at the sites noted above. We also note that during the 2011 – 2012 water year at our site approximately 25% of annual precipitation occurred during two intense storm events—during late December and January—and these likely induced more rapid transit times of subsurface flow than would occur under the more typical low intensity storm events.

#### *4.42 Plants control the water balance, but exert little influence on mean-transit time*

Even though the perennial grassland species maintain some metabolic activity during the wet and cool winter months in this Mediterranean climate [Phillips *et al.*, 2011], the photosynthetic rates (and presumably root uptake) were low and the presence of vegetation did not result in dramatically different soil-moisture trends than were observed under bare soil from December through April—when most recharge occurred. Pangle ([2013], and chapter 3 of this document) hypothesized that the primary effect of vegetation on subsurface flow processes during this winter period would be the enhancement of rapid macropore flow due to root-induced changes to soil structural properties [Angers and Caron, 1998]. However, the evidence did not support this expectation, at least at the time scale of individual storm events. This analysis also suggests that over weeks to months, water transit-times were generally unaffected by growth and establishment of the grassland root systems. The maximum-likelihood estimates of mean-transit time were slightly shorter after six years of grassland growth, though the broadly overlapping posterior parameter distributions suggest these differences were not significant (and probably not accurate to the order of a few days, as discussed in section 4.43 below).

The LTIC approach we applied here provided estimates of soil-water mean-transit times based on sampling of the recharge flux, and considering the  $\delta^{18}\text{O}$  composition of precipitation and recharge only during the quasi-steady-state soil-moisture conditions. In this Mediterranean climate, the most pronounced effect of grassland establishment and growth was the abrupt shift in the soil-water balance (occurring within the first year of growth) from recharge-dominated (R:P = 0.67 in L1bs) to evapotranspiration-dominated

(R:P = 0.42 and 0.4 in L1g and L10, respectively). This shift reduced the amount of effective precipitation and the time span over which quasi-steady-state conditions existed, but did not significantly alter the mean-transit time of soil water that ultimately contributed to recharge. However, this does not preclude the possibility that plants may affect mean-transit times by altering seasonal evapotranspiration and soil-moisture trends—but in ways that would not be detected in our application of the LTIC approach.

Figure 4.5 shows how root-water uptake and transpiration caused substantially lower soil-moisture content throughout the summer drought period, particularly at greater soil depths. Evaporation from bare soil is supplied by liquid water at the soil surface, and occurs at low rates late in the summer due to limited vertical-liquid-water transport from below, whereas root systems utilize more water overall and from greater depth. Water age increases with soil depth [Asano *et al.*, 2002; Munoz-Villers and McDonnell, 2012; Stewart and McDonnell, 1991], therefore progressive root-expansion and greater uptake of water stored in the deep soil during the summer would reduce the volume of relatively “old” water persisting at depth that could contribute to recharge during the following rainy season. This mechanism could strongly influence the magnitude of the longest times represented in the overall transit-time distribution, and perhaps the mean. We did not quantify the age distribution of water that left the soil by evapotranspiration during the summer, and therefore only offer this mechanism as speculative. We also acknowledge that it is based on the assumption that water stored in the deep soil during the summer had similar entry times to the bare soil and grassland lysimeters. Brooks *et al.* [2010] showed isotopic-evidence that precipitation entering the soil during the early fall season in a Mediterranean climate may occupy pore spaces that render it relatively immobile, where it may persist until being extracted by tree roots during the following summer. Hence, the assumption of similar entry time could be questionable, considering the stark difference in the amount of vacant soil-pore space that existed at the onset of fall rains in the bare soil versus grassland lysimeters.

#### 4.43 *On the accuracy of the $\delta^{18}O_R$ simulations and derived transit times*

The overall accuracy of the simulated  $\delta^{18}O_R$  time series limits somewhat the inference that can be made from the small differences observed in the derived transport

parameters. The simulated time series of  $\delta^{18}\text{O}_R$  generally follow the same seasonal trend as the measured values, though with notable deviations occurring among individual weeks and lower overall range. For example, measured  $\delta^{18}\text{O}_R$  from L10 steadily increased after recharge was initiated during late December (Figures 4.6) to values that were actually less negative than any included in the  $\delta^{18}\text{O}_{\text{Peff}}$  time series for that lysimeter (Figure 4.4). Even less negative  $\delta^{18}\text{O}$  values did occur during precipitation events in early October, though these precipitation events occurred prior to the establishment of near-steady-state soil-moisture conditions, and were not included in the  $\delta^{18}\text{O}_{\text{Peff}}$  time series for L1g or L10. Hence, assuming the water from these initial rains filled “immobile” pore space and did not contribute to the  $\delta^{18}\text{O}_R$  may be a source of error in our simulations. Also,  $\delta^{18}\text{O}_R$  for L1bs decreased by 0.88 ‰ between two weeks in late January, 2012 (Figure 4.4)—a change that was not accurately simulated. This shift may have been influenced by rapid transport of some precipitation from the very large storm event that occurred days prior, and showed very negative  $\delta^{18}\text{O}$  values. If such rapid transport did contribute to this shift in  $\delta^{18}\text{O}_R$ , it would not be accurately simulated by the best fitting transit-time distribution (Figure 4.4) since that distribution suggests near zero probability of transit-times shorter than about 40 days.

The most negative  $\delta^{18}\text{O}$  values occurred during March, 2012 (Figure 4.4), and were likely influenced by the 200 mm of precipitation that fell from January 16<sup>th</sup> through 22<sup>nd</sup>, which included the most negative  $\delta^{18}\text{O}_{\text{Peff}}$  values observed throughout the year. None of the simulations were able to replicate these seasonal lows, suggesting that the transport of water originating from this large storm event could not be fully described by the fitted transit time distributions. However, the fact that these minimum  $\delta^{18}\text{O}_R$  values occurred during the same week for all lysimeters does indicate general similarity in their mean transit-times. The greater total range of  $\delta^{18}\text{O}_R$  observed in L10 and L1g as compared to L1bs suggests that at some times of the year water moved through the vegetated soil profiles while undergoing less mixing with stored soil water than occurred under the bare soil condition. The differences in transport and mixing that may have caused a greater range of  $\delta^{18}\text{O}_R$  values under grassland were not consistently represented by the maximum likelihood parameters. Similar ranges of  $\delta^{18}\text{O}_R$  were observed for L1g and L10, although  $D/vx$  for L1g was much more similar to L1bs than L10. Given these

inaccuracies in the model simulations, and the uncertainties associated with the final parameter values (Figure 4.3), we conclude that water transport in this soil was not significantly affected by establishment and growth of grassland vegetation.

#### 4.5 Conclusions

Vegetation establishment and growth has been shown to enhance water infiltration rates at the soil surface in agricultural soils [Jarvis, 2007] and arid environments [Thompson *et al.*, 2010], and the mechanisms by which plant-root systems may influence soil hydraulic properties are well documented [Angers and Caron, 1998; Bengough, 2012]. However, little is known about how these physical effects, and vegetation control on soil-moisture dynamics, may influence flow and transport processes in the subsurface. We examined soil-water transit times using a series of lysimeters with the same soil, but with surface conditions ranging from bare soil through two age classes of aggrading grassland vegetation. We found that vegetation establishment and growth had no significant effect on mean-transit times of soil water that contributed to potential groundwater recharge over the water year, which corroborated the finding of Pangle ([2013], Chapter 3 of this document) that aggrading vegetation also had no discernible effect on rapid-transport during individual precipitation events. This was surprising considering that the soil in our study had silty-clay loam texture and shrink-swell tendencies that made it susceptible to plant-induced structural changes that may enhance rapid flow through macropores [Jarvis *et al.*, 2009]. Grassland establishment and growth did shift abruptly the soil-water balance from being recharge-dominated under bare soil to evapotranspiration-dominated. This measurable shift in the water balance shortened the period of time during the rainy season when quasi-steady-state soil-moisture conditions existed, and reduced the amount of precipitation that effectively contributed to groundwater recharge, but did not significantly alter the mean-soil-water transit time.

#### 4.6 References

Allen, R. G., L. S. Pereira, D. Raes, and M. Smith (1998), *Crop evapotranspiration - Guidelines for computing crop water requirements*.

- Angers, D. A., and J. Caron (1998), Plant-induced changes in soil structure: Processes and feedbacks, *Biogeochemistry*, 42(1-2), 55-72.
- Asano, Y., T. Uchida, and N. Ohte (2002), Residence times and flow paths of water in steep unchannelled catchments, Tanakami, Japan, *J. Hydrol.*, 261(1-4), 173-192.
- Bastviken, D., P. Sandén, T. Svensson, C. Ståhlberg, M. Magounakis, and G. Öberg (2006), Chloride Retention and Release in a Boreal Forest Soil: Effects of Soil Water Residence Time and Nitrogen and Chloride Loads, *Environmental Science & Technology*, 40(9), 2977-2982.
- Bengough, A. G. (2012), Water dynamics of the root zone: rhizosphere biophysics and its control on soil hydrology, *Vadose Zone Journal*, 11(2).
- Botter, G., E. Bertuzzo, and A. Rinaldo (2010), Transport in the hydrologic response: Travel time distributions, soil moisture dynamics, and the old water paradox, *Water Resources Research*, 46.
- Botter, G., E. Bertuzzo, and A. Rinaldo (2011), Catchment residence and travel time distributions: The master equation, *Geophysical Research Letters*, 38.
- Brooks, J. R., H. R. Barnard, R. Coulombe, and J. J. McDonnell (2010), Ecohydrologic separation of water between trees and streams in a Mediterranean climate, *Nat. Geosci.*, 3(2), 100-104.
- Bureau of Reclamation, D. o. t. I., USA (2013), The Pacific Northwest Cooperative Agricultural Weather Network, edited by C. A. Station, <http://www.usbr.gov/pn/agrimet/>.
- Heidbuchel, I., P. A. Troch, S. W. Lyon, and M. Weiler (2012), The master transit time distribution of variable flow systems, *Water Resources Research*, 48.
- Hrachowitz, M., C. Soulsby, D. Tetzlaff, and I. A. Malcolm (2011), Sensitivity of mean transit time estimates to model conditioning and data availability, *Hydrol. Process.*, 25(6), 980-990.
- Hrachowitz, M., C. Soulsby, D. Tetzlaff, I. A. Malcolm, and G. Schoups (2010), Gamma distribution models for transit time estimation in catchments: Physical interpretation of parameters and implications for time-variant transit time assessment, *Water Resources Research*, 46.
- Jarvis, N. J. (2007), A review of non-equilibrium water flow and solute transport in soil macropores: principles, controlling factors and consequences for water quality, *Eur. J. Soil Sci.*, 58(3), 523-546.

- Jarvis, N. J., J. Moeys, J. M. Hollis, S. Reichenberger, A. M. L. Lindahl, and I. G. Dubus (2009), A Conceptual Model of Soil Susceptibility to Macropore Flow, *Vadose Zone Journal*, 8(4), 902-910.
- Johnson, M. S., M. Weiler, E. G. Couto, S. J. Riha, and J. Lehmann (2007), Storm pulses of dissolved CO<sub>2</sub> in a forested headwater Amazonian stream explored using hydrograph separation, *Water Resources Research*, 43(11).
- Kennedy, V. C., G. W. Zellweger, and R. J. Avanzino (1979), Variations of rain chemistry during storms at two sites in Northern California, *Water Resources Research*, 15, 687-702.
- Kreft, A., and A. Zuber (1978), On the physical meaning of the dispersion equation and its solutions for different initial and boundary conditions, *Chemical Engineering Science*, 33, 1471-1480.
- Maciejewski, S., P. Maloszewski, C. Stumpp, D. Klotz, (2006), Modelling of water flow through typical Bavarian soils: 1. Estimation of hydraulic characteristics of the unsaturated zone, *Hydrological Sciences Journal*, 51(2), 285-297.
- Maloszewski, P., and A. Zuber (1982), Determining the turnover time of groundwater systems with the aid of environmental tracers. 1. Models and their applicability, *J. Hydrol.*, 57(3-4), 207-231.
- Maloszewski, P., S. Maciejewski, C. Stumpp, W. Stichler, P. Trimborn, and D. Klotz (2006), Modelling of water flow through typical Bavarian soils: 2. Environmental deuterium transport, *Hydrological Sciences Journal-Journal Des Sciences Hydrologiques*, 51(2), 298-313.
- McGuire, K. J., and J. J. McDonnell (2006), A review and evaluation of catchment transit time modeling, *J. Hydrol.*, 330(3-4), 543-563.
- McGuire, K. J., and J. J. McDonnell (2010), Hydrological connectivity of hillslopes and streams: Characteristic time scales and nonlinearities, *Water Resources Research*, 46.
- Munoz-Villers, L. E., and J. J. McDonnell (2012), Runoff generation in a steep, tropical montane cloud forest catchment on permeable volcanic substrate, *Water Resources Research*, 48.
- Pangle, L. A. (2013), Ecohydrological mediation of water budget partitioning and time scales of subsurface flow in a seasonally semi-arid grassland, Oregon State University, Corvallis, Oregon.

Phillips, C. L., J. W. Gregg, and J. K. Wilson (2011), Reduced diurnal temperature range does not change warming impacts on ecosystem carbon balance of Mediterranean grassland mesocosms, *Glob. Change Biol.*, 17(11), 3263-3273.

Rinaldo, A., K. J. Beven, E. Bertuzzo, L. Nicotina, J. Davies, A. Fiori, D. Russo, and G. Botter (2011), Catchment travel time distributions and water flow in soils, *Water Resources Research*, 47.

Schoups, G., and J. A. Vrugt (2010), A formal likelihood function for parameter and predictive inference of hydrologic models with correlated, heteroscedastic, and non-Gaussian errors, *Water Resources Research*, 46.

Stewart, M. K., and J. J. McDonnell (1991), Modeling base-flow soil-water residence times from deuterium concentrations, *Water Resources Research*, 27(10), 2681-2693.

Stumpp, C., W. Stichler, and P. Maloszewski (2009a), Application of the environmental isotope delta O-18 to study water flow in unsaturated soils planted with different crops: Case study of a weighable lysimeter from the research field in Neuherberg, Germany, *J. Hydrol.*, 368(1-4), 68-78.

Stumpp, C., P. Maloszewski, W. Stichler, and J. Fank (2009b), Environmental isotope (delta O-18) and hydrological data to assess water flow in unsaturated soils planted with different crops: Case study lysimeter station "Wagna" (Austria), *J. Hydrol.*, 369(1-2), 198-208.

Ter Braak, C. J. F., and J. A. Vrugt (2008), Differential evolution Markov Chain with snooker updater and fewer chains, *Statistical Computing*, 18, 435-446.

Thompson, S. E., C. J. Harman, P. Heine, and G. G. Katul (2010), Vegetation-infiltration relationships across climatic and soil type gradients, *J. Geophys. Res.-Biogeosci.*, 115.

van der Velde, Y., P. Torfs, S. van der Zee, and R. Uijlenhoet (2012), Quantifying catchment-scale mixing and its effect on time-varying travel time distributions, *Water Resources Research*, 48.

van der Velde, Y., G. H. de Rooij, J. C. Rozemeijer, F. C. van Geer, and H. P. Broers (2010), Nitrate response of a lowland catchment: On the relation between stream concentration and travel time distribution dynamics, *Water Resources Research*, 46.

van Genuchten, M.T., 1980, A closed-form equation for predicting the hydraulic conductivity of unsaturated soils, *Soil Science Society of America Journal*, 44(5), 892-898.

Vitvar, T., and W. Balderer (1997), Estimation of mean water residence times and runoff generation by <sup>18</sup>O measurements in a Pre-Alpine catchment (Rietholzbach, Eastern Switzerland), *Applied Geochemistry*, 12, 787-796.

Vrugt, J. A., C. J. F. ter Braak, C. G. H. Diks, B. A. Robinson, J. M. Hyman, and D. Higdon (2009), Accelerating Markov Chain Monte Carlo Simulation by Differential Evolution with Self-Adaptive Randomized Subspace Sampling, *International Journal of Nonlinear Sciences and Numerical Simulation*, 10(3), 273-290.

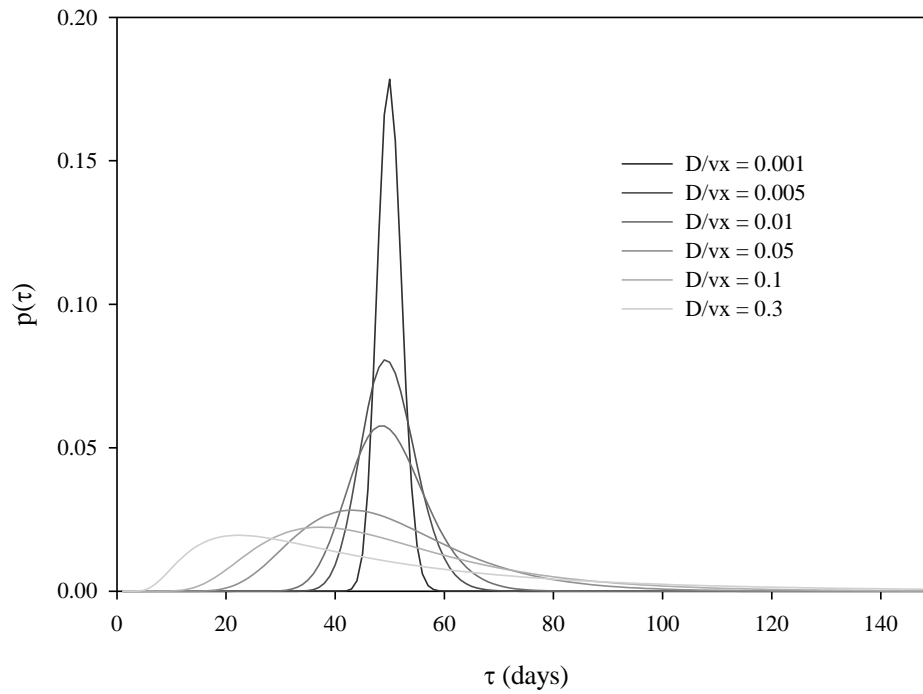


**Figure 4.1** Exemplary shapes of the dispersion model (equation 4.3) used as a transit-time distribution function given a constant mean-transit time,  $T$ , of 50 days and a range of  $D/vx$  values that indicate varying relative contributions of diffusive versus advective transport.

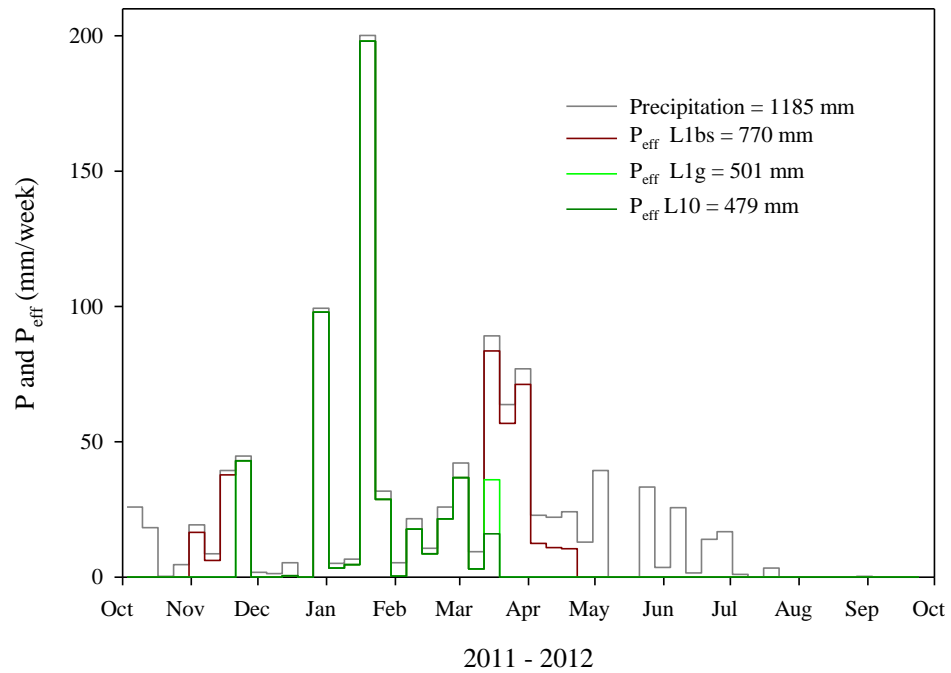


**Figure 4.2** Measured rates of weekly precipitation and calculated rates of effective precipitation (i.e. precipitation that contributes to recharge) for each lysimeter, based on equations 4.4 – 4.6.

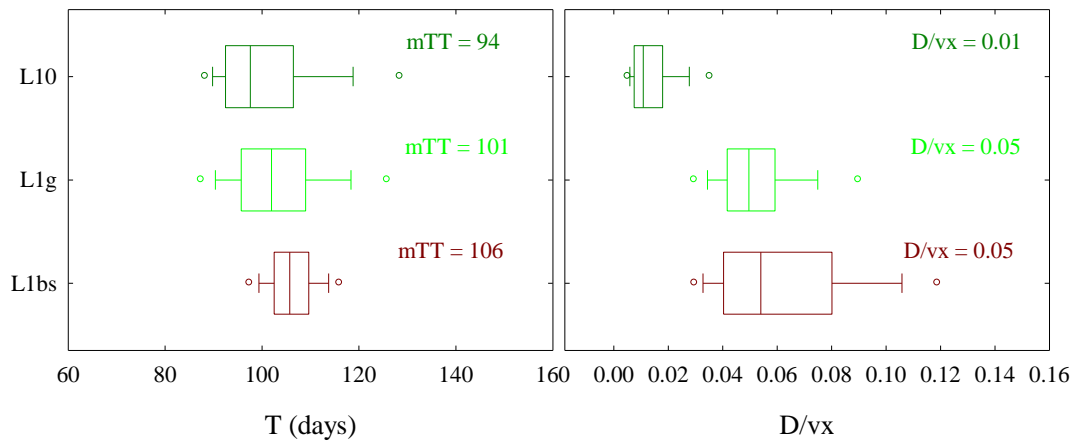


**Figure 4.3** Boxplots showing the median, inter-quartile range, 10<sup>th</sup> and 90<sup>th</sup> (whiskers) and 5<sup>th</sup> and 95<sup>th</sup> (dots) percentiles of the posterior distribution of the parameter space for the mean-transit time,  $T$ , and the parameter  $D/vx$  for each lysimeter. The maximum-likelihood value of each parameter is indicated in text.

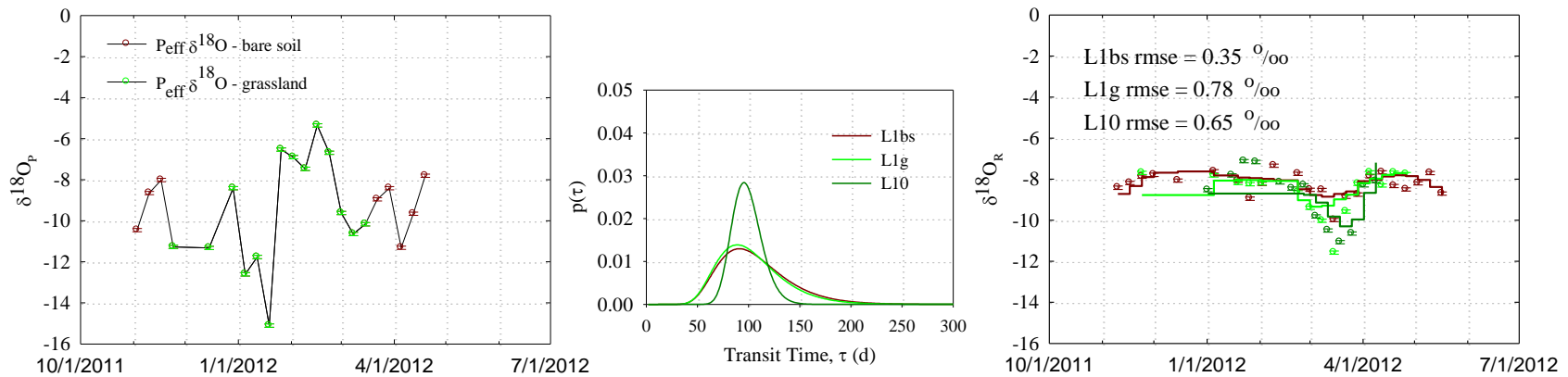


**Figure 4.4** (Left) Time series of the  $\delta^{18}O$  composition of effective precipitation for the bare soil and grassland-covered lysimeters during the 2011-2012 water year. The ratio of effective to actual precipitation was greater under the bare-soil condition than under grassland cover, including precipitation that fell earlier in the fall and later into the spring season, hence the time series of  $\delta^{18}O$  is also longer. (Middle) Shapes of the transit-time distributions for each lysimeter based on the maximum likelihood values of  $T$  and  $D/vx$ . (Right) Measured (dots) and simulated (lines) time series of  $\delta^{18}O$  in recharge during the 2011-2012 water year. Root-mean-squared error statistics describing the overall accuracy of the simulations are shown in text.

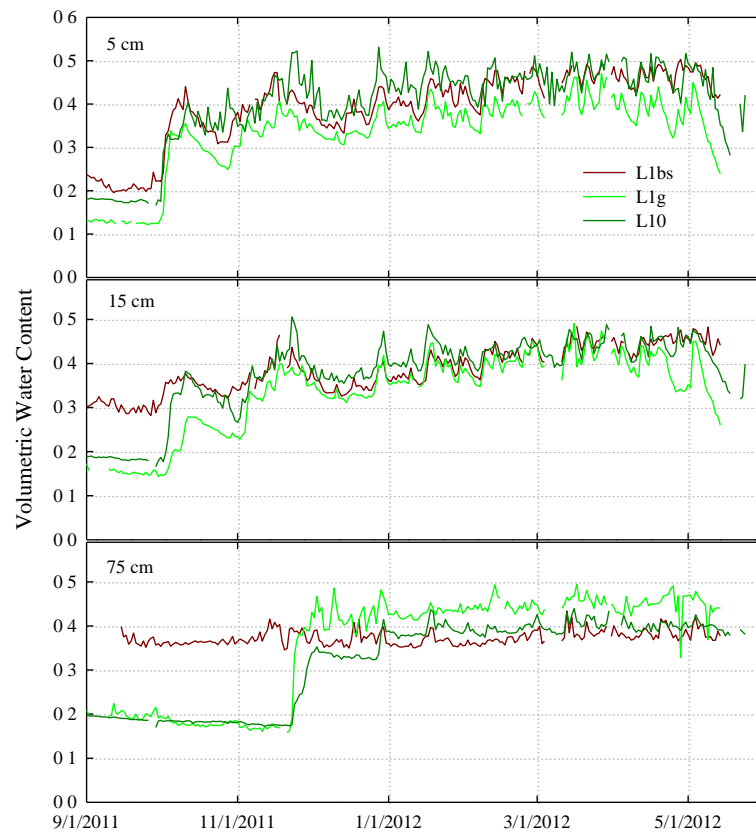
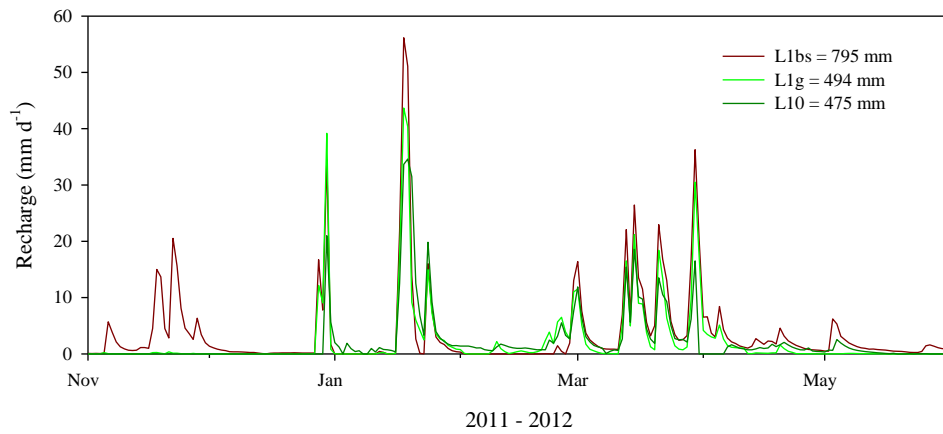


Figure 4.5 Volumetric water content at 0.05, 0.15, and 0.75 m soil depth within each lysimeter. Discontinuities in the lines indicate periods when data were missing or omitted due to equipment malfunction.



**Figure 4.6** Time series of recharge from each lysimeter during the 2011-2012 water year. Annual-total recharge for each lysimeter is indicated in the figure legend.

## **5. CONCLUSIONS**

## 5.1 Synopsis of research findings

Plants mediate water flows through the environment, both above and belowground, confounding our ability to describe the terrestrial hydrologic cycle based on physical principles alone. This dissertation aimed to improve our understanding of potential ecohydrological mechanisms that may alter the quantities and time-scales of water flow in soils, in particular, focusing on 1) the interrelationships between plant-water use, temporal soil-moisture dynamics, and potential groundwater recharge, and 2) how the physical alteration of soils by inhabiting vegetation may alter the magnitude and transit-times of water flowing through soils. To address these research foci I utilized well controlled lysimeter-based field studies: in one case a precision-controlled and replicated climate-change experiment that enabled analysis of the total soil-water balance under multiple air-temperature treatments, and in the other case a series of lysimeters with similar soil but with either a bare soil surface or two stages of aggrading vegetation, which allowed me to isolate the effect of aggrading vegetation on subsurface flow processes.

In the first study we found that on an annual time scale warming did not alter the soil-water balance in this Mediterranean climate. Warmer temperatures did increase evapotranspiration during the spring when soil-water was abundant, but there was an important ecohydrological feedback mechanism whereby this enhancement of evapotranspiration also accelerated the depletion of soil water, resulting in less evapotranspiration under warmer air temperature during the summer drought period than occurred under ambient temperature. Importantly, we also discovered that the groundwater recharge flux was mostly unaffected by the plant and soil-moisture response to warming in this Mediterranean climate. Though soil-moisture decline occurred earlier under warmer temperatures (relative to ambient temperature) the difference was insufficient to influence recharge rates for most of the spring.

In the second and third studies we found no evidence that plant root systems enhanced the rapid transport of precipitation through the soil profile. The contributions of event water versus stored-soil water to the recharge flux were very low in all cases, and always zero for grasslands ranging in age from three to six years. We also found that

mean-transit times of soil water over the entire water year were not significantly affected by establishment and growth of vegetation. The local precipitation regime and soil-specific hydraulic properties were the predominant controls on water transport during storms. Physical alteration of soil-hydraulic properties has been shown to be a hydrologically important mechanism in arid-regions and agricultural soils, mainly by influencing the partitioning of precipitation between rapid-surface runoff versus infiltration. Our data suggest this mechanism may have little impact on the magnitude and transit-time of water flow at greater soil depth.

The consistency in soil-water transport we observed occurred despite major vegetation impacts on the overall soil-water balance. During individual storms, interception, storage, and evaporative loss from the aboveground biomass and detritus substantially reduced effective precipitation and the total recharge response, and at the annual time scale aggrading vegetation truncated the period when recharge occurred during the rainy season, and shifted the soil-water balance from being recharge dominated to evapotranspiration dominated, even within the first year of plant growth.

## **5.2 Synthesis**

These results support some general conclusions about which ecohydrological processes have the most important impacts on the soil-water balance and transit-times of subsurface flow, and provide some guidance for future climate- and environmental-change research:

### *5.2.1 Ecosystem water-use efficiency*

The grassland response to drought in this Mediterranean climate was tissue senescence and physiological dormancy. This contributed to the negative feedback mechanism we observed, which caused no annual difference in evapotranspiration. Other plant functional types (e.g. trees) with different leaf-and canopy-level water-use efficiency and rooting depths may exhibit totally different temporal patterns of soil-water extraction and transpiration, resulting in different magnitudes of total evapotranspiration. Variable water-use efficiency by different plant functional groups could affect the

magnitudes and transit-times of subsurface flows as well, during the fall and spring transitional periods in this Mediterranean climate, and by controlling soil-moisture dynamics during inter-storm periods in climates where precipitation is distributed more evenly throughout the year.

#### *5.22 Vegetation control on effective precipitation and accessible soil water*

The analysis in Chapter 3 revealed rather remarkable interception losses from these grassland communities, even when total leaf area was relatively low. These interception losses were influenced apparently by substantial accumulation of detritus, and perhaps by the unique architecture of some of the grassland species (e.g. *Festuca romeri*). This aboveground effect translated into marked differences in subsurface flow as well, proving more significant than the hypothesized effects of plant roots systems on soil-hydraulic properties. In principle, modification of effective precipitation could also influence soil-water transit times: plant canopies with different area, structure, and detrital deposition rates could substantially influence the amount and timing of precipitation that actually infiltrates the soil. While there have been many studies of land-use change effects on water-balance partitioning, the potential impact of changes in vegetation cover on transit-times of subsurface flow has not been well investigated, and could be an important mechanism influencing water quality under land-use change.

Effects of plant root systems on soil hydraulics have been well documented, and shown to have a significant effect on the partitioning of rainfall between infiltration and surface runoff, especially in arid lands and cultivated soils. Also, root systems may provide conduits for rapid lateral flow of water down steep-forested hillslopes during intense rain storms. While plant-altered soil-hydraulics may support ecosystem function by increasing infiltration, the results presented here suggest this is not an ecohydrological mechanism that significantly alters groundwater recharge rates and soil-water transit times. This appears to be due to the low precipitation intensity, high water-storage capacity of the soil, and relatively shallow rooting habit of the grassland vegetation. This research did affirm the critical importance of plant-rooting depth for controlling short-term and seasonal soil moisture fluctuations, and therefore the timing and magnitude of subsurface water flow.

## REFERENCES

- Abbaspour, K. C., R. Schulin, and M. T. van Genuchten (2001), Estimating unsaturated soil hydraulic parameters using ant colony optimization, *Adv. Water Resour.*, 24(8), 827-841.
- Angers, D. A., and J. Caron (1998), Plant-induced changes in soil structure: Processes and feedbacks, *Biogeochemistry*, 42(1-2), 55-72.
- Angert, A., S. Biraud, C. Bonfils, C.C. Henning, W. Buermann, J. Pinzon, C.J. Tucker, I. Fung, (2005), Drier summers cancel out the CO<sub>2</sub> uptake enhancement induced by warmer springs, *Proceedings of the National Academy of Sciences of the United States of America*, 102(31), 10823-10827, doi: 10.1073/pnas.0501647102.
- Asano, Y., T. Uchida, and N. Ohte (2002), Residence times and flow paths of water in steep unchannelled catchments, Tanakami, Japan, *J. Hydrol.*, 261(1-4), 173-192.
- Bachmair, S., M. Weiler, and P. A. Troch (2012), Intercomparing hillslope hydrological dynamics: spatio-temporal variability and vegetation cover effects, *Water Resources Research*, 48.
- Baldocchi, D. (2011), Global change: The grass response, *Nature*, 476(7359), 160-161, doi: 10.1038/476160a.
- Baldocchi, D. D., L. K. Xu, and N. Kiang (2004), How plant functional-type, weather, seasonal drought, and soil physical properties alter water and energy fluxes of an oak-grass savanna and an annual grassland, *Agricultural and Forest Meteorology*, 123(1-2), 13-39, doi: 10.1016/j.agrformet.2003.11.006.
- Bastviken, D., P. Sandén, T. Svensson, C. Ståhlberg, M. Magounakis, and G. Öberg (2006), Chloride Retention and Release in a Boreal Forest Soil: Effects of Soil Water Residence Time and Nitrogen and Chloride Loads, *Environmental Science & Technology*, 40(9), 2977-2982.
- Bell, J. E., E. S. Weng, and Y. Q. Luo (2010a), Ecohydrological responses to multifactor global change in a tallgrass prairie: A modeling analysis, *J. Geophys. Res.-Biogeosci.*, 115, G04042, doi: 10.1029/2009JG001120.
- Bell, J. E., R. Sherry, and Y. Q. Luo (2010b), Changes in soil water dynamics due to variation in precipitation and temperature: An ecohydrological analysis in a tallgrass prairie, *Water Resources Research*, 46, W03523, doi: 10.1029/2009WR007908.
- Bengough, A. G. (2012), Water dynamics of the root zone: rhizosphere biophysics and its control on soil hydrology, *Vadose Zone Journal*, 11(2).

- Beven, K. (2006), Searching for the Holy Grail of scientific hydrology:  $Q(t) = (S, R, \Delta t)A$  as closure, *Hydrology and Earth System Sciences*, 10(5), 609-618, doi: 10.5194/hess-10-609-2006.
- Beven, K. (1981), Microporosity, mesoporosity, macroporosity and channeling flow phenomena in soils, *Soil Sci. Soc. Am. J.*, 45(6), 1245-1245.
- Beven, K., and P. Germann (1982), Macropores and water flow in soils, *Water Resources Research*, 18(5), 1311-1325.
- Beven, K., and P. Germann (2013), Macropores and water flow in soils revisited, *Water Resources Research*, Available online, DOI: 10.1002/wrcr.20156.
- Botter, G., E. Bertuzzo, and A. Rinaldo (2010), Transport in the hydrologic response: Travel time distributions, soil moisture dynamics, and the old water paradox, *Water Resources Research*, 46.
- Botter, G., E. Bertuzzo, and A. Rinaldo (2011), Catchment residence and travel time distributions: The master equation, *Geophysical Research Letters*, 38.
- Brooks, J. R., H. R. Barnard, R. Coulombe, and J. J. McDonnell (2010), Ecohydrologic separation of water between trees and streams in a Mediterranean climate, *Nat. Geosci.*, 3(2), 100-104.
- Bronick, C. J., and R. Lal (2005), Soil structure and management: a review, *Geoderma*, 124(1-2), 3-22.
- Bruand, A., I. Cousin, B. Nicoulaud, O. Duval, and J. C. Begon (1996), Backscattered electron scanning images of soil porosity for analyzing soil compaction around roots, *Soil Sci. Soc. Am. J.*, 60(3), 895-901.
- Budyko, M. I. (1974), *Climate and Life*, 508 pp., Academic, New York.
- Bureau of Reclamation, Dept. of the Interior, The Pacific Northwest Cooperative Agricultural Weather Network, <http://www.usbr.gov/pn/agrimet/>, accessed June, 2013.
- Buttle, J. M. (1994), Isotope hydrograph separations and rapid delivery of pre-event water from drainage basins, *Prog. Phys. Geogr.*, 18(1), 16-41.
- Cai, W., T. Cowan, P. Briggs, and M. Raupach (2009), Rising temperature depletes soil moisture and exacerbates severe drought conditions across southeast Australia, *Geophysical Research Letters*, 36, L21709, doi: 10.1029/2009GL040334.

Caron, J., B. D. Kay, and J. A. Stone (1992), Improvement of structural stability of a clay loam with drying, *Soil Sci. Soc. Am. J.*, 56(5), 1583-1590.

Clark, O. R. (1940), Interception of rainfall by prairie grasses, weeds, and certain crop plants, *Ecol. Monogr.*, 10(2), 243-277.

Couturier, D. E., and E. A. Ripley (1973), Rainfall interception in mixed grass prairie, *Canadian Journal of Plant Science*, 53(3), 659-663.

Crockford, R. H., and D. P. Richardson (2000), Partitioning of rainfall into throughfall, stemflow and interception: effect of forest type, ground cover and climate, *Hydrol. Process.*, 14(16-17), 2903-2920.

Cullum, R.F. (2009), Macropore flow estimations under no-till and till systems, *Catena*, 78(1), 87-91.

Cuthbert, M.O., C. Tindimugaya (2010), The importance of preferential flow in controlling groundwater recharge in tropical Africa and implications for modelling the impact of climate change on groundwater resources, *Journal of Water and Climate Change*, 1(4), 234-245.

De Boeck, H. J., C. Lemmens, H. Bossuyt, S. Malchair, M. Carnol, R. Merckx, I. Nijs, and R. Ceulemans (2006), How do climate warming and plant species richness affect water use in experimental grasslands?, *Plant and Soil*, 288(1-2), 249-261, doi: 10.1007/s11104-006-9112-5.

Dermody, O., J. F. Weltzin, E. C. Engel, P. Allen, and R. J. Norby (2007), How do elevated CO<sub>2</sub>, warming, and reduced precipitation interact to affect soil moisture and LAI in an old field ecosystem?, *Plant and Soil*, 301(1-2), 255-266, doi: 10.1007/s11104-007-9443-x.

Dexter, A. R. (1987), Compression of soil around roots, *Plant Soil*, 97(3), 401-406.

Donohue, R. J., M. L. Roderick, and T. R. McVicar (2007), On the importance of including vegetation dynamics in Budyko's hydrological model, *Hydrology and Earth System Sciences*, 11(2), 983-995, doi: 10.5194/hess-11-983-2007.

Dragila, M.-I., and S. W. Wheatcraft (2001), Free Surface Films, in *Conceptual Models of Flow and Transport in the Fractured Vadose Zone*, edited, pp. 217-241, National Research Council, National Academy Press, Washington, D.C.

Eagleson, P. S. (2002), *Ecohydrology: Darwinian expression of vegetation form and function*, Cambridge University Press, Cambridge, UK.

Edwards, W. M., L. D. Norton, and C. E. Redmond (1988), Characterizing macropores that affect infiltration into nontilled soil, *Soil Sci. Soc. Am. J.*, 52(2), 483-487.

Ellerbrock, R. H., and H. H. Gerke (2004), Characterizing organic matter of soil aggregate coatings and biopores by Fourier transform infrared spectroscopy, *Eur. J. Soil Sci.*, 55(2), 219-228.

Fay, P. A., J. D. Carlisle, B. T. Danner, M. S. Lett, J. K. McCarron, C. Stewart, A. K. Knapp, J. M. Blair, and S. L. Collins (2002), Altered rainfall patterns, gas exchange, and growth in grasses and forbs, *Int. J. Plant Sci.*, 163(4), 549-557, doi: 10.1086/339718.

Field, C.B., C.P. Lund, N.R. Chiariello, and B.E. Mortimer, (1997), CO<sub>2</sub> effects on the water budget of grassland microcosm communities, *Glob. Change Biol.*, 3(3), 197-206, doi: 10.1046/j.1365-2486.1997.t01-1-00096.x.

Fredeen, A.L., J.T. Randerson, N.M. Holbrook, C.B. Field, (1997), Elevated atmospheric CO<sub>2</sub> increases water availability in a water-limited grassland ecosystem, *Journal of the American Water Resources Association*, 33(5), 1033-1039, doi: 10.1111/j.1752-1688.1997.tb04122.x.

Gee, G. W., and J. W. Bauder (1986), Particle-size Analysis, in *Methods of Soil Analysis. Part I. Physical and Mineralogical Methods*, edited by E. A. Klute, American Society of Agronomy-Soil Science Society, Madison, WI.

Genereux, D. (1998), Quantifying uncertainty in tracer-based hydrograph separations, *Water Resources Research*, 34(4), 915-919.

Ghestem, M., R. C. Sidle, and A. Stokes (2011), The Influence of Plant Root Systems on Subsurface Flow: Implications for Slope Stability, *Bioscience*, 61(11), 869-879.

Gish, T. J., K. J. S. Kung, D. C. Perry, J. Posner, G. Bubenzer, C. S. Helling, E. J. Kladivko, and T. S. Steenhuis (2004), Impact of preferential flow at varying irrigation rates by quantifying mass fluxes, *J. Environ. Qual.*, 33(3), 1033-1040.

Green, T. R., B.C. Bates, S.P. Charles, and P.M. Fleming (2007), Physically based simulation of potential effects of carbon dioxide-altered climates on groundwater recharge, *Vadose Zone J.*, 6(3), 597-609, doi: 10.2136/vzj2006.0099.

- Green, T. R., M. Taniguchi, H. Kooi, J. J. Gurdak, D. M. Allen, K. M. Hiscock, H. Treidel, and A. Aureli (2011), Beneath the surface of global change: Impacts of climate change on groundwater, *J. Hydrol.*, 405(3-4), 532-560, doi: 10.1016/j.jhydrol.2011.05.002.
- Grevers, M. C. J., and E. Dejong (1990), The characterization of soil macroporosity of a clay soil under 10 grasses using image-analysis, *Can. J. Soil Sci.*, 70(1), 93-103.
- Groisman, P. Y., R. W. Knight, T. R. Karl, D. R. Easterling, B. M. Sun, and J. H. Lawrimore (2004), Contemporary changes of the hydrological cycle over the contiguous United States: Trends derived from in situ observations, *J. Hydrometeorol.*, 5(1), 64-85, doi: 10.1175/1525-7541(2004)005<0064:CCOTHC>2.0.CO;2.
- Hardie, M. A., W. E. Cotching, R. B. Doyle, G. Holz, S. Lisson, and K. Mattern (2011), Effect of antecedent soil moisture on preferential flow in a texture-contrast soil, *J. Hydrol.*, 398(3-4), 191-201.
- Heidbuchel, I., P. A. Troch, S. W. Lyon, and M. Weiler (2012), The master transit time distribution of variable flow systems, *Water Resources Research*, 48.
- Herbst, M., W. Fialkiewicz, T. Chen, T. Putz, D. Thiery, C. Mouvet, G. Vachaud, and H. Vereecken (2005), Intercomparison of flow and transport models applied to vertical drainage in cropped lysimeters, *Vadose Zone Journal*, 4(2), 240-254.
- Horton, J. H., and R. H. Hawkins (1965), Flow path of rain from the soil surface to the water table, *Soil Sci.*, 100(6), 377-383.
- Hrachowitz, M., C. Soulsby, D. Tetzlaff, and I. A. Malcolm (2011), Sensitivity of mean transit time estimates to model conditioning and data availability, *Hydrol. Process.*, 25(6), 980-990.
- Hrachowitz, M., C. Soulsby, D. Tetzlaff, I. A. Malcolm, and G. Schoups (2010), Gamma distribution models for transit time estimation in catchments: Physical interpretation of parameters and implications for time-variant transit time assessment, *Water Resources Research*, 46.
- Huntington, T. G. (2006), Evidence for intensification of the global water cycle: Review and synthesis, *J. Hydrol.*, 319(1-4), 83-95, doi: 10.1016/j.jhydrol.2005.07.003.
- Hwang, T., L.E.Band, J.M. Vose, C. Tague, (2012), Ecosystem processes at the watershed scale: hydrologic vegetation gradient as an indicator for lateral hydrologic connectivity of headwater catchments, *Water Resources Research*, 48.

- Jakeman, A. J., and G. M. Hornberger (1993), How much complexity is warranted in a rainfall-runoff model, *Water Resources Research*, 29(8), 2637-2649.
- Jarvis, N. J. (2007), A review of non-equilibrium water flow and solute transport in soil macropores: principles, controlling factors and consequences for water quality, *Eur. J. Soil Sci.*, 58(3), 523-546.
- Jarvis, N. J., J. Moeys, J. M. Hollis, S. Reichenberger, A. M. L. Lindahl, and I. G. Dubus (2009), A conceptual model of soil susceptibility to macropore flow, *Vadose Zone Journal*, 8(4), 902-910.
- Jastrow, J. D. (1987), Changes in soil aggregation associated with tallgrass prairie restoration, *American Journal of Botany*, 74(11), 1656-1664.
- Jaynes, D. B., S. I. Ahmed, K. J. S. Kung, and R. S. Kanwar (2001), Temporal dynamics of preferential flow to a subsurface drain, *Soil Sci. Soc. Am. J.*, 65(5), 1368-1376.
- Johnson, M. S., and J. Lehmann (2006), Double-funneling of trees: Stemflow and root-induced preferential flow, *Ecoscience*, 13(3), 324-333.
- Johnson, M. S., M. Weiler, E. G. Couto, S. J. Riha, and J. Lehmann (2007), Storm pulses of dissolved CO<sub>2</sub> in a forested headwater Amazonian stream explored using hydrograph separation, *Water Resources Research*, 43(11).
- Jones, J. P., E. A. Sudicky, A. E. Brookfield, and Y. J. Park (2006), An assessment of the tracer-based approach to quantifying groundwater contributions to streamflow, *Water Resources Research*, 42(2), W02407.
- Jung, M., G. Bonan, A. Cescattii, J.Q. Chen, R. de Jeu, A.J. Dolman, W. Eugster, D. Gerten, D. Gianelle, N. Gobron, J. Heinke, J. Kimball, B.E. Law, L. Montagnani, Q.Z. Mu, B. Mueller, K. Oleson, D. Papale, A.D. Richardson, O. Roupsard, S. Running, E. Tomelleri, N. Viovy, U. Weber, C. Williams, E. Wood, S. Zaehle, K. Zhang (2010), Recent decline in the global land evapotranspiration trend due to limited moisture supply, *Nature*, 467(7318), 951-954, doi: 10.1038/nature09396.
- Katul, G. G., R. Oren, S. Manzoni, C. Higgins, and M. B. Parlange (2012), Evapotranspiration: A process driving mass transport and energy exchange in the soil-plant-atmosphere-climate system, *Rev. Geophys.*, 50(3), RG3002.
- Keim, R. F., and A. E. Skaugset (2004), A linear system model of dynamic throughfall rates beneath forest canopies, *Water Resources Research*, 40(5).

- Keim, R. F., H. Meerveld, and J. J. McDonnell (2006), A virtual experiment on the effects of evaporation and intensity smoothing by canopy interception on subsurface stormflow generation, *J. Hydrol.*, 327(3-4), 352-364.
- Kennedy, V. C., G. W. Zellweger, and R. J. Avanzino (1979), Variations of rain chemistry during storms at two sites in Northern California, *Water Resources Research*, 15, 687-702.
- Kirchner, J. W., X. H. Feng, and C. Neal (2000), Fractal stream chemistry and its implications for contaminant transport in catchments, *Nature*, 403(6769), 524-527.
- Kleinhans, M. G., M. F. P. Bierkens, and M. van der Perk (2010), HESS Opinions On the use of laboratory experimentation: 'Hydrologists, bring out shovels and garden hoses and hit the dirt', *Hydrol. Earth Syst. Sci.*, 14(2), 369-382.
- Kool, J. B., and J. C. Parker (1987), Development and evaluation of closed-form expressions for hysteretic soil hydraulic properties, *Water Resources Research*, 23(1), 105-114.
- Kreft, A., and A. Zuber (1978), On the physical meaning of the dispersion equation and its solutions for different initial and boundary conditions, *Chemical Engineering Science*, 33, 1471-1480.
- Kundzewicz, Z. W., L. J. Mata, N. W. Arnell, P. Doll, B. Kabat, K. A. Jimenez, T. Miller, Z. Oki, S. Shiklomanov, and I. A. Shiklomanov (2007), Freshwater resources and their management, *Climate Change 2007: Impacts, Adaptation and Vulnerability, Contribution of Working Group II to the Fourth Assessment Report of the Intergovernmental Panel on Climate Change*, M.L. Parry, O.F. Canziani, J.P. Palutikof, P.J. van der Linden and C.E. Hanson, Eds., Cambridge University Press, Cambridge, UK, 173-210..
- Kung, K. J. S., E. J. Kladvko, T. J. Gish, T. S. Steenhuis, G. Bubenzer, and C. S. Helling (2000), Quantifying preferential flow by breakthrough of sequentially applied tracers: Silt loam soil, *Soil Sci. Soc. Am. J.*, 64(4), 1296-1304.
- Kutner, M. H., C. J. Nachtsheim, J. Neter, and W. Li (2005), *Applied Linear Statistical Models*, McGraw-Hill/Irwin, New York, NY.
- Lange, B., P. Luescher, and P. F. Germann (2009), Significance of tree roots for preferential infiltration in stagnant soils, *Hydrol. Earth Syst. Sci.*, 13(10), 1809-1821.
- Lehmann, P., C. Hinz, G. McGrath, H. J. Tromp-van Meerveld, and J. J. McDonnell (2007), Rainfall threshold for hillslope outflow: an emergent property of flow pathway

connectivity, *Hydrology and Earth System Sciences*, 11(2), 1047-1063, doi: 10.5194/hessd-3-2923-2006.

Li, Y. M., and M. Ghodrati (1994), Preferential transport of nitrate through soil columns containing root channels, *Soil Sci. Soc. Am. J.*, 58(3), 653-659.

Luo, Y. Q., D. Gerten, G. Le Maire, W.J. Parton, E.S. Weng, X.H. Zhou, C. Keough, C. Beier, P. Ciais, W. Cramer, J.S. Dukes, B. Emmett, P.J. Hanson, A. Knapp, S. Linder, D. Nepstad, L. Rustad, (2008), Modeled interactive effects of precipitation, temperature, and [CO<sub>2</sub>] on ecosystem carbon and water dynamics in different climatic zones, *Glob. Change Biol.*, 14(9), 1986-1999, doi: 10.1111/j.1365-2486.2008.01629.x.

Luxmoore, R. J. (1981), Microporosity, mesoporosity, and macroporosity of soil, *Soil Sci. Soc. Am. J.*, 45(3), 671-672.

Lyon, S. W., S. L. E. Desilets, and P. A. Troch (2009), A tale of two isotopes: differences in hydrograph separation for a runoff event when using delta D versus delta O-18, *Hydrol. Process.*, 23(14), 2095-2101.

Ma, S., D.D. Baldocchi, X. Liukang, and T. Hehn, (2007), Inter-annual variability in carbon dioxide exchange of an oak/grass savanna and open grassland in California, *Agricultural and Forest Meteorology*, 147, 157-171, doi: 10.1016/j.agrformet.2007.07.008.

Maciejewski, S., P. Maloszewski, C. Stumpp, D. Klotz, (2006), Modelling of water flow through typical Bavarian soils: 1. Estimation of hydraulic characteristics of the unsaturated zone, *Hydrological Sciences Journal*, 51(2), 285-297.

Macleod, C. J. A., A. Binley, S. L. Hawkins, M. W. Humphreys, L. B. Turner, W. R. Whalley, and P. M. Haygarth (2007), Genetically modified hydrographs: what can grass genetics do for temperate catchment hydrology?, *Hydrol. Process.*, 21(16), 2217-2221.

Maloszewski, P., and A. Zuber (1982), Determining the turnover time of groundwater systems with the aid of environmental tracers. 1. Models and their applicability, *J. Hydrol.*, 57(3-4), 207-231.

Maloszewski, P., S. Maciejewski, C. Stumpp, W. Stichler, P. Trimborn, and D. Klotz (2006), Modelling of water flow through typical Bavarian soils: 2. Environmental deuterium transport, *Hydrological Sciences Journal-Journal Des Sciences Hydrologiques*, 51(2), 298-313.

Marquardt, D. W. (1963), An algorithm for least-squares estimation of nonlinear parameters, *SIAM Journal of Applied Mathematics*, 11, 431-441.

Materechera, S. A., A. R. Dexter, and A. M. Alston (1992), Formation of aggregates by plant-roots in homogenized soils, *Plant Soil*, 142(1), 69-79.

McGuire, K. J., and J. J. McDonnell (2006), A review and evaluation of catchment transit time modeling, *J. Hydrol.*, 330(3-4), 543-563.

McGuire, K. J., and J. J. McDonnell (2010), Hydrological connectivity of hillslopes and streams: Characteristic time scales and nonlinearities, *Water Resources Research*, 46.

McMillan, H. K. (2012), Effect of spatial variability and seasonality in soil moisture on drainage thresholds and fluxes in a conceptual hydrological model, *Hydrol. Process.*, 26(18), 2838-2844, doi: 10.1002/hyp.9396.

Milly, P. C. D. (1994), Climate, interseasonal storage of soil-water, and the annual water-balance, *Adv. Water Resour.*, 17(1-2), 19-24, doi: 10.1016/0309-1708(94)90020-5.

Milly, P. C. D., and K. A. Dunne (2002), Macroscale water fluxes - 2. Water and energy supply control of their interannual variability, *Water Resources Research*, 38(10), 9.

Mitchell, A. R., T. R. Ellsworth, and B. D. Meek (1995), Effect of root systems on preferential flow in swelling soil, *Commun. Soil Sci. Plant Anal.*, 26(15-16), 2655-2666.

Montaldo, N., J. D. Albertson, and M. Mancini (2008), Vegetation dynamics and soil water balance in a water-limited Mediterranean ecosystem on Sardinia, Italy, *Hydrol. Earth Syst. Sci.*, 12(6), 1257-1271, doi: 10.5194/hess-12-1257-2008.

Morgan, J. A., D. R. LeCain, E. Pendall, D. M. Blumenthal, B. A. Kimball, Y. Carrillo, D. G. Williams, J. Heisler-White, F. A. Dijkstra, and M. West (2011), C4 grasses prosper as carbon dioxide eliminates desiccation in warmed semi-arid grassland, *Nature*, 476(7359), 202-205, doi: 10.1038/nature10274.

Morgan, J. A., D.E. Pataki, C. Korner, H. Clark, S.J. Del Grosso, J.M. Grunzweig, A.K. Knapp, A.R. Mosier, P.C.D. Newton, P.A. Niklaus, J.B. Nippert, R.S. Nowak, W.J. Parton, H.W. Polley, M.R. Shaw (2004), Water relations in grassland and desert ecosystems exposed to elevated atmospheric CO<sub>2</sub>, *Oecologia*, 140(1), 11-25, doi: 10.1007/s00442-004-1550-2.

Mote, P. W., and E. P. Salathe (2010), Future climate in the Pacific Northwest, *Clim. Change*, 102(1-2), 29-50, doi: 10.1007/s10584-010-9848-z.

- Munoz-Villers, L. E., and J. J. McDonnell (2012), Runoff generation in a steep, tropical montane cloud forest catchment on permeable volcanic substrate, *Water Resources Research*, 48.
- Nash, J. E., and J. V. Sutcliffe (1970), River flow forecasting through conceptual models part 1 - A discussion of principles, *J. Hydrol.*, 10(3), 282-290.
- Nimmo, J. R. (2007), Simple predictions of maximum transport rate in unsaturated soil and rock, *Water Resources Research*, 43(5).
- Nimmo, J. R. (2012), Preferential flow occurs in unsaturated conditions, *Hydrol. Process.*, 26(5), 786-789.
- Noguchi, S., Y. Tsuboyama, R. C. Sidle, and I. Hosoda (1997), Spatially distributed morphological characteristics of macropores in forest soils of Hitachi Ohta Experimental Watershed, Japan, *Journal of Forest Research*, 2(4), 207-215.
- Norby, R. J., and Y. Q. Luo (2004), Evaluating ecosystem responses to rising atmospheric CO<sub>2</sub> and global warming in a multi-factor world, *New Phytologist*, 162(2), 281-293, doi: 10.1111/j.1469-8137.2004.01047.x.
- Pangle, L. A. (2013), Ecohydrological mediation of water budget partitioning and time scales of subsurface flow in a seasonally semi-arid grassland, Oregon State University, Corvallis, Oregon.
- Pangle, L. A., J. W. Gregg, and J. J. McDonnell (2013a), Seasonal rainfall and an ecohydrological feedback offset the potential impact of climate warming on evapotranspiration and groundwater recharge, *Water Resources Research*, *In Review*.
- Pangle, L. A., J. Klaus, E. S. F. Berman, M. Gupta, and J. J. McDonnell (2013b), A new multi-source and high-frequency approach to measuring  $\delta^2\text{H}$  and  $\delta^{18}\text{O}$  in hydrological field studies, *Water Resources Research*, *In Review*.
- Phillips, C. L., J. W. Gregg, and J. K. Wilson (2011), Reduced diurnal temperature range does not change warming impacts on ecosystem carbon balance of Mediterranean grassland mesocosms, *Glob. Change Biol.*, 17(11), 3263-3273, doi: 10.1111/j.1365-2486.2011.02483.x.
- Ponton, S., L. B. Flanagan, K. P. Alstad, B. G. Johnson, K. Morgenstern, N. Kljun, T. A. Black, and A. G. Barr (2006), Comparison of ecosystem water-use efficiency among Douglas-fir forest, aspen forest and grassland using eddy covariance and carbon isotope techniques, *Glob. Change Biol.*, 12(2), 294-310, doi: 10.1111/j1365-2486.2005.01103.x.

Porporato, A., E. Daly, and I. Rodriguez-Iturbe (2004), Soil water balance and ecosystem response to climate change, *American Naturalist*, 164(5), 625-632, doi: 10.1086/424970.

Porporato, A., F. Laio, L. Ridolfi, and I. Rodriguez-Iturbe (2001), Plants in water-controlled ecosystems: active role in hydrologic processes and response to water stress - III. Vegetation water stress, *Adv. Water Resour.*, 24(7), 725-744, doi: 10.1016/S0309-1708(01)00006-9.

Potter, N. J., L. Zhang, P. C. D. Milly, T. A. McMahon, and A. J. Jakeman (2005), Effects of rainfall seasonality and soil moisture capacity on mean annual water balance for Australian catchments, *Water Resour. Res.*, 41(6), W06007, doi: 10.1029/2004WR003697.

Price, K., C. R. Jackson, and A. J. Parker (2010), Variation of surficial soil hydraulic properties across land uses in the southern Blue Ridge Mountains, North Carolina, USA, *J. Hydrol.*, 383(3-4), 256-268.

Pumo, D., F. Viola, and L. V. Noto (2008), Ecohydrology in Mediterranean areas: a numerical model to describe growing seasons out of phase with precipitations, *Hydrology and Earth System Sciences*, 12(1), 303-316, doi: 10.5194/hess-12-303-2008.

Rasse, D. P., A. J. M. Smucker, and D. Santos (2000), Alfalfa root and shoot mulching effects on soil hydraulic properties and aggregation, *Soil Sci. Soc. Am. J.*, 64(2), 725-731.

Rillig, M. C., S. F. Wright, and V. T. Eviner (2002), The role of arbuscular mycorrhizal fungi and glomalin in soil aggregation: comparing effects of five plant species, *Plant Soil*, 238(2), 325-333.

Rinaldo, A., K. J. Beven, E. Bertuzzo, L. Nicotina, J. Davies, A. Fiori, D. Russo, and G. Botter (2011), Catchment travel time distributions and water flow in soils, *Water Resources Research*, 47.

Rodriguez-Iturbe, I., A. Porporato, L. Ridolfi, V. Isham, and D. R. Cox (1999), Probabilistic modelling of water balance at a point: the role of climate, soil and vegetation, *Proc. R. Soc. London Ser. A-Math. Phys. Eng. Sci.*, 455, 3789-3805, doi: 10.1098/rspa.1999.0477.

Ryu, Y., D. D. Baldocchi, S. Ma, and T. Hehn (2008), Interannual variability of evapotranspiration and energy exchange over an annual grassland in California, *Journal of Geophysical Research-Atmospheres*, 113, doi: 10.1029/2007JD009263.

Sanders, E. C., M. R. Abou Najm, R. H. Mohtar, E. Klavivko, and D. Schulze (2012), Field method for separating the contribution of surface-connected preferential flow pathways from flow through the soil matrix, *Water Resources Research*, 48, doi: 10.1029/2011WR011103.

Schaap, M. G., F. J. Leij, and M. T. van Genuchten (2001), Rosetta: a computer program for estimating soil hydraulic parameters with hierarchical pedotransfer functions, *J. Hydrol.*, 251, 163-176.

Schenk, H. J., and R. B. Jackson (2002), The global biogeography of roots, *Ecol. Monogr.*, 72(3), 311-328.

Schoups, G., and J. A. Vrugt (2010), A formal likelihood function for parameter and predictive inference of hydrologic models with correlated, heteroscedastic, and non-Gaussian errors, *Water Resources Research*, 46.

Simunek, J., M. Sejna, H. Saito, M. Sakai, and M. T. Van Genuchten (2012), The HYDRUS-1D software package for simulating the movement of water, heat, and multiple solutes in variably saturated media, Version 4.15, *HYDRUS Software Series*, 3, Department of Environmental Sciences, University of California Riverside, Riverside, California, USA, .

Stewart, M. K., and J. J. McDonnell (1991), Modeling base-flow soil-water residence times from deuterium concentrations, *Water Resources Research*, 27(10), 2681-2693.

Stumpp, C. and P. Maloszewski (2010), Quantification of preferential flow and flow heterogeneities in an unsaturated soil planted with different crops using the environmental isotope delta O-18, *Journal of Hydrology*, 394(3-4), 407-415.

Stumpp, C., W. Stichler, and P. Maloszewski (2009a), Application of the environmental isotope delta O-18 to study water flow in unsaturated soils planted with different crops: Case study of a weighable lysimeter from the research field in Neuherberg, Germany, *J. Hydrol.*, 368(1-4), 68-78.

Stumpp, C., P. Maloszewski, W. Stichler, and J. Fank (2009b), Environmental isotope (delta O-18) and hydrological data to assess water flow in unsaturated soils planted with different crops: Case study lysimeter station "Wagna" (Austria), *J. Hydrol.*, 369(1-2), 198-208.

Stumpp, C., P. Maloszewski, W. Stichler, and S. Maciejewski (2007), Quantification of the heterogeneity of the unsaturated zone based on environmental deuterium observed in lysimeter experiments, *Hydrological Sciences Journal-Journal Des Sciences Hydrologiques*, 52(4), 748-762.

Survey, N. C. S. (2012), National Cooperative Soil Characterization Database, edited, Natural Resource Conservation Service; United States Department of Agriculture.

Tague, C., K. Heyn, and L. Christensen (2009), Topographic controls on spatial patterns of conifer transpiration and net primary productivity under climate warming in mountain ecosystems, *Ecohydrology*, 2(4), 541-554, doi: 10.1002/eco.88.

Taylor, R.G., B. Scanlon, P. Doll, M. Rodell, R. van Beek, Y. Wada, L. Longuevergne, M. Leblanc, J.S. Famiglietti, M. Edmunds, L. Konikow, T.R. Green, J. Chen, M. Taniguchi, M.F.P. Bierkens, A. MacDonald, Y. Fan, R.M. Maxwell, Y. Yecheili, J.J. Gurdak, D.M. Allen, M. Shamsudduha, K. Hiscock, P.J.F. Yeh, I. Holman, H. Treidel (2012), Ground water and climate change, *Nature Climate Change*, 3(4), 322-329, doi: 10.1038/nclimate1744.

Ter Braak, C. J. F., and J. A. Vrugt (2008), Differential evolution Markov Chain with snooker updater and fewer chains, *Statistical Computing*, 18, 435-446.

Teuling, A. J., S.I. Seneviratne, R. Stöckli, M. Reichstein, E. Moors, P. Ciais, S. Luyssaert, B. van den Hurk, C. Ammann, C. Bernhofer, E. Dellwik, D. Gianelle, B. Gielen, T. Grünwald, K. Klumpp, L. Montagnani, C. Moureaux, M. Sottocornola, and G. Wohlfahrt (2010), Contrasting response of European forest and grassland energy exchange to heatwaves, *Nat. Geosci.*, 3(10), 722-727, doi: 10.1038/geo950.

Thompson, S. E., C. J. Harman, P. A. Troch, P. D. Brooks, and M. Sivapalan (2011), Spatial scale dependence of ecohydrologically mediated water balance partitioning: A synthesis framework for catchment ecohydrology, *Water Resources Research*, 47, doi: 10.1029/2010WR009998.

Thompson, S. E., C. J. Harman, P. Heine, and G. G. Katul (2010), Vegetation-infiltration relationships across climatic and soil type gradients, *J. Geophys. Res.-Biogeosci.*, 115.

Thompson, S. E., C. J. Harman, A. G. Konings, M. Sivapalan, A. Neal, and P. A. Troch (2011), Comparative hydrology across AmeriFlux sites: The variable roles of climate, vegetation, and groundwater, *Water Resources Research*, 47.

Tippkötter, R. (1983), Morphology, spatial arrangement and origin of macropores in some hapludalfs, West-Germany, *Geoderma*, 29(4), 355-371.

Tingey, D. T., R. S. Waschmann, D. L. Phillips, and D. M. Olszyk (2000), The carbon dioxide leakage from chambers measured using sulfur hexafluoride., *Environmental and Experimental Botany*, 43, 101-110, doi: 10.1016/S0098-8472(99)00051-9.

Udawatta, R. P., S. H. Anderson, C. J. Gantzer, and H. E. Garrett (2008), Influence of prairie restoration on CT-measured soil pore characteristics, *J. Environ. Qual.*, 37(1), 219-228.

van der Velde, Y., P. Torfs, S. van der Zee, and R. Uijlenhoet (2012), Quantifying catchment-scale mixing and its effect on time-varying travel time distributions, *Water Resources Research*, 48.

van der Velde, Y., G. H. de Rooij, J. C. Rozemeijer, F. C. van Geer, and H. P. Broers (2010), Nitrate response of a lowland catchment: On the relation between stream concentration and travel time distribution dynamics, *Water Resources Research*, 46.

van Genuchten, M.T., 1980, A closed-form equation for predicting the hydraulic conductivity of unsaturated soils, *Soil Science Society of America Journal*, 44(5), 892-898.

Viola, F., E. Daly, G. Vico, M. Cannarozzo, and A. Porporato (2008), Transient soil-moisture dynamics and climate change in Mediterranean ecosystems, *Water Resources Research*, 44, doi: 10.1029/2007WR006371.

Vitvar, T., and W. Balderer (1997), Estimation of mean water residence times and runoff generation by  $^{18}\text{O}$  measurements in a Pre-Alpine catchment (Rietholzbach, Eastern Switzerland), *Applied Geochemistry*, 12, 787-796.

Vrugt, J. A., C. J. F. ter Braak, C. G. H. Diks, B. A. Robinson, J. M. Hyman, and D. Higdon (2009), Accelerating Markov Chain Monte Carlo Simulation by Differential Evolution with Self-Adaptive Randomized Subspace Sampling, *International Journal of Nonlinear Sciences and Numerical Simulation*, 10(3), 273-290.

Weiler, M., and F. Naef (2003), An experimental tracer study of the role of macropores in infiltration in grassland soils, *Hydrol. Process.*, 17(2), 477-493.

Weiler, M., B. L. McGlynn, K. J. McGuire, and J. J. McDonnell (2003), How does rainfall become runoff? A combined tracer and runoff transfer function approach, *Water Resources Research*, 39(11).

Williams, A., D. Scholefield, J. Dowd, N. Holden, and L. Deeks (2000), Investigating preferential flow in a large intact soil block under pasture, *Soil Use and Management*, 16(4), 264-269.

Williams, A. G., J. F. Dowd, and E. W. Meyles (2002), A new interpretation of kinematic stormflow generation, *Hydrol. Process.*, 16, 2791-2803.

Wu, Z. T., P. Dijkstra, G. W. Koch, J. Penuelas, and B. A. Hungate (2011), Responses of terrestrial ecosystems to temperature and precipitation change: a meta-analysis of experimental manipulation, *Glob. Change Biol.*, 17(2), 927-942.

Yu, K. L., T. G. Pypker, R. F. Keim, N. Chen, Y. B. Yang, S. Q. Guo, W. J. Li, and G. Wang (2012), Canopy rainfall storage capacity as affected by sub-alpine grassland degradation in the Qinghai-Tibetan Plateau, China, *Hydrol. Process.*, 26(20), 3114-3123.

Zavaleta, E. S., B. D. Thomas, N. R. Chiariello, G. P. Asner, M. R. Shaw, and C. B. Field (2003a), Plants reverse warming effect on ecosystem water balance, *Proceedings of the National Academy of Sciences of the United States of America*, 100(17), 9892-9893, doi: 10.1073/pnas.1732012100.

Zavaleta, E. S., M. R. Shaw, N. R. Chiariello, B. D. Thomas, E. E. Cleland, C. B. Field, and H. A. Mooney (2003b), Grassland responses to three years of elevated temperature, CO<sub>2</sub>, precipitation, and N deposition, *Ecological Monographs*, 73(4), 585-604, doi: 10.1890/02-4053.

Zhongmin, H., Y. Guirui, Z. Yanlian, S. Xiaomin, L. Yingnian, S. Peili, W. Yanfen, S. Xia, Z. Zemei, Z. Li, and L. Shenggong (2009), Partitioning of evapotranspiration and its controls in four grassland ecosystems: Application of a two-source model, *Agricultural and Forest Meteorology*, 149, 1410-1420, doi: 10.1016/j.agrformet.2009.03.014.

**APPENDICES**

## Appendix A: Field deployable laser spectrometer and automated-high-frequency sampling system.<sup>1</sup>

### A1.1 Sample-acquisition system and field-deployable laser spectrometer

We utilized a new sample-acquisition system that combined a four-channel peristaltic pump and a four-port stainless steel sampling manifold that was mounted on a CTC LCPAL auto-sampler tray (Figure A1.1). The peristaltic pump (Ismatec MS-CA Stand-mounted Pump) had a fixed-speed motor and eight rollers that turned on the drive shaft at 20 rpm. The maximum pressure differential created by the pump was up to 100 kPa depending on the type of compressible tubing used. We used PharMed Ismaprene compressible tubing (1.65 mm inside diameter) with vinyl tubing (9.5 mm inside diameter) connected to the intake and output sides of the compressible tubing to deliver water from the discharge point to the sampling manifold. We sustained consistent flow rates of 5.56—5.72 mL min<sup>-1</sup> depending on the length of the particular sample line and the total head gradient.

The custom manifold was designed to attach to the tray holder of a CTC LCPAL auto-sampler (Figure A1.1). Water flowed vertically through the base of the manifold through four vertical stainless steel tubes. The top of the manifold had a Plexiglas cover with drilled openings above each tube that allowed the 1.2 µL syringe to draw from the inflowing water. The slanted interior of the stainless steel manifold allowed the water to drain out of an attached waste line. This design prevented the accumulation of any residual water within the four tubes, which reduced the risk of particle matter accumulation that could cause the injection syringe to malfunction. The moving arm of the LCPAL auto-sampler was calibrated to locate the horizontal and vertical position of each inlet tube.

The ratio of <sup>2</sup>H/<sup>1</sup>H and <sup>18</sup>O/<sup>16</sup>O of liquid water samples was measured with a Los Gatos Research liquid water isotope analyzer (LWIA), and converted to δ<sup>2</sup>H and δ<sup>18</sup>O using the Vienna Standard Mean Ocean Water (VSMOW). Recent advances in sample heating and gas transport within the LWIA, along with software modifications, enabled

---

<sup>1</sup> This appendix is an excerpt from the manuscript: Pangle, L.A., J. Klaus, E.S.F. Berman, M. Gupta, and J.J. McDonnell, *In Review*, A new multi-source and high-frequency approach to measuring δ<sup>2</sup>H and δ<sup>18</sup>O in hydrological field studies. *Water Resources Research*.

the measurement of the stable isotope composition of one injection of sample water every 102 s. We used a sampling scheme that included three external standards interleaved with nine samples. Each sample was injected five times; the first two injections were omitted to account for the carryover effect resulting from traces of residual vapor molecules from the previous sample remaining in the cavity, and the last three injections were averaged. These three injections were not drawn from exactly the same volume of water, since the flow through the manifold was continuous. The average  $\delta^2\text{H}$  and  $\delta^{18}\text{O}$  of three injections represented a normalized flux of 0.0056 – 0.079 mm across the range of observed flux rates. This scheme enabled one sample (average of  $n=3$  injections) to be analyzed from each of three water sources every 34 minutes.

### *A1.2 Field deployment*

We deployed the sample acquisition system and LWIA at a lysimeter study site at the Terracosm research facility in Corvallis, OR (44.57°N, -123.29°W; 77 m elevation) during March, 2012. The instrumentation was placed inside acrylic boxes to protect it from dust and humidity and located inside a non-climate-controlled shed with 120 VAC power. We measured  $\delta^2\text{H}$  and  $\delta^{18}\text{O}$  in the potential groundwater recharge flux (i.e. lysimeter drainage) from L1bs and L1g. A funnel was attached to the base of the tipping bucket that measured recharge from each lysimeter, which directed the water flow into a closed container (0.040 L volume) that was connected to the sample acquisition system by vinyl tubing (Figure A1.1). Similarly, a rainfall collector was connected with vinyl tubing to route precipitation to the sample acquisition system

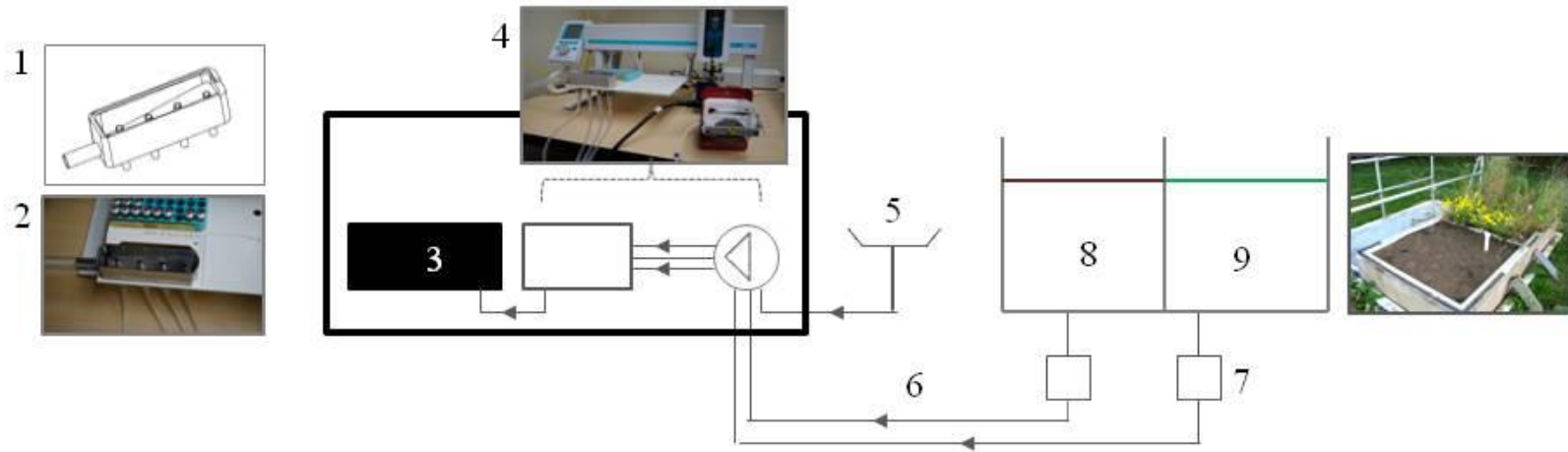


**Figure A1.1** Diagram illustrating the components of the new sample-acquisition system and site of field-deployment: 1) sketch of the custom manifold, 2) photo of manifold mounted to sample tray of a CTC LCPAL auto-sampler, with four incoming sample lines and outgoing waste line, 3) LGR Liquid Water Isotope Analyzer, 4) photograph illustrating the flow path from the four-channel peristaltic pump to the sample inflow ports on the base of the manifold, 5) precipitation collector, 6) vinyl tubing connecting each water source to the peristaltic pump, 7) tipping bucket gages, 8) lysimeter with bare soil surface, 9) lysimeter with grassland vegetation.

## **Appendix 2: Variably-saturated-flow modeling to evaluate the potential effect of rainfall-interception, storage, and evaporative loss from grassland canopies on potential groundwater recharge.**

We modeled water flow within the L1bs lysimeter during the storm event spanning March 12<sup>th</sup> 12:00 to March 14<sup>th</sup> 8:00 using a 1-dimensional version of the governing equation for variably-saturated flow in porous media (a.k.a. the Richards Equation) combined with the van Genuchten-Mualem soil hydraulic model [*van Genuchten*, 1980] that describes the relationships between volumetric-water content and water-pressure head, and between saturated-hydraulic conductivity and water-pressure head. The model was implemented using a finite-element numerical solution to the Richards Equation executed with the HYDRUS-1D software [*Simunek et al.*, 2012].

### *A2.1 Model domain, boundary and initial conditions*

The model domain was a 1-dimensional soil profile with 0.95 m depth and consisting of a single soil material. The upper boundary condition (i.e. the soil surface) was defined as a variable-flux boundary subject to measured-incoming precipitation and evaporation that was estimated using a variant of the Penman-Monteith equation [*Allen et al.*, 1998]. Meteorological data used to drive the evaporation model included solar radiation and wind-speed data that were obtained from the Corvallis Agrimet station [*Bureau of Reclamation*, 2013] located approximately 10 km northeast of our study site, and temperature and relative humidity data collected locally at the Terracosm facility. The bottom boundary condition (i.e. the soil-gravel interface) was modeled as a seepage face where water-pressure head must exceed atmospheric pressure ( $h = 0$  m gage) before drainage can occur. Variable boundary conditions at the soil surface were simulated at a time step of 15 minutes. Initial conditions at each node in the model domain were specified based on measured volumetric-water content at 0.05, 0.15, and 0.75 m soil depth. The values at each node in between these depths were estimated by linear interpolation. The values from 0-0.04 m soil depth were assumed to be the same as measured at 0.05, and values from 0.76-0.95 m were assumed to be the same as measured at 0.75 m depth.

### A2.2 Soil hydraulic model and parameter identification

We used an inverse-solution procedure to find an optimal parameter set for the van Genuchten-Mualem hydraulic model. The ROSETTA neural network tool [Schaap *et al.*, 2001] was used to generate initial estimates of the parameters  $\theta_r$ ,  $\theta_s$ ,  $\alpha$ ,  $n$ , and  $K_{\text{sat}}$  for the hydraulic model based on the measured sand, silt, and clay fractions of the soil, measured bulk-density, and  $\theta$  at 0.34 kPa of applied pressure (measured using repacked soil columns and a pressure chamber). We also simulated hysteresis in the  $h(\theta)$  relationship using the estimation procedure described by Kool and Parker [1987] that was executed within the HYDRUS-1D software. In total this required the identification of eight parameters, and their optimal values were determined through an iterative-optimization procedure [Marquardt, 1963] based on minimization of the summed-squared differences between observed and simulated drainage flux from the base of the lysimeter.

### A2.3 Model evaluation

The resulting drying and wetting curves of the van Genuchten-Mualem hydraulic model with hysteresis are shown in figure A2.1, in comparison with measured values of  $h(\theta)$  (during drying from an initial saturated state) obtained using a pressure chamber and repacked soil columns (5 cm height x 5 cm diameter). The fitted hydraulic model provides a reasonable representation of the wet-end of the moisture retention curves, even with the substantial decline in  $\theta$  that occurs under very low applied pressures. Figure A2.2 compares the measured and simulated R. The model accurately simulated R during this storm event (RMSE = 0.06 mm 15 min<sup>-1</sup>), including the magnitude of peak R and the timing of the rising limb of the hydrograph, though the model did tend to overestimate flow during the initial falling limb of the hydrograph and slightly underestimate the prolonged recession flow.

Since the soil profile in L10 was 0.05 m deeper than in L1bs and L1g, and the incident precipitation was slightly different, an additional simulation was performed to address the potential influence of these factors. The simulation used the same hydraulic model and parameters, but the model domain was extended to 1 m total depth and the irrigation rates applied to L10 were used to define the upper boundary condition. Figure

A2.2 shows the results of this simulation, in comparison with the measured data and the simulation described above. The difference in soil-profile depth had a negligible effect, whereas the different incident precipitation actually increased total R and the maximum flux rate. Based on this simulation, it was concluded that the difference in soil depth and incident precipitation on L10 versus L1bs and L1g did not influence the contrasting R trends we observed (Figure 3.1 and Table 3.1).

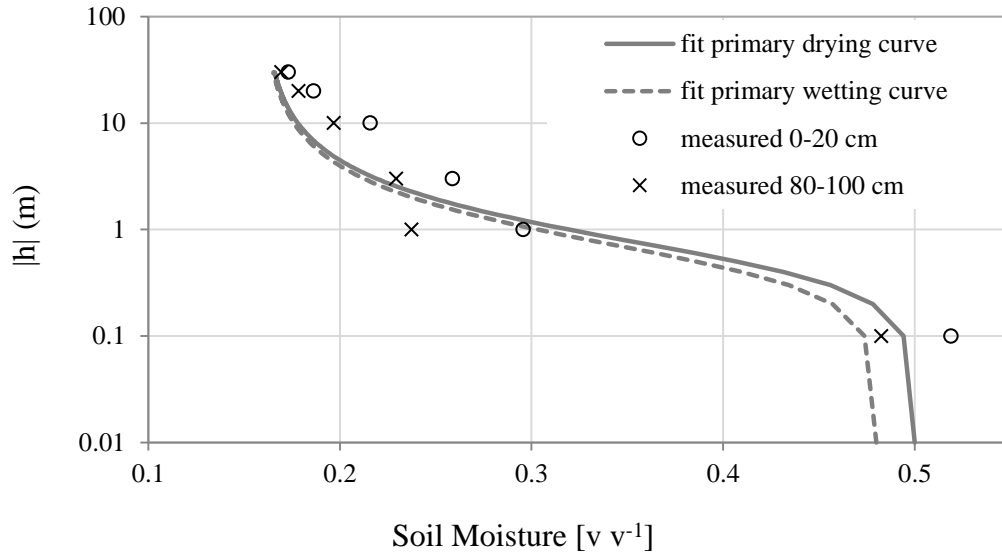


**Figure A2.1** Measured moisture retention curves for the soil layers installed at 0-0.20 and 0.80-1 m depth within the lysimeters. Lines indicate the fitted primary drying curve based on the van Genuchten-Mualem model and an optimized primary wetting curve that were used in the model simulations of the lysimeter rainfall-recharge response.

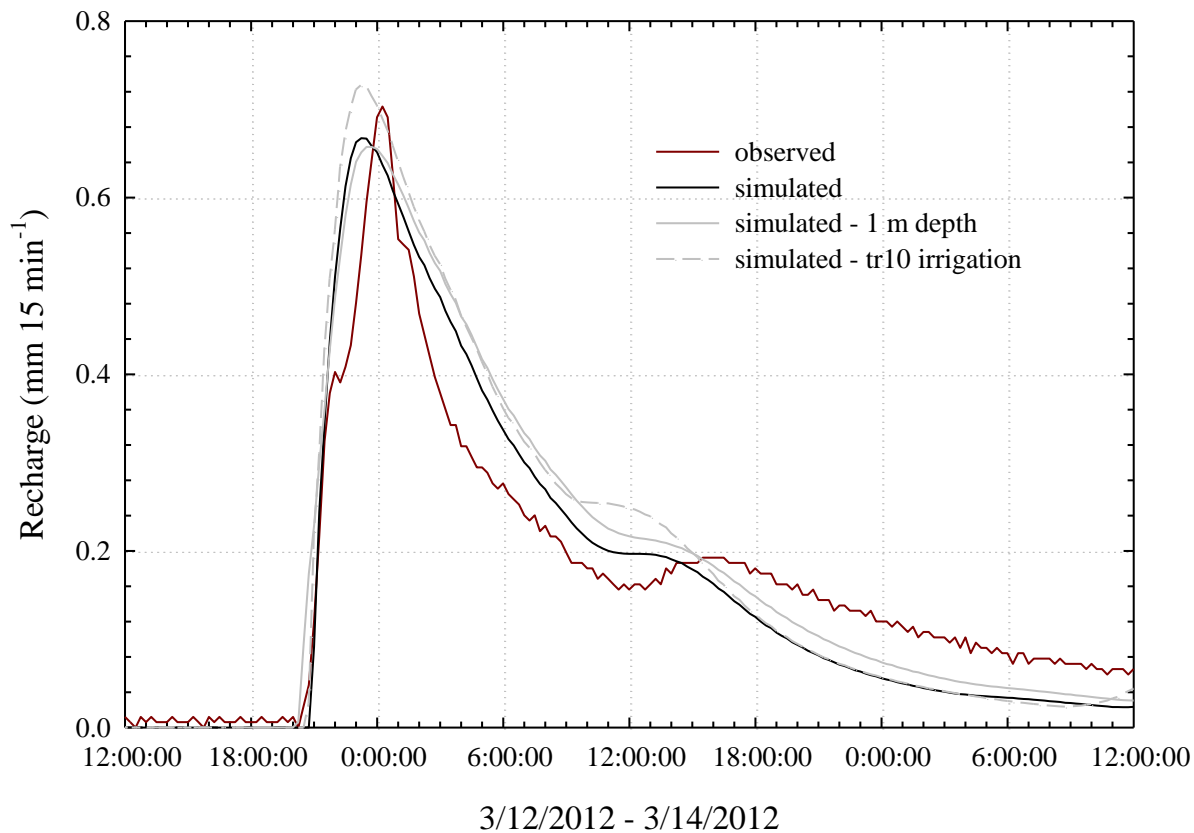


**Figure A2.2** Measured and simulated recharge that occurred under the bare soil condition (L1bs) in response to precipitation on March 12<sup>th</sup> through March 14<sup>th</sup>, 2012. Also shown are simulations using the same model parameters but with a 1-m-deep soil profile (reflecting the additional 0.05 m of soil depth in L10), and a fourth simulation where the irrigation regime specific to L10 was used to drive the model in contrast to the incident precipitation experienced by L1bs and L1g.

## References

- Allen, R. G., L. S. Pereira, D. Raes, and M. Smith (1998), *Crop evapotranspiration - Guidelines for computing crop water requirements*.
- Bureau of Reclamation, D. o. t. I., USA (2013), The Pacific Northwest Cooperative Agricultural Weather Network, edited by C. A. Station, <http://www.usbr.gov/pn/agrimet/>.
- Kool, J. B., and J. C. Parker (1987), Development and evaluation of closed-form expressions for hysteretic soil hydraulic properties, *Water Resources Research*, 23(1), 105-114.
- Marquardt, D. W. (1963), An algorithm for least-squares estimation of nonlinear parameters, *SIAM Journal of Applied Mathematics*, 11, 431-441.
- Schaap, M. G., F. J. Leij, and M. T. van Genuchten (2001), Rosetta: a computer program for estimating soil hydraulic parameters with hierarchical pedotransfer functions, *J. Hydrol.*, 251, 163-176.
- Simunek, J., M. Sejna, H. Saito, M. Sakai, and M. T. Van Genuchten (2012), The HYDRUS-1D software package for simulating the movement of water, heat, and multiple solutes in variably saturated media, Version 4.15, *HYDRUS Software Series*, 3, Department of Environmental Sciences, University of California Riverside, Riverside, California, USA, .
- van Genuchten, M. T. (1980), A closed-form equation for predicting the hydraulic conductivity of unsaturated soils, *Soil Sci. Soc. Am. J.*, 44(5), 892-898.